

Ground states of quantum antiferromagnets in two dimensions

Subir Sachdev^{1,2} and Kwon Park¹

¹*Department of Physics, Yale University, P.O. Box 208120, New Haven, CT 06520-8120*

²*Department of Physics, Harvard University, Cambridge MA 02138*

(December 2, 2024)

We explore the ground states and quantum phase transitions of two-dimensional, spin $S = 1/2$, antiferromagnets by generalizing lattice models and duality transforms introduced by Sachdev and Jalabert (Mod. Phys. Lett. B **4**, 1043 (1990)). The ‘minimal’ model for square lattice antiferromagnets is a lattice discretization of the quantum non-linear sigma model, along with Berry phases which impose quantization of spin. With full SU(2) spin rotation invariance, we find a magnetically ordered ground state with Néel order at weak coupling, and a confining paramagnetic ground state with bond charge (*e.g.* spin Peierls) order at strong coupling. We study the mechanisms by which these two states are connected in intermediate coupling. We extend the minimal model to study different routes to fractionalization and deconfinement in the ground state, and also generalize it to cases with a uniaxial anisotropy (the spin symmetry group is then U(1)). For the latter systems, fractionalization can appear by the pairing of vortices in the staggered spin order in the easy-plane; however, we argue that this route does not survive the restoration of SU(2) spin symmetry. For SU(2) invariant systems we study a separate route to fractionalization associated with the Higgs phase of a complex boson measuring *non-collinear*, spiral spin correlations: we present phase diagrams displaying competition between magnetic order, bond charge order, and fractionalization, and discuss the nature of the quantum transitions between the various states. A strong check on our methods is provided by their application to $S = 1/2$ frustrated antiferromagnets in one dimension: here, our results are in complete accord with those obtained by bosonization and by the solution of integrable models.

Contents

| | | | | |
|------------|---|-----------|--------------------------------------|---|
| | | B | Phases with magnetic order | 31 |
| | | 1 | HN phase | 31 |
| | | 2 | P phase | 31 |
| | | 3 | HN+F phase | 32 |
| | | C | Multicritical points | 32 |
| I | Introduction | 2 | | |
| | A Fractionalization | 5 | | |
| | B Outline | 6 | | |
| II | Duality and Bond Order | 7 | VII | Conclusions |
| III | Connecting the Néel and Bond order states | 8 | APPENDIXES | 34 |
| | A Spin wave expansion | 9 | A | CP^1 formulation |
| | B Critical φ^4 field theory | 9 | B | Large g limit with SU(2) symmetry |
| | 1 U(1) symmetry | 11 | C | Properties and mappings of the height model |
| | 2 Remarks | 12 | 1 | Quantum dimer model |
| IV | Antiferromagnets in one dimension | 12 | 2 | Coulomb plasma of instantons |
| | A Results from bosonization | 12 | 3 | Sine-Gordon model |
| | B Dual lattice models | 13 | D | Correlations of defects in the φ^4 field theory |
| | 1 Observables and limiting cases | 15 | E | Field theory in one dimension |
| | 2 Field theory and phase diagram | 16 | F | CP^1 models with easy-plane anisotropy |
| V | U(1) symmetry in two dimensions | 17 | G | Field theory in two dimensions |
| | A Observables and limiting cases | 18 | H | Gauge theory with $\langle N \rangle \neq 0$ |
| | B Field theories | 18 | | |
| | C Generalized phase diagrams and restoration of SU(2) symmetry | 21 | | |
| | 1 HN order in the XY+I phase | 22 | | |
| | 2 SU(2) symmetry with bond order | 24 | | |
| | 3 Interplay with fractionalization | 25 | | |
| VI | Fractionalization with SU(2) symmetry, and non-collinear spin correlations | 26 | | |
| | A Connection with Z_2 gauge theory | 28 | | |

I. INTRODUCTION

A central problem¹ in the study of correlated electron systems is the classification of the quantum phases and critical points of two-dimensional quantum antiferromagnets at zero temperature (T). Of particular interest, because of its association with the physics of the cuprate superconductors, is the spin $S = 1/2$ antiferromagnet on the square lattice:

$$H = J \sum_{\langle ij \rangle} \hat{\mathbf{S}}_i \cdot \hat{\mathbf{S}}_j + \dots \quad (1.1)$$

Here $\hat{\mathbf{S}}_j$ are $S = 1/2$ quantum spin operators on the sites, j , of a square lattice, the sum $\langle ij \rangle$ is over nearest neighbor links, and $J > 0$ is the antiferromagnetic exchange energy. The ellipsis represents smaller further neighbor or ring exchange terms that can be added to deform the purely nearest neighbor model: we allow a wide class of such terms. Without these additional terms, the ground state of H is well known: it is the Néel state with a spontaneous staggered magnetic moment

$$\langle \hat{\mathbf{S}}_j \rangle = \eta_j N_0 \mathbf{e} \quad , \quad T = 0, \quad (1.2)$$

where $\eta_j = \pm 1$ identifies the square sublattice of site j , \mathbf{e} is a unit vector with an arbitrary, fixed, orientation in spin space, and $N_0 > 0$ is the magnitude of the moment. We will refer to this state as the Heisenberg-Néel (HN) state, the qualifier denoting the SU(2) (Heisenberg) symmetry of H (this allows us to distinguish from cases in which the SU(2) spin symmetry has been reduced to U(1), which we consider later in the paper). The low energy, elementary excitations of the HN state are a doublet of gapless spin wave modes, associated with slow modulations in the orientation \mathbf{e} .

This paper will address the following question and related issues²: what are the possible ground states of H which are “near” the HN state? More precisely, imagine slowly reducing the value of N_0 (while (1.2) maintains its spatial structure) by modifying some of the unspecified non-nearest-neighbor terms in H ; at some critical point in parameter space, N_0 will vanish and spin rotation invariance will be restored; how does the ground state of H evolve towards and beyond this critical point? What is the field theoretic description of the quantum critical point at which N_0 vanishes, and of any additional quantum critical points that may be encountered? How do these results get modified when exchange anisotropies in H (like an additional $J\zeta \sum_{\langle ij \rangle} \hat{S}_{iz} \hat{S}_{jz}$ term) reduce the global spin symmetry of H from SU(2) to U(1)?

Along some lines in parameter space, the spatial form of (1.2) may change before spin rotation invariance is restored *e.g.* the spontaneous magnetization can become incommensurate and non-collinear. This is a situation of fundamental importance, but in the interests of simplicity we will postpone discussion of phases associated with non-collinear spin correlations to Section VI, where

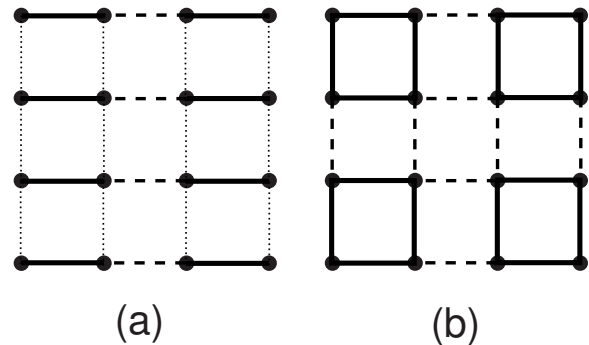


FIG. 1. Sketch of the two simplest possible states with bond-centered charge (BC) order: (a) the columnar spin-Peierls states, and (b) plaquette state. The different values of the Q_{ij} on the links are encoded by the different line styles; the state in (a) has 3 distinct values of Q_{ij} , while that in (b) has 2. Both states are 4-fold degenerate; an 8-fold degenerate state, with superposition of the above orders, also appears as a possible ground state of the generalized action for BC order in Appendix C

we present in (6.4) our ‘global’ theory for $S = 1/2$ quantum antiferromagnets in two dimensions. The phases and phase transitions in Section VI are generalizable to other lattices with non-collinear spin correlations *e.g.* the triangular lattice. Also, although we will only explicitly consider the square lattice antiferromagnet in this paper, all our results can also be applied to other two-dimensional, bipartite lattices, like the honeycomb lattice.

Apart from the HN state, states which will play a central role in our considerations are those with bond-centered charge order (BC order); these states have been argued^{3–5} to be generically contiguous to the HN state, and we will also find this here. See Refs. 6,7, and references therein, for recent numerical evidence for BC order in systems like (1.1). The BC states are characterized by spontaneous spatial modulations in the expectation values of the bond fields

$$Q_{ij} = \hat{\mathbf{S}}_i \cdot \hat{\mathbf{S}}_j, \quad (1.3)$$

where i, j are on nearest neighbor sites. Modulations in Q_{ij} will lead to corresponding modulations in other spin-singlet, charge-conserving observables, including the charge density associated with the orbitals that reside on the link (i, j) (in the cuprates, this is the location of the O ions). In the simplest cases, the modulation doubles the unit cell, with the largest values of $\langle Q_{ij} \rangle$ residing either in parallel columns (also referred to as a spin-Peierls state) or in disjoint plaquettes (see Fig 1).

This paper will address the nature of the quantum critical points the system must encounter in evolving from the HN to a BC state. On the basis of numerical analysis of the square lattice antiferromagnet with first and second neighbor exchange interactions, Sushkov, Oitmaa, and Zheng⁶ have proposed that this evolution occurs via

an intermediate phase with co-existence of the two order parameters *i.e.* there is first a dimerization transition from the HN state to a state with co-existing Néel and bond-charge orders (the HN+BC state; see Table I for our convention for identifying ground states), and then a second transition to the BC state where spin rotation invariance is restored. (Such a scenario was also mentioned in the early work of Ref. 4.) As is discussed at length below, we shall find a number of situations in which our field theories display precisely this sequence of transitions. The other possibility, which general field theoretic considerations can never rule out, is a direct first-order transition from the HN to the BC state. We will not find any clear-cut scenario for a generic (*i.e.* not multicritical) second order transition between the HN and BC states, but cannot definitively rule out the possibility that such a transition exists (further discussion of this point is at the end of Section V C 2).

Another class of our main results concerns the issue of spin fractionalization. These will be reviewed below in Section I A. We will find that paramagnetic fractionalized states (F in the notation of Table I) are not connected by a second-order phase boundary to the HN state in the SU(2) symmetric H . In contrast, in spin systems with a reduced, easy-plane U(1) symmetry, there can be a second-order transition between the XY and F states^{8–10}.

We introduce the computations of this paper by recalling some essential facts about quantum and thermal fluctuations near the HN state. At long wavelengths, it is accepted that these are well described by the O(3) nonlinear sigma model in 2+1 dimensions¹¹, with the action

$$S_\sigma = \frac{1}{2c\tilde{g}} \int d^2x d\tau [(\partial_\tau \mathbf{n})^2 + c^2(\nabla_x \mathbf{n})^2], \quad (1.4)$$

where x is the continuum spatial co-ordinate, τ is imaginary time, c is the spin-wave velocity, and \tilde{g} is a (dimensionful) coupling constant which controls the strength of quantum fluctuations. The field $\mathbf{n}(x, \tau)$ satisfies $\mathbf{n}^2 = 1$ everywhere in spacetime, and denotes the local orientation, \mathbf{e} , of the short-range Néel order; so

$$\hat{\mathbf{S}}_j \sim \eta_j \mathbf{n}(x_j, \tau). \quad (1.5)$$

However, as the value of N_0 decreases with increasing \tilde{g} , the action S_σ ceases to be a complete description of the underlying antiferromagnet H . The essential missing ingredients are residual Berry phases associated with the precession of the lattice spins¹². These appear in the coherent state path integral representation of the quantum spin Hamiltonian H in (1.1); they do not have an obvious continuum limit, and to specify them, we have to return to a lattice regularization of S_σ and its degrees of freedom.

For the spatial co-ordinates, we return to the original square lattice associated with H , while we also discretize the imaginary time direction: consequently, spacetime is replaced by a cubic lattice, on which reside the \mathbf{n}_j degrees of freedom (the label j is now a three-dimensional

| Label | Property |
|-------|---|
| HN | The Hamiltonian is invariant under SU(2) spin rotations, and spin rotation symmetry is broken by (1.2) with $N_0 > 0$ and \mathbf{e} an arbitrary unit vector in spin space. There are two gapless spin-wave excitations. |
| XY | The Hamiltonian has only a U(1) spin rotation symmetry about the z axis (due to the presence of exchange anisotropies), and (1.2) is obeyed with $N_0 > 0$ and \mathbf{e} a unit vector in the x - y plane. There is one gapless spin-wave excitation. |
| I | The Hamiltonian has only a U(1) spin rotation symmetry about the z axis (due to the presence of exchange anisotropies), and (1.2) is obeyed with $N_0 > 0$ an Ising order parameter, and \mathbf{e} a unit vector along the $\pm z$ directions. There are no gapless spin-wave excitations. |
| BC | Lattice space group symmetry is broken by a spontaneous modulation in the values of the bond-centered charge order parameter Q_{ij} defined in (1.3). The simplest patterns, in Fig 1, double the unit cell to two sites. |
| F | The ground state has topological order and fractionalization. There are one or more gapped excitations with spin $S = 1/2$, and also a spinless Z_2 vortex excitation. |
| P | Spin rotation symmetry is broken by a non-collinear, polarization of the spins. There are three gapless spin-wave excitations if the Hamiltonian has full SU(2) symmetry, and only one if the symmetry is U(1). |

TABLE I. We identify states by a label which specifies all of the properties from the above list which are satisfied by the state. It is assumed that if a property not contained in a state's label, that state does not satisfy its requirements; so *e.g.* while both the HN and HN+F states obey (1.2), the HN state does not obey property F, while the HN+F state does. Along the same lines, the F state is invariant under spin rotations, as it does not obey properties HN, XY, I, or P.

cubic lattice index, rather than a two-dimensional index in (1.1)—the interpretation of j should usually be clear from the context). On this cubic lattice, the Berry phase term in the partition function is e^{-S_B} with

$$S_B = i \sum_j \eta_j \mathcal{A}_{j\tau}, \quad (1.6)$$

where, as before, $\eta_j = 1$ on one of the square sublattices and $\eta_j = -1$ on the other (note η_j is independent of τ), and the leading $i = \sqrt{-1}$. The quantity $\mathcal{A}_{j\mu}$ is defined to be *half* (for $S = 1/2$) the signed area of the spherical triangle formed between \mathbf{n}_j , $\mathbf{n}_{j+\hat{\mu}}$ and \mathbf{n}_0 , with \mathbf{n}_0 an arbitrary reference unit vector (the index μ extends over the spacetime directions x, y, τ). We can choose \mathbf{n}_0 at our convenience, and a convenient choice is usually $\mathbf{n}_0 = (0, 0, 1)$. The explicit expression for half the area, \mathcal{A} , of the spherical triangle bounded by $\mathbf{n}_{1,2,3}$ is¹³

$$e^{i\mathcal{A}} \equiv \frac{1 + \mathbf{n}_1 \cdot \mathbf{n}_2 + \mathbf{n}_2 \cdot \mathbf{n}_3 + \mathbf{n}_3 \cdot \mathbf{n}_1 + i \mathbf{n}_1 \cdot (\mathbf{n}_2 \times \mathbf{n}_3)}{\{2(1 + \mathbf{n}_1 \cdot \mathbf{n}_2)(1 + \mathbf{n}_2 \cdot \mathbf{n}_3)(1 + \mathbf{n}_3 \cdot \mathbf{n}_1)\}^{1/2}}. \quad (1.7)$$

It can be shown from this definition, or more geometrically from the interpretation of \mathcal{A} as a spherical area, that changes in the choice of \mathbf{n}_0 amount to a gauge transformation of the $\mathcal{A}_{j\mu}$, with

$$\mathcal{A}_{j\mu} \rightarrow \mathcal{A}_{j\mu} + \phi_{j+\hat{\mu}} - \phi_j, \quad (1.8)$$

where ϕ_j is half the area of the spherical triangle formed by \mathbf{n}_j and the old and new choices for \mathbf{n}_0 . It is easily seen that (1.6) is invariant under (1.8) provided we choose periodic boundary conditions in the τ direction—this we will always do. As a companion to S_B , we also write down the continuum S_σ in (1.4) on the same hypercubic lattice:

$$S_{\mathbf{n}} = -\frac{1}{g} \sum_{j, \hat{\mu}} \mathbf{n}_j \cdot \mathbf{n}_{j+\hat{\mu}} \quad (1.9)$$

where the $\hat{\mu}$ are vectors of length equal to the lattice spacing, and extending over the x, y , and τ directions. The dimensionless coupling constant g is proportional to \tilde{g} , while c has been absorbed by the choice of the temporal lattice spacing. For the above discretizations to be meaningful representations of the underlying antiferromagnet, we exclude values of g so large that the \mathbf{n} correlation length is of order a lattice spacing or smaller.

In the analogous formulation of *one*-dimensional antiferromagnets¹², a natural continuum representation of the Berry phase term does exist. A careful examination of S_B for smooth configurations of \mathbf{n}_j shows that it can be written as

$$S_\theta = \frac{i\theta}{4\pi} \int dx d\tau \mathbf{n} \cdot \left(\frac{\partial \mathbf{n}}{\partial \tau} \times \frac{\partial \mathbf{n}}{\partial x} \right) \quad (1.10)$$

with $\theta = \pi$. This is a topological term, and the continuum theory $S_\sigma + S_\theta$ (the integral in (1.4) now extends

over one spatial dimension) was used by Haldane to argue for the fundamental distinction between integer and half-integer spin chains. While the continuum theory has been valuable in establishing this distinction, very little information on the physics at $\theta = \pi$ has been obtained directly from the continuum functional integral of $S_\sigma + S_\theta$. Rather, the most efficient approach has been to refer back to the lattice $S=1/2$ spin chains, and to analyze them by the methods of abelian bosonization. This paper will perform a direct analysis of the lattice actions $S_{\mathbf{n}} + S_B$, in both spatial dimensions $d = 1$ and $d = 2$. We will use parallel methods in the two cases, and the comparison with the known bosonization results in $d = 1$ will act as a significant consistency check of our conclusions.

Although it is not essential, it is convenient to introduce another term in the final form lattice action we shall study—this has the advantage of yielding an independent dimensionless coupling constant (in addition to g) which can be used to explore a potentially richer phase diagram. We wish to write down a term associated with the gauge potential $\mathcal{A}_{j\mu}$. Any such term must clearly be invariant under the gauge transformation (1.8). Further, as only the values of \mathbf{n}_j are observable, (1.7) indicates that the term should be periodic under $\mathcal{A}_{j\mu} \rightarrow \mathcal{A}_{j\mu} + 2\pi$. These requirements strongly constrain the allowed terms, and the simplest permissible one is

$$S'_A = -\frac{1}{e^2} \sum_{\square} \cos(\epsilon_{\mu\nu\lambda} \Delta_\nu \mathcal{A}_{j\lambda}). \quad (1.11)$$

This term is written in notation standard in lattice gauge theory: the sum over \square extends over all plaquettes of the cubic lattice, the indices μ, ν, λ extend over the x, y, τ directions. The symbol Δ_μ represents a discrete lattice derivative ($\Delta_\mu f_j \equiv f_{j+\hat{\mu}} - f_j$), and so S_A depends on the \mathcal{A} flux threading each plaquette. In principle, we should allow for different coupling constants associated with fluxes in the spatial and temporal directions, but we have chosen them equal for convenience. As we will discuss shortly, an important tool in our analysis is a dual lattice representation of (1.11). It is somewhat more convenient to perform this in a “Villain representation” of (1.11), which replaces the exponential of a cosine by a periodic sum over gaussians. So we shall replace S'_A by

$$S_A = \frac{1}{2e^2} \sum_{\square} (\epsilon_{\mu\nu\lambda} \Delta_\nu \mathcal{A}_{j\lambda} - 2\pi q_{j\mu})^2, \quad (1.12)$$

where $q_{j\mu}$ is an integer-valued vector field on the sites, j , of the dual cubic lattice; q couples to the \mathcal{A} flux on the plaquette it pierces. It is also clear that S_A becomes singular as $e^2 \rightarrow 0$, and we shall therefore exclude this limit from our considerations; we are primarily interested in moderately large values of e^2 , where the connection to Heisenberg antiferromagnets is evident. However, the limit $e^2 \rightarrow \infty$ is not expected to be singular, and the properties at $e^2 = \infty$ should be smoothly connected to those for large e^2 .

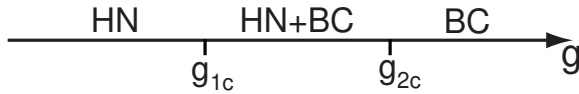


FIG. 2. Proposed phase diagram of the model Z in (1.13) as a function of g for a range of e^2 . The transition at $g = g_{1c}$ involves onset of BC order like that in Fig 1: this is in the universality class of the 2+1 dimensional Z_4 clock model, which is in turn described by the φ^4 field theory with $O(2)$ symmetry. The HN order vanishes at $g = g_{2c} > g_{1c}$ with a transition described by the 2+1 dimensional φ^4 field theory with $O(3)$ symmetry. A direct first order transition between the HN and BC phases is also possible. We have not find any clear-cut scenario for a direct second order transition between the HN and BC states, but cannot definitively rule out the possibility that such a transition exists for some values of e^2 (further discussion of this point is at the end of Section V C 2).

It is useful to collect all the terms introduced so far. One of the central purposes of this paper is to understand the phase diagram of the partition function

$$Z = \sum_{\{q_{j\mu}\}} \int \prod_j d\mathbf{n}_j \delta(\mathbf{n}_j^2 - 1) \exp(-S_{\mathbf{n}} - S_A - S_B) \quad (1.13)$$

in the plane of the coupling constants g and e^2 . Z constitutes a “minimal model” for a theory of $S = 1/2$ quantum antiferromagnets in two dimensions: it incorporates the essential ingredients—quantum fluctuations of the short-range Néel order represented by the non-linear sigma model plus the Berry phases accounting for the quantization of spin. This model, and the duality methods we shall employ, are closely related to those introduced in Ref. 4; see also Appendix A where we introduce an alternative formulation of Z using fields in CP^1 —this formulation is more convenient for some purposes, and is closer to the approach of Ref. 4. The presence of the complex Berry phases associated with S_B means that a Monte Carlo evaluation of Z will not be straightforward; nevertheless, we hope that such evaluations will be attempted by experts in the future. Our strategy will be to employ a variety of duality and field-theoretic techniques to delineate the phase diagram of Z . We will present strong arguments that only phases with HN and BC order appear in this phase diagram, and that there are no states with spin fractionalization in the $SU(2)$ symmetric Z . (see also Section IA below). A likely scenario for the sequence of phases as a function of increasing g is HN, HN+BC, BC, for all non-zero values of e^2 , as shown in Fig 2.

As we have already indicated, the connection of our models with the successful theory of one-dimensional antiferromagnets will be an important guide to our analysis. For these systems, a complete understanding of the physics was achieved by considering the phase diagram in a wider space: the spin-symmetry was reduced to $U(1)$ by introducing an easy-plane or easy-axis anisotropy,

and the phase diagram was studied as a function of the strength of the anisotropy. After mapping to continuum field theories by abelian bosonization methods applicable for systems with only a $U(1)$ symmetry, it was found that one could nevertheless identify lines in the parameter space of the field theories where the Heisenberg $SU(2)$ symmetry was restored. Thus one achieved an understanding of $SU(2)$ symmetric antiferromagnets by completely exploring the phase diagram of less-symmetric, and simpler, systems. A similar strategy will be an important ingredient in our arsenal here: we will reduce the symmetry in the \mathbf{n} space to $U(1)$, by introducing exchange anisotropy in $S_{\mathbf{n}}$ and so deforming Z to $Z_{U(1)}$ (the explicit form is below in (1.15)). We find then that duality transforms of $Z_{U(1)}$ can be carried through to completion. This yields models which we will study by mappings to continuum field theories in 2+1 dimensions which are amenable to standard renormalization group analyses. We will then search for lines in the parameter space of these dual models at which $SU(2)$ symmetry is present; the properties of such lines will allow us to reach important conclusions about the $SU(2)$ symmetric partition function Z .

A. Fractionalization

Much attention has focused on ground states of two-dimensional antiferromagnets with an “order” quite distinct from those discussed so far. These are states with fractionalized spin excitations (spin $S = 1/2$) and associated topological, spin-singlet, excitations. States with this property are denoted by F, see Table I). In a theory^{14–18} of paramagnetic F states in systems with $SU(2)$ symmetry, fractionalization was linked with non-collinear spin correlations¹⁹. In particular, restoring spin rotation invariance in a state with long-range, non-collinear, magnetic order (a P state, see Table I) by a second-order quantum phase transition led naturally to a paramagnetic F state. Such P states are not expected to appear in the model Z in (1.13), and so the theory of Ref. 14 leads to the conclusion that the $SU(2)$ symmetric Z does not contain the F state either. Our results here will support this conclusion.

As already noted above, we will also study a deformation of Z to anisotropic spin models, $Z_{U(1)}$ with only a $U(1)$ spin symmetry. For easy-plane anisotropy, this will deform the HN state into the XY state (see Table I). In such a situation, the \mathbf{n}_j field will fluctuate primarily in the x - y plane in spin space, and it is therefore useful to parameterize in terms of an angular variable θ_j by

$$\mathbf{n}_j = (\cos \theta_j, \sin \theta_j, 0). \quad (1.14)$$

We will show in Sections IV B and V that in such an easy-plane limit, the model Z in (1.13) is equivalent to the following XY model coupled to a Z_2 gauge theory in 2+1 dimensions:

$$Z_{U(1)} = \sum_{\{s_{j,j+\hat{\mu}}=\pm 1\}} \int \prod_j d\theta_j \exp \left(K \sum_{\square} \prod_{\square} s_{j,j+\hat{\mu}} + \frac{4}{g} \sum_{j,\hat{\mu}} s_{j,j+\hat{\mu}} \cos \left(\frac{\Delta_{\mu}\theta_j}{2} \right) - i \frac{\pi}{2} \sum_j (1 - s_{j,j+\hat{\tau}}) \right), \quad (1.15)$$

with the coupling K is related to e^2 by (4.11); actually the precise equivalence is to a model in which the cosine in (1.15) is replaced a periodic Gaussian-Villain form, as in (4.10). The Z_2 gauge field $s_{j,j+\hat{\mu}}$ resides on the links of the direct lattice; apart from the usual Maxwell term, it also carries the last Berry phase term which is the remnant of S_B in (1.6). Models closely related to (1.15) have recently been studied by Senthil and Fisher and collaborators⁸⁻¹⁰: we have thus established a surprising connection between their work and the easy-plane limit of model Z of Ref. 4 and the present paper.

We make a brief aside to place the work of Senthil and Fisher in the context of the models being studied here: their work has shed new light on subject of fractionalization in spin systems with U(1) symmetry. In their first paper⁸, Senthil and Fisher considered a model with charge fluctuations and SU(2) spin symmetry, but examined fractionalization of the Cooper pairs associated with superfluid order and the U(1) charge symmetry. Alternatively, we could replace the Cooper pair bosons by the hard-core bosons associated with S=1/2 spin systems (with the spin raising operators $S^+ = b^\dagger \sim e^{i\theta}$, the operator creating the hard-core boson (see (4.21) later)), and transcribe their results to quantum spin systems with only a U(1) symmetry. Precisely such a point of view was taken in Section II of Ref. 10.

Our analysis of $Z_{U(1)}$ will follow and generalize the framework laid by these studies of Z_2 gauge theories. Duality transformations of the model $Z_{U(1)}$ show that, unlike Z , $Z_{U(1)}$ does indeed contain a paramagnetic F state in two dimensions; further, it appears possible to directly connect the XY and F states by a second-order quantum phase transition. The appearance of these F phases is intimately linked to the half-angle variable appearing as the argument of the cosine term in (1.15); indeed $e^{i\theta/2}$ is the ‘square root’ of the $S_z = 1$ spin-flip boson b^\dagger , and so the former is the creation operator a $S_z = 1/2$ spinon. For large K and large g , the fluctuations of the Z_2 gauge field $s_{j,j+\hat{\mu}}$ and the XY order will both be suppressed, and this will introduce a paramagnetic F state in which such spinons can propagate freely by the $1/g$ term in (1.15).

Our main interest here is in spin systems with SU(2) symmetry, and so in Sections IV B 2 and V C we will consider a wide class of generalizations of $Z_{U(1)}$ in the hope of identifying special regimes of parameter space where the full SU(2) symmetry may be restored. Our search for such spaces for enhanced symmetry will be successful: one of our main findings will be that such F states do not survive the restoration of SU(2) symmetry. Along with other reasons to be discussed in Sections II and III,

this leads to our conclusion that the SU(2) symmetric Z in (1.13) does not contain any fractionalized states. Similar reasoning will also allow us to conclude that the HN and F states cannot be separated by a single, second-order quantum critical point, in contrast to that found in $Z_{U(1)}$ between the XY and F states.

To further clarify the issues of fractionalization in systems with SU(2) symmetry, we will introduce a distinct lattice model, Z_P , in Section VI. This model generalizes Z to explicitly allow for a non-collinear, magnetically ordered state (a P state). We will argue that it also contains an F state, and discuss the structure of the phase diagram of Z_P . This will allow us to delineate the routes by which it is possible to connect states with HN, BC, and/or F order in systems with full SU(2) spin symmetry. We expect the conclusions in this section to be rather general, and apply to a wide class of SU(2) symmetric models with phases characterized as in Table I.

B. Outline

This is a lengthy paper, and so it is helpful for the reader to have an overview of the logical relationships between the sections at the outset. We will begin in Section II by a direct assault on the SU(2) invariant partition function Z in (1.13). We will argue that BC order appears at large g and then proceed in Section III to a discussion of how the system interpolates between the small g HN phase and the large g BC phase. We will present a number of arguments based upon the statistical mechanics of defects in the φ^4 field theory in 3 spacetime dimensions that support the proposal of an intermediate phase with co-existing HN and BC order. The next two sections take the reader on a long detour. In Section IV we turn our attention to one dimensional antiferromagnets and allow for the system to acquire a uniaxial anisotropy and a reduced U(1) symmetry. For such systems, we are able to develop rather precise duality methods which completely account for the defects and their Berry phases; we are also able to restore SU(2) symmetry along special lines in parameter space. The results obtained in this manner are found to be in excellent accord with those obtained earlier by bosonization methods. Emboldened by this success, we proceed with the application of the same methods in two dimensions in Section V. The main results again support the co-existence of HN and BC order in the SU(2) invariant systems, in agreement with Section III. Finally, in Section VI we return to the main road, and focus direct attention on SU(2) invariant antiferromagnets in two dimensions. We introduce a generalization of Z , denoted Z_P , which explicitly accounts for non-collinear spin correlations expected in frustrated antiferromagnets. This model does contain paramagnetic fractionalized phases, and we present phase diagrams which describe competition between HN, BC, and F orders.

II. DUALITY AND BOND ORDER

The model Z in (1.13) has a clear association with the HN state: in the limit of small g , the coupling in $S_{\mathbf{n}}$ prefers that all the \mathbf{n}_j align along a common direction in spin space, and this leads to a ground state with HN order, as in (1.2). This section will introduce a duality transformation of Z which demonstrates its intimate connection with BC states. We will argue that BC order appears for large g in the $SU(2)$ -symmetric Z . We will also indicate why there is no such requirement for $Z_{U(1)}$.

This first step in the duality transformation, as usual, is to rewrite (1.12) by the Poisson summation formula:

$$\sum_{\{q_{\bar{j}\mu}\}} e^{-S_{\mathcal{A}}} = \sum_{\{a_{\bar{j}\mu}\}} \exp\left(-\frac{e^2}{2} \sum_{\bar{j}} a_{\bar{j}\mu}^2 - i \sum_{\square} \epsilon_{\mu\nu\lambda} a_{\bar{j}\mu} \Delta_{\nu} \mathcal{A}_{j\lambda}\right), \quad (2.1)$$

where $a_{\bar{j}\mu}$ (like $q_{\bar{j}\mu}$) is an integer-valued vector field on the links of the dual lattice. Here, and henceforth, we drop overall normalization constants in front of partition functions. The last term in (2.1) has the structure of a ‘Chern-Simons’ coupling, and connects $a_{\bar{j}\mu}$ to the \mathcal{A} flux on the plaquette of the direct lattice that it pierces.

Next, we write S_B in a form more amenable to duality transformations. Choose a ‘background’ $a_{\bar{j}\mu} = a_{\bar{j}}^0$ flux which satisfies

$$\epsilon_{\mu\nu\lambda} \Delta_{\nu} a_{\bar{j}\lambda}^0 = \eta_j \delta_{\mu\tau}, \quad (2.2)$$

where j is the direct lattice site in the center of the plaquette defined by the curl on the left-hand-side. Any integer-valued solution of (2.2) is an acceptable choice for $a_{\bar{j}\mu}^0$, and a convenient choice is shown in Fig 3. With (2.2), the Berry phase term also takes the form of Chern-Simons coupling:

$$S_B = i \sum_{\square} \epsilon_{\mu\nu\lambda} a_{\bar{j}\mu}^0 \Delta_{\nu} \mathcal{A}_{j\lambda} \quad (2.3)$$

We can now combine (2.1) and (2.3) and, after a shift of $a_{\bar{j}\mu}$ by $a_{\bar{j}\mu}^0$, obtain a new exact representation of Z :

$$Z = \sum_{\{a_{\bar{j}\mu}\}} \int \prod_j d\mathbf{n}_j \delta(\mathbf{n}_j^2 - 1) \exp\left(-S_{\mathbf{n}} - S_a - i \sum_{\square} \epsilon_{\mu\nu\lambda} a_{\bar{j}\mu} \Delta_{\nu} \mathcal{A}_{j\lambda}\right), \quad (2.4)$$

where

$$S_a = \frac{e^2}{2} \sum_{\bar{j}, \mu} (a_{\bar{j}\mu} - a_{\bar{j}\mu}^0)^2. \quad (2.5)$$

The structure of this representation of Z also allows us to give a simple physical interpretation of $a_{\bar{j}\mu}$. The quantity

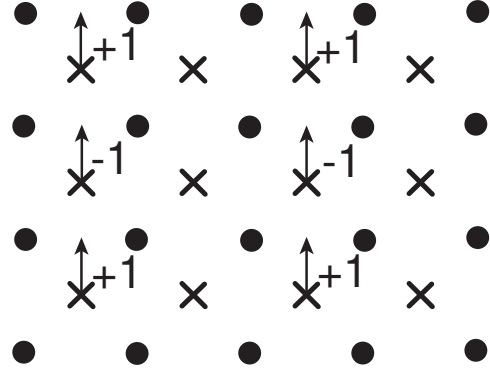


FIG. 3. Specification of the non-zero values of the fixed field $a_{\bar{j}\mu}^0$. The circles are the sites of the direct lattice, j , while the crosses are the sites of the dual lattice, \bar{j} ; the latter are also offset by half a lattice spacing in the direction out of the paper (the $\mu = \tau$ direction). The $a_{\bar{j}\mu}^0$ are all zero for $\mu = \tau, x$, while the only non-zero values of $a_{\bar{j}\mu}^0$ are shown above. Notice that the a^0 flux obeys (2.2).

$(a_{\bar{j}\mu} - a_{\bar{j}\mu}^0)^2$ for $\mu = x, y$ is a term in action associated with a spatial link on the dual lattice, and is therefore surely associated with a measure of the energy of the bond on the direct lattice which intersects it. We may therefore identify the bond variable in (1.3) as

$$Q_{j, j+\hat{x}} \sim (a_{\bar{j}y} - a_{\bar{j}y}^0)^2, \quad (2.6)$$

where the direct lattice link on the left-hand-side intersects the dual lattice link on the right-hand-side. A similar relation holds for $x \leftrightarrow y$.

We have now assembled the ingredients necessary to address the physics of the large g regime. Here the \mathbf{n} field will fluctuate strongly, and so it appears natural to integrate it out. To do this, we need to evaluate the average

$$W(a_{\mu}) \equiv \left\langle \exp\left(-i \sum_{\square} \epsilon_{\mu\nu\lambda} a_{\bar{j}\mu} \Delta_{\nu} \mathcal{A}_{j\lambda}\right) \right\rangle_{S_{\mathbf{n}}}; \quad (2.7)$$

In terms of $W(a_{\mu})$, the partition function is

$$Z = \sum_{\{a_{\bar{j}\mu}\}} W(a_{\mu}) \exp(-S_a). \quad (2.8)$$

Strong fluctuations in \mathbf{n} will lead to concomitant fluctuations in the flux $\epsilon_{\mu\nu\lambda} \Delta_{\nu} \mathcal{A}_{j\lambda}$ over all real values between 0 and 2π . This means that the average in (2.7) will be strongly dominated by configurations in $a_{\bar{j}\mu}$ which obey

$$\epsilon_{\mu\nu\lambda} \Delta_{\nu} a_{\bar{j}\lambda} = 0. \quad (2.9)$$

In other words, the large g region is in a ‘ a -Meissner’ phase which expels the flux of $a_{\bar{j}\mu}$. We will restrict attention to $a_{\bar{j}\mu}$ configurations which satisfy (2.9) in most of the remainder of this section. A more careful discussion of the origin of (2.9) is given in Appendix B; there

we show that the configurations which violate (2.9) lead mainly to a renormalization of the coupling constant e in S_a . The discussion in Appendix B also shows that the analysis of this section also applies to models which a bare value $e = \infty$; the renormalized e appearing in S_a is finite even in that case.

This is also a convenient point to make a brief aside on systems with an easy-plane anisotropy, and a reduced $U(1)$ symmetry. Here \mathbf{n} lies in the x - y plane as indicated in (1.14), and the flux $\epsilon_{\mu\nu\lambda}\Delta_\nu\mathcal{A}_{j\lambda}$ on any plaquette is typically zero. Only if plaquette happens to contain a *vortex* in the angle θ is the flux non-zero, and then it takes the *discrete* values $\pm\pi$ (half the area of a hemisphere). More generally, allowing for multiple vortices, the allowed values of the flux $\epsilon_{\mu\nu\lambda}\Delta_\nu\mathcal{A}_{j\lambda}$ are $m\pi$ with m integer. In the large g region, we can assume that there were be strong fluctuations in the value of m in the plaquettes, and so the average in (2.7) will be dominated by configurations in $a_{\bar{j}\mu}$ which satisfy

$$\epsilon_{\mu\nu\lambda}\Delta_\nu a_{\bar{j}\lambda} = 0 \pmod{2}, \quad (2.10)$$

and the flux of $a_{\bar{j}\mu}$ is only expelled modulo 2. The difference between (2.9) and (2.10) is the key reason from the strong distinction between the properties of $SU(2)$ and $U(1)$ symmetric spin systems. We will show in Section V A that the partition function (2.8), when evaluated under the constraint (2.10), reduces exactly to an Ising model on the cubic lattice in $D = 3$ dimensions, with the signs of the couplings chosen so that every spatial plaquette is frustrated; this Ising model is dual to the Ising gauge theory plus Berry phases obtained in the large g limit of (1.15). Precisely the same Ising model was considered in Refs. 16,18 in a context somewhat different from the present, but closely related to the models of frustrated antiferromagnets to be considered in Section VI. We can also already notice here that double vortices (with $m = \pm 2$) don't couple at all to fluctuations in $a_{\bar{j}\mu}$, and so can selectively proliferate for large g : this is the effect responsible for appearance of F states in $Z_{U(1)}$.

Returning to $SU(2)$ -invariant systems, and the a -Meissner phase obeying (2.9), we can solve the constraint by writing

$$a_{\bar{j}\mu} = \Delta_\mu h_{\bar{j}} \quad (2.11)$$

where $h_{\bar{j}}$ is a ‘‘height’’ on the sites of the dual lattice. The partition function Z is now equivalent to the three-dimensional height-model partition function

$$Z_h = \sum_{\{h_{\bar{j}}\}} \exp\left(-\frac{e^2}{2} \sum_{\bar{j}} (\Delta_\mu h_{\bar{j}} - a_{\bar{j}\mu}^0)^2\right). \quad (2.12)$$

The model Z_h has been studied previously on a number of occasions^{5,22–24} and we now state the main results. The most important property of Z_h is that the heights are in a *smooth* phase for all values of e ; in other words,

any state of Z_h has a definite value for its average height $\langle h_{\bar{j}} \rangle$, where the average is over both quantum fluctuations and over sites of the dual lattice—this is a generic property of height models in three dimensions. Furthermore, the combination of the background $a_{\bar{j}\mu}^0$ terms in (2.12) and the existence of an average height implies that the translational symmetry will be broken by a modulation in the Q_{ij} in (2.6). In other words, the ground state of Z_h has BC order.

A review of the prior analyses of Z_h which led to the above results is provided in Appendix C. There, we also establish the close connection between Z_h and a number of other models for quantum paramagnets that have appeared in the literature. In particular, there is a simple and direct connection between Z_h and the ‘‘quantum dimer’’ model^{25,26}. Furthermore, Z_h can also be written as a Coulomb gas of point instanton charges, each of which carries a Berry phase: these instantons are nothing but ‘hedgehog’ defects in the \mathbf{n} field, and the Berry phases implied by Z_h are precisely equal to the hedgehog Berry phases computed by Haldane²⁷. Finally, Z_h can also be written as a frustrated sine-Gordon model. This last form is the most useful in determining the ground states of Z_h . This simplest state which emerges is the 4-fold degenerate columnar BC state shown in Fig 1a. However, within the generalized parameter space of the sine-Gordon model we also find²⁴ the 4-fold degenerate plaquette ground state of Fig 1b, and an 8-fold degenerate states involving co-existence of the orders in Fig 1a and b. The symbol BC refers collectively to any one of these states; an antiferromagnet could also have quantum phase transitions between different BC states—these transitions can also be discussed easily within the framework of the frustrated sine-Gordon model²⁴, but we will not dwell on them here.

III. CONNECTING THE NÉEL AND BOND ORDER STATES

We have so far examined the phases of the $SU(2)$ symmetric model Z (Eqn (1.13)) in the limits of small and large g . For small g we have the HN state with broken spin rotation symmetry, while for large g we have $SU(2)$ symmetric ground states with BC order. This section will comment on the evolution of the ground state as g moves between these two limits. Our analysis will focus of the behavior of the function $W(a_\mu)$ in (2.7) as a function of g : this will permit us to study the influence of the HN order parameter \mathbf{n} on the fluctuations of the $a_{\bar{j}\mu}$ which control the BC order. We will begin in Section III A with limit of small g , where \mathbf{n} fluctuations can be computed in the spin-wave approximation. Next, in Section III B, we will consider the point where \mathbf{n} fluctuations are critical *i.e.* at the point where $SU(2)$ symmetry is broken, and describe the associated structure of $W(a_\mu)$. The critical point is a strongly coupled theory in three spacetime

dimensions, and so our arguments here do have ad hoc steps which are based mainly on physical arguments.

A. Spin wave expansion

First, we describe the small g spin-wave expansion. Here, we assume $\langle \mathbf{n} \rangle = N_0(0, 0, 1)$. We perform the familiar spin-wave expansion of the non-linear sigma model by parameterizing $\mathbf{n} = (\pi_x, \pi_y, \sqrt{1 - \pi_x^2 - \pi_y^2})$ and expanding the action, including the expressions for $\mathcal{A}_{j\mu}$ in powers of π_x, π_y . Integrating out the π_x, π_y fluctuations to lowest order in g we obtain

$$\begin{aligned} W(a_\mu) &= \exp(-S_{sw}(a_\mu)) \\ S_{sw}(a_\mu) &= \frac{g}{8} \sum_{i,j,\mu,\nu} (\epsilon_{\mu\rho\sigma} \Delta_\rho a_\sigma)_i (\epsilon_{\nu\lambda\gamma} \Delta_\lambda a_\gamma)_j \\ &\times [G(i-j)G(i-j+\hat{\mu}-\hat{\nu}) - G(i-j+\hat{\mu})G(i-j-\hat{\nu})] \\ G(j) &= \int_{-\pi}^{\pi} \frac{d^3k}{8\pi^3} \frac{g e^{ik \cdot j} / 2}{3 - \cos k_x - \cos k_y - \cos k_z} \quad (3.1) \end{aligned}$$

We now need to study the $a_{j\mu}$ fluctuations, as controlled by the action $S_a + S_{sw}$, to determine the fate of the bond order in this framework. A closely related action was numerically simulated earlier in Ref. 4, with an action in which the double summation in S_{sw} over i and j was replaced with a single summation over the on-site term with $i = j$, and $\mu = \nu$. Numerical evaluation of the expression for G in (3.1) shows that this on-site term is over 10 times larger than the off-site terms, and so the truncation involved in mapping to the model of Ref. 4 is reasonable. The primary result of Ref. 4, which we expect to apply to the full action in (3.1), was that there is a critical value of g above which there is an onset of BC order. However, the present small g expansion does not allow us to determine if this onset occurs in a regime where the small g spin-wave expansion about the HN state is valid. If the transition in $S_a + S_{sw}$ occurs in its regime of applicability, then the ground state has HN+BC order beyond the critical point. So the structure of the spin-wave expansion in powers of g is compatible with both the HN and HN+BC states, but does not allow us to definitively conclude that the HN+BC state must exist.

B. Critical φ^4 field theory

To study the competition between the HN and BC states further, we imagine turning up the value of g to the critical point where SU(2) symmetry is first restored, and N_0 vanishes. This section will make the assumption that the fluctuations of \mathbf{n} at this critical point are described by the field theory associated with the critical point in $S_{\mathbf{n}}$ itself *i.e.* the 3-component φ^4 field theory in 2+1 dimensions with O(3) symmetry. We will argue, by an evaluation of $W(a_\mu)$ at the critical point of the φ^4 field

theory, that this assumption is justified only if HN order vanishes at a transition between the HN+BC and BC states. In other words, we will find that a critical point described by the 3-component φ^4 field theory has finite, non-critical BC order. The alert reader will notice that these arguments do not logically exclude the possibility that there is some other unknown critical field theory describing the vanishing of HN order, and which describes a second-order phase transition between the HN and BC states; however, we will not find any likely candidates for such a critical theory here.

To evaluate $W(a_\mu)$ we need some understanding of the fluctuations of the \mathcal{A} flux. As we saw in the large g theory in Section II, these are controlled by the fluctuations of the hedgehog point-defects in the \mathbf{n} fluctuations. So as a first step, we should determine the correlations of the hedgehogs at the critical point of the φ^4 field theory. We will be able to make a number of statements about these correlations in an expansion in $\epsilon = 4 - D$ (where D is the dimensionality of spacetime) by an extension of methods developed by Halperin²⁸ some time ago, which are described in Appendix D. We begin by outlining the physical ideas behind our analysis, and will then apply them to the computation of $W(a_\mu)$.

It is useful to first contrast the critical behavior of the hedgehogs with a well-known and familiar example: vortices in the $D = 2$ XY model which exhibit the Kosterlitz-Thouless (KT) transition. Imagine we are examining a model with a short-distance momentum cutoff, Λ . Let the mean density of vortices be $\bar{\rho}_v$, and a dimensionless measure of this is $\bar{\rho}_v \Lambda^{-2}$. Now we perform an RG transformation, integrating out tightly-bound dipoles of vortices, and gradually reduce the value of Λ . It is known that at the KT critical point the vortex fugacity ultimately flows to zero; in other words, as we scale Λ to smaller values, the dimensionless vortex density, $\bar{\rho}_v \Lambda^{-2}$, ultimately scales to zero. This is the precise form of the statement that there are no free vortices at the KT critical point. The behavior of the density of hedgehogs, $\bar{\rho}_h$, at the critical point of the $D = 3$ O(3) model is known^{28,29} to be dramatically different: $\bar{\rho}_h \Lambda^{-3}$ remains a finite number of order unity even after RG scaling to the longest scales. So, loosely speaking, there is finite density of “free” hedgehogs at the critical point. We will compute correlations of this critical ensemble of defects of below. Our main physical observation will be that these critical decay correlations decay sufficiently rapidly (see (3.6) and (3.7) below) that there is little material difference from the corresponding correlations in the paramagnetic phase. The consequences of the latter correlations were explored earlier in the large g theory: we saw in Section II that they led to BC order in the paramagnetic phase. So it is reasonable to conclude that finite BC order is also present at the critical point of the HN order.

Let us now describe the correlations of the hedgehogs at the critical point of the O(3) φ^4 field theory in 2+1 dimensions. Let $\rho_h(r)$ be the topological charge density

operator of hedgehogs at the spacetime point r (so $\bar{\rho}_h = \langle |\rho_h(r)| \rangle$). We consider first the two-point correlator

$$C_h(r) = \langle \rho_h(r) \rho_h(0) \rangle \quad (3.2)$$

The topological character of the $\rho_h(r)$, and its association with a continuum field $\varphi(r)$ implies that this correlator obeys an overall charge neutrality condition

$$\int d^3r C_h(r) = 0. \quad (3.3)$$

We explicitly evaluate $C_h(r)$ in an expansion in $\epsilon = 4 - D$ in Appendix D. The topological character is special to $D = 3$, and so the constraints of the conservation law (3.3) are not reflected in this computation. We find that the long-distance decay of $C_h(r)$ is controlled by the scaling dimension

$$\dim[\rho_h(r)] \equiv (9 + \eta_h)/2 \quad (3.4)$$

where η_h has the ϵ expansion

$$\begin{aligned} \eta_h &= 3\eta + \mathcal{O}(\epsilon^3) \\ &= \frac{15}{242}\epsilon^2 + \mathcal{O}(\epsilon^3), \end{aligned} \quad (3.5)$$

where η is the anomalous dimension of the field φ . This scaling dimension implies that C_h has the long distance behavior

$$C_h(r \rightarrow \infty) \sim \frac{1}{|r|^{9+\eta_h}}, \quad (3.6)$$

One might question the applicability of such an expansion to $D = 3$, given the neglect of the conservation law (3.3) to all orders in the ϵ expansion. Indeed, if (3.3) was obeyed by the scaling limit of the field theory, then we would expect $\dim[\rho_h(r)] = 3$, or $\eta_h = -3$. We think this is extremely unlikely, and the more plausible scenario is that the conservation (3.3) is not obeyed by the scaling limit field theory (this is analogous to the appearance of an ‘‘anomaly’’ in a field theory): to properly define the field theory, some consistent short-distance regularization has to be introduced, and this regularized theory does obey (3.3) after including short distance contributions which are beyond the scaling limit. The reason for the presence of the ‘‘anomaly’’ becomes clear after implementing the consequences of (3.3) and (3.6) in momentum space: $C_h(k)$, the Fourier transform of $C_h(r)$, has the following small k expansion

$$C_h(k \rightarrow 0) \sim c_1 k^2 + \dots + c_2 k^{6+\eta_h} + \dots \quad (3.7)$$

where the first set of ellipsis in (3.7) refer to various analytic terms in integer powers k^2 , and $c_{1,2}$ are constants. Even for $\eta_h = -3$, note that the second singular term remains subdominant to the analytic term proportional to c_1 . The latter is controlled by non-universal short-distance effects, and it appears that these are the primary degrees of freedom controlling the conservation of

total topological charge. For the scaling limit theory to be tightly constrained by the conservation law, we would require $c_1 = 0$, something that does not seem likely in general, given its dependence on non-universal features. So we conclude that the critical theory can ignore the conservation law, and the ϵ expansion for η_h remains applicable in $D = 3$. The singular piece of C_h decays very rapidly with r , and the small momentum behavior of C_h is dominated by a non-universal, analytic term with coefficient $c_1 \neq 0$: these are the primary conclusions on the properties of $C_h(r)$ that we will need in our analysis below.

The ϵ expansion also allows computation of higher order correlations of ρ_h . To leading order in ϵ and at small k , we can neglect higher order cumulants in the correlations of ρ_h . So we will assume that the fluctuations of ρ_h are controlled by the distribution controlled only by the second cumulant, which is

$$\exp\left(-\frac{1}{2} \sum_k \frac{|\rho_h(k)|^2}{C_h(k)}\right). \quad (3.8)$$

It now remains to evaluate the distribution of the \mathcal{A} flux associated with the above distribution of ρ_h , and to thence obtain $W(a_\mu)$. Let us define the ‘electromagnetic’ field

$$\mathcal{E}_\mu = \epsilon_{\mu\nu\lambda} \partial_\nu \mathcal{A}_\lambda. \quad (3.9)$$

As we are focusing attention on long-wavelengths here, we have replaced the lattice derivative by a continuum partial derivative. In the presence of a fixed hedgehog density ρ_h , the \mathcal{E} field obeys the ‘Maxwell’ equations of motion

$$\partial_\mu \mathcal{E}_\mu = 2\pi\rho_h \quad \epsilon_{\mu\nu\lambda} \partial_\nu \mathcal{E}_\lambda = 0 \quad (3.10)$$

From these equations, and from (3.8), we can deduce that the distribution of \mathcal{E} is controlled by

$$\exp\left(-\frac{1}{2} \sum_k \frac{k^2 |\mathcal{E}_\mu(k)|^2}{4\pi^2 C_h(k)}\right). \quad (3.11)$$

At this point, it is tempting to compute $W(a_\mu) = \langle e^{ia_\mu \mathcal{E}_\mu} \rangle$ from the distribution (3.11) and to conclude that

$$W(a_\mu) \sim \exp\left(-\frac{1}{2} \sum_k \frac{4\pi^2 C_h(k)}{k^2} |a_\mu(k)|^2\right). \quad (3.12)$$

However, this expression is not invariant under the integer-valued gauge transformations $a_{j\mu} \rightarrow a_{j\mu} - \Delta_\mu \ell_j$ which are respected by the original definition in (2.7). To remedy this, we will have to put (3.11) back on the lattice, and compute the average over \mathcal{E}_μ while respecting the periodicity $\mathcal{A}_{j\mu} \rightarrow \mathcal{A}_{j\mu} + 2\pi$. This we do in the following paragraph. Readers not interested in this technical step may skip ahead to the main result (3.15) which replaces (3.12).

First we decouple the distribution in (3.11) by a Hubbard-Stratonovich field \mathcal{S}_μ

$$\int \mathcal{D}\mathcal{S}_\mu \exp \left(-\frac{1}{2} \sum_k \frac{4\pi^2 C_h(k)}{k^2} |\mathcal{S}_\mu(k)|^2 + i \sum_k \mathcal{E}_\mu(k) \mathcal{S}_\mu(-k) \right). \quad (3.13)$$

Then we restore the proper flux-periodicity in the last term by replacing (3.13) by

$$\sum_{\{q_{\bar{j}\mu}\}} \int \mathcal{D}\mathcal{S}_\mu \exp \left(-\frac{1}{2} \sum_k \frac{4\pi^2 C_h(k)}{k^2} |\mathcal{S}_\mu(k)|^2 + i \sum_{\bar{j}} \mathcal{S}_{\bar{j}\mu} (\epsilon_{\mu\nu\lambda} \Delta_\nu \mathcal{A}_{j\lambda} - 2\pi q_{\bar{j}\mu}) \right). \quad (3.14)$$

We can now evaluate $W(a_\mu)$ with the distribution of \mathcal{A} controlled by (3.14): the sum over $q_{\bar{j}\mu}$ implies that $\mathcal{S}_{\bar{j}\mu}$ must be an integer, while the integral over \mathcal{A} implies that $\mathcal{S}_{\bar{j}\mu} = a_{\bar{j}\mu} - \Delta_\mu h_{\bar{j}\mu}$ where h is integer-valued field on the sites of the dual lattice. From this we obtain our main result,

$$W(a_\mu) \sim \sum_{\{h_{\bar{j}\mu}\}} \exp \left(-\sum_k \frac{2\pi^2 C_h(k)}{k^2} |a_\mu(k) - \Delta_\mu h(k)|^2 \right) \quad (3.15)$$

for $W(a_\mu)$ at the critical point of the $O(3)$ φ^4 field theory. The expression (3.15) modifies (3.12) to allow invariance under integer-valued gauge transformations of the a_μ .

The status of the BC order at this critical point is now controlled by the a_μ fluctuations associated with the distribution $e^{-S_a} W(a_\mu)$. It is surely acceptable to replace C_h in (3.15) by its leading small k expansion in (3.7): $C_h(k) = c_1 k^2$, with $c_1 \neq 0$. Then, the distribution (3.15) for a_μ becomes precisely that in (B4) in Appendix B for the case of the large g limit. Our conclusions here are therefore the same as those in the discussion following (B4): the systems expels a flux, and is in the a -Meissner phase. There is, therefore, *well-developed BC order at the critical point of the $O(3)$ φ^4 model*. The BC order fluctuations are also not critical and this justifies, a posteriori, that the fluctuations of the HN order at the critical point at which N_0 vanishes are described by the $O(3)$ φ^4 model alone.

This section has therefore delineated an explicit route for the destruction of the HN order by second-order quantum transitions, which was sketched in Fig 2. With increasing g , and *before* the HN order vanishes, there is an onset of BC order at $g = g_{1c}$; for BC order of the two types shown in Fig 1, this transition is described by the Z_4 clock model, which is in turn in the universality class of the $O(2)$ φ^4 field theory. For $g > g_{1c}$, the system is in the HN+BC state. At a larger value of $g = g_{2c}$ HN order disappears by a continuous transition described by

the $O(3)$ φ^4 model; the BC order is finite on both sides of this transition, as well as the critical point, and does not play an essential role in its critical theory at g_{2c} .

1. $U(1)$ symmetry

We mention in this subsection the application of the analysis above to systems with only a $U(1)$ spin symmetry. We will consider such models in much detail in Section V using rather more precise methods. So we can test our present approach and see if consistent conclusions are obtained. For $Z_{U(1)}$, as we already noted in Section II, the ‘flux’ $\mathcal{E}_\mu = \epsilon_{\mu\nu\lambda} \Delta_\nu \mathcal{A}_\lambda$ through any plaquette is simply π times the vortex number piercing that plaquette. In other words, we can write $\mathcal{E}_\mu = \pi \mathcal{J}_\mu$, where \mathcal{J}_μ is the vortex current of a 2+1 dimensional XY model. Assuming the latter is described by the critical point of the $O(2)$ φ^4 field theory in 2+1 dimensions, we can compute the correlations of \mathcal{J}_μ by Halperin’s analysis²⁸, as generalized in Appendix D to the critical point. A computation very similar to that leading to (3.7) now yields

$$C_{v,\mu\nu}(k) \equiv \langle \mathcal{J}_\mu(k) \mathcal{J}_\nu(-k) \rangle = (k^2 \delta_\mu - k_\mu k_\nu) (\tilde{c}_1 + \tilde{c}_2 k^{1+\eta_v} + \dots), \quad (3.16)$$

where now we choose to define (see Appendix D) $\dim[\mathcal{J}_\mu(r)] \equiv (6 + \eta_v)/2$. The transverse nature of the right-hand-side is a consequence of the conservation of the vortex current, which is now expressed by the local law

$$\partial_\mu C_{v,\mu\nu} = 0. \quad (3.17)$$

If (3.17) was not violated by an anomaly, then we would expect that $\dim[\mathcal{J}_\mu(r)] = 2$ or $\eta_v = -2$. Inserting the latter value in (3.16) we see that the singular contribution from the scaling theory *dominates* the non-singular piece proportional to \tilde{c}_1 . This is the opposite of the situation in the $SU(2)$ symmetric case considered in the body of this section. In the present case, we do *not* expect an anomaly in the conservation of vortex current as the conservation law is dominated by the scaling theory contributions, and so the result $\eta_v = -2$ should be exact in $D = 3$. Integrating out the \mathcal{J}_μ fluctuations using (3.16) and this value of η_v , we conclude that

$$W(a_\mu) \sim \exp \left(-\frac{\tilde{c}_2}{2} \sum_k \frac{1}{k} a_\mu(-k) (k^2 \delta_\mu - k_\mu k_\nu) a_\nu(k) \right) \quad (3.18)$$

for the case of $Z_{U(1)}$. The strong contrast between (3.18) and (3.15) should be noted. The present result (3.18) is midway between the a -Meissner result (3.15) which expels a_μ flux, and the ‘ a -Maxwell’ result (3.1) which allows penetration of a_μ flux. A more careful analysis is required to understand the consequences of (3.18) and

this will be taken up in Section V. We will find there that the BC order can either present, absent, or critical at the point at which U(1) spin-rotation invariance is restored; the situation depends upon the details of the model being studied. For our purposes here, it is satisfying to note that, unlike the SU(2) case, the present methods do not place the U(1) critical point in the a -Meissner phase, which would have required BC order.

2. Remarks

We conclude this section by a few remarks on SU(2)-invariant systems, motivated by the previous subsection on U(1) symmetry. It is interesting to observe that if the SU(2) symmetric spin system had $C_h(k) \sim k^3$ (the value suggested naively by (3.3)), then its $W(a_\mu)$ would have had a power of k in the exponent which was the same as that in (3.18) for systems with U(1) symmetry; in such a situation one could envisage a direct second order phase transition between the HN and BC phases, as had been conjectured in earlier work by one of us³⁰. We have argued above that this behavior of $W(a_\mu)$ is not present at the critical point described by the O(3) symmetric φ^4 field theory. This paper does not find a clear-cut scenario under which this behavior could arise generically, as we will discuss further at the end of Section V C 2.

IV. ANTIFERROMAGNETS IN ONE DIMENSION

There is now a rather complete understanding of $S = 1/2$ quantum antiferromagnets, like those in (1.1), in one spatial dimension. This is largely due to the powerful bosonization technique, which not only allows classification of various gapless critical states, but also describes the renormalization group flow between gapped states with numerous possible broken discrete symmetries. We will use these well-established results as a convenient laboratory for testing the methods developed here for two-dimensional antiferromagnets. As we show below, when adapted to one dimension, our methods reproduce all the important universal results obtained by the bosonization method. This agreement significantly boosts our confidence that our lattice models and duality methods are also successfully capturing the physics of antiferromagnets in two dimensions.

Our discussion is divided into two subsections. In Section IV A, we recall the phase diagram of a $S = 1/2$ quantum antiferromagnet in one dimension obtained by the abelian bosonization method. In Section IV B we show that an essentially identical phase diagram is obtained by an analysis of the partition function Z in (1.13) when applied to one dimension.

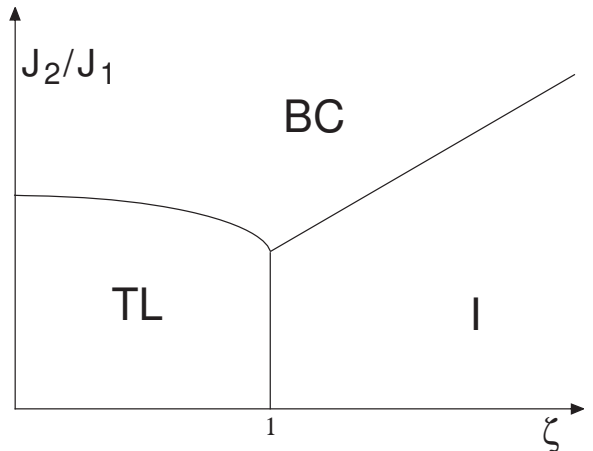


FIG. 4. Phase diagram³¹ of the $S = 1/2$, one-dimensional antiferromagnet $H^{(1)}$ in (4.1). The BC and I phases are as in Table I, and have a gap to all excitations. The Tomonaga-Luttinger (TL) phase is special to one dimension: it is gapless and has power-law spin correlations. There is SU(2) spin symmetry along the line $\zeta = 1$.

A. Results from bosonization

A convenient frustrated $S = 1/2$ antiferromagnet in one dimension is that studied by Haldane³¹ with first and second neighbor exchange interactions:

$$H^{(1)} = \sum_j \left[J_1 \left(\hat{S}_{ix} \hat{S}_{j+1,x} + \hat{S}_{iy} \hat{S}_{j+1,y} + \zeta \hat{S}_{iz} \hat{S}_{j+1,z} \right) + J_2 \hat{\mathbf{S}}_j \cdot \hat{\mathbf{S}}_{j+2} \right]. \quad (4.1)$$

We have also introduced a uniaxial anisotropy parameter ζ so that the spin symmetry is SU(2) only at $\zeta = 1$, and is U(1) otherwise. Both exchange constants are positive, $J_{1,2} > 0$, so the second neighbor coupling is frustrating.

A review of the abelian bosonization analysis of (4.1) may be found in Ref. 32. The resulting phase diagram is shown in Fig 4. There are two phases with a gap to all excitations, the BC and I, and these are as described in Table I. The I phase occurs for large ζ , when the spins clearly prefer to be polarized along the $\pm z$ directions. The BC phase appears for moderate values of the frustration, J_2/J_1 , and the spatial pattern of the bond order, $Q_{j,j+1}$, is sketched in Fig 4: this phase contains the special Majumdar-Ghosh point³³ $\zeta = 1$, $J_2/J_1 = 1/2$ where the fully dimerized wavefunction, consisting simply of products of singlet pairs of nearest neighbor sites, is the exact ground state.

The Tomonaga-Luttinger (TL) phase is gapless, and special to one dimension. It is the analog of the XY phase in two dimensions, but instead of exhibiting true long-range order, spin-correlations in the x - y plane have a slow power-law decay,

$$\langle \hat{S}_{ix} \hat{S}_{j+n,x} + \hat{S}_{iy} \hat{S}_{j+n,y} \rangle \sim \frac{(-1)^n}{|n|^{\eta_{XY}}} \quad (4.2)$$

for large $|n|$, where the exponent $\eta_{XY} \leq 1$ varies continuously within the TL phase ($\eta_{XY} = 1/2$ at $\zeta = 0$, $J_2/J_1 = 0$). Similarly, the correlations of the Ising order $(-1)^j \hat{S}_{j,z}$ decay with an exponent $\eta_I = 1/\eta_{XY}$, while those of the BC order decay with an exponent also equal to η_I .

At boundary between the TL and BC phases, and also at the boundary between the TL and I phases, we have $\eta_{XY} = \eta_I = 1$; actually, there is also a logarithmic correction to (4.2) at these boundaries—we do not display this here but note that our methods in Section IV B also reproduce this correction. Within the TL phase we have $\eta_{XY} < 1$. The boundary between the BC and I phases is also critical, and has $\eta_{XY} > 1$.

The manner in which the BC and I orders vanish at the boundaries of their respective phases is also reviewed in Ref 32: both order parameters vanish with an essential singularity at their boundaries to the TL phase, while they vanish with the same continuously varying power-law on opposite sides of the BC-I boundary.

B. Dual lattice models

We will now describe the properties of the lattice model Z in (1.13) adapted to one dimension: this latter model will be denoted $Z^{(1)}$. We will see that the phase diagram of a generalized class of such models is identical in structure to that of Fig 4.

First, let us explicitly write down the form of $Z^{(1)}$; we have

$$Z^{(1)} = \sum_{\{a_{\bar{j}}\}} \int \prod_j d\mathbf{n}_j \delta(\mathbf{n}_j^2 - 1) \exp\left(-S_{\mathbf{n}} - S_{\mathcal{A}}^{(1)} - S_B\right). \quad (4.3)$$

In present situation in two spacetime dimensions, the site indices j and \bar{j} extend over the square and dual-square lattices respectively, and the Greek indices $\mu, \nu, \lambda \dots$ extend over x, τ , and the parameter η_j in the Berry phase term is now $(-1)^{j_x}$. Furthermore, the \mathcal{A} flux can point in only one direction, and so $S_{\mathcal{A}}$ in (1.11) is replaced by

$$S_{\mathcal{A}}^{(1)} = \frac{1}{2e^2} \sum_{\square} (\epsilon_{\mu\nu} \Delta_{\mu} \mathcal{A}_{j\nu} - 2\pi q_{\bar{j}})^2, \quad (4.4)$$

so that the integer $q_{\bar{j}}$ is simply a scalar and carries no spacetime vector index. We wish to map the phase diagram of $Z^{(1)}$ in a parameter space where the coupling in $S_{\mathbf{n}}$ in (1.9) is allowed to acquire a uniaxial anisotropy and reduce the spin symmetry to $U(1)$.

We proceed with the duality transformations as in Section II. Then the expression for the partition function in (2.4) is replaced by

$$Z^{(1)} = \sum_{\{a_{\bar{j}}\}} \int \prod_j d\mathbf{n}_j \delta(\mathbf{n}_j^2 - 1) \exp\left(-S_{\mathbf{n}} - S_a^{(1)} - i \sum_{\square} \epsilon_{\mu\nu} a_{\bar{j}} \Delta_{\mu} \mathcal{A}_{j\nu}\right), \quad (4.5)$$

where now the integers $a_{\bar{j}}$ carry no spacetime vector index, and the action S_a is replaced by

$$S_a^{(1)} = \frac{e^2}{2} \sum_{\bar{j}} (a_{\bar{j}} - a_{\bar{j}}^0)^2, \quad (4.6)$$

with $a_{\bar{j}}^0$ now satisfying $\epsilon_{\mu\nu} a_{\bar{j}}^0 = \eta_j \delta_{\mu\tau}$ instead of (2.2); a convenient choice has $a_{\bar{j}}^0$ taking the values 1 and 0 on alternating spatial columns *i.e.* $a_{\bar{j}}^0 = (1 + (-1)^{\bar{j}_x})/2$.

We now need to understand the consequences of the integration over the \mathbf{n}_j in (4.5). Because our purpose is to compare with the properties of the model (4.1) which has a uniaxial anisotropy and only a $U(1)$ symmetry, we choose to introduce a similar anisotropy in $S_{\mathbf{n}}$. Actually it is convenient to take the easy-plane limit, and to assume that the \mathbf{n} fields are completely localized in the x - y plane in spin space. In such a limit the integral over the \mathbf{n} fields in (4.5) can be evaluated completely, and a precise mapping to a dual lattice model is obtained. We will then examine at the general structure of the resulting dual lattice model, and discuss how its parameter space allows us to relax the easy-plane restriction, and even find regimes in which the spins are localized in the $\pm z$ directions, and also special parameter values for which full $SU(2)$ spin symmetry is restored. So, in the easy-plane limit, we parameterize \mathbf{n}_j in terms of an angular field θ_j as noted in (1.14). To aid the integration over the θ_j , we perform the usual innocuous change of writing the action $S_{\mathbf{n}}$ in the periodic Gaussian (Villain) form

$$S_{\mathbf{n},U(1)} = \frac{1}{2g} \sum_{j,\bar{\mu}} (\Delta_{\mu} \theta_j - 2\pi m_{j\bar{\mu}})^2, \quad (4.7)$$

where the $m_{j\bar{\mu}}$ are the integers on the links of the direct lattice which ensure the periodicity of the action in the angular θ_j . These integers also have the utility of allowing us to measure the vorticity within each plaquette: this is simply $\epsilon_{\mu\nu} \Delta_{\mu} m_{j\nu}$. Now recall the discussion in Section III, in the paragraph containing (3.16), where we noted that in the easy-plane limit the \mathcal{A} flux through a plaquette is simply π times the vorticity. Using this result, and the modified form of the action in (4.7), the partition function $Z^{(1)}$ transforms to the following form in the easy-plane limit

$$Z_{U(1)}^{(1)} = \sum_{\{a_{\bar{j}}, m_{j\bar{\mu}}\}} \int \prod_j d\theta_j \exp\left(-S_{\mathbf{n},U(1)} - S_a^{(1)} - i\pi \sum_{\square} \epsilon_{\mu\nu} a_{\bar{j}} \Delta_{\mu} m_{j\nu}\right). \quad (4.8)$$

Before proceeding to a duality mapping of (4.8), we present an alternative representation of (4.8) which exposes its close relationship to the Z_2 gauge theories of Refs. 8,34. We notice that the last term in (4.8) is only sensitive to whether the integer $m_{j\mu}$ is even or odd. So we write

$$m_{j\mu} \equiv 2f_{j\mu} + \frac{1 - s_{j,j+\hat{\mu}}}{2} \quad (4.9)$$

where $f_{j\mu}$ is an integer vector field on the direct lattice, and $s_{j,j+\hat{\mu}} = \pm 1$ is an Ising variable on the links of the direct lattice; notice that $s_{j,j+\hat{\mu}}$ is *unoriented* (unlike $m_{j\mu}$ and $f_{j\mu}$) and this is reflected in the choice of notation. At this stage, it is now easy to perform the summation over the $a_{\bar{j}}$ independently on every dual lattice site, and to obtain the alternative representation of $Z_{U(1)}^{(1)}$:

$$\begin{aligned} Z_{U(1)}^{(1)} = & \sum_{\{s_{j,j+\hat{\mu}}=\pm 1\}} \sum_{\{f_{j\mu}\}} \int \prod_j d\theta_j \exp \left(K \sum_{\square} \prod_{\square} s_{j,j+\hat{\mu}} \right. \\ & - \frac{2}{g} \sum_{j,\hat{\mu}} \left(\frac{\Delta_{\mu}\theta_j}{2} - 2\pi f_{j\mu} - \frac{\pi}{2}(1 - s_{j,j+\hat{\mu}}) \right)^2 \\ & \left. - i\frac{\pi}{2} \sum_j (1 - s_{j,j+\hat{\tau}}) \right). \end{aligned} \quad (4.10)$$

The first term in the action of this form of $Z_{U(1)}^{(1)}$ is the standard Maxwell term of a Z_2 gauge theory, with $s_{j,j+\hat{\mu}}$ the Z_2 gauge field. The coupling K is related to e^2 by

$$e^{2K} \equiv \frac{\sum_{n=-\infty}^{\infty} e^{-e^2 n^2/2}}{\sum_{n=-\infty}^{\infty} (-1)^n e^{-e^2 n^2/2}}; \quad (4.11)$$

K is a monotonically decreasing function of e^2 , with $K = \pi^2/(4e^2) - (\ln 2)/2$ as $e^2 \rightarrow 0$ and $K = 2e^{-e^2/2}$ as $e^2 \rightarrow \infty$. The last term in (4.10) is the Berry phase of the Z_2 gauge theory: this is identical in form to that in Ref. 8, and was obtained after using the identity $\epsilon_{\mu\nu}\Delta_{\nu}a_{\bar{j}}^0 = \eta_j\delta_{\mu\tau}$. The connection to the models of Ref. 8 becomes clearer if we write (4.10) using the simple cosine interaction of the angle θ_j , rather than the periodic Gaussian, Villain form:

$$\begin{aligned} Z_{U(1)}^{(1)} \approx & \sum_{\{s_{j,j+\hat{\mu}}=\pm 1\}} \int \prod_j d\theta_j \exp \left(K \sum_{\square} \prod_{\square} s_{j,j+\hat{\mu}} \right. \\ & \left. + \frac{4}{g} \sum_{j,\hat{\mu}} s_{j,j+\hat{\mu}} \cos \left(\frac{\Delta_{\mu}\theta_j}{2} \right) - i\frac{\pi}{2} \sum_j (1 - s_{j,j+\hat{\tau}}) \right). \end{aligned} \quad (4.12)$$

This is the action of an XY model coupled to a Z_2 gauge field, with an additional Berry phase term associated with the $S = 1/2$ nature of the underlying antiferromagnet. Note that the angular variable in the XY coupling

is $\theta/2$, which is *half* the angle determining the orientation of \mathbf{n} in (1.14): this half-angle variable is of course the reason for the appearance of the Z_2 gauge degrees of freedom. Thus we have established the rather surprising result that simply by introducing an easy-plane anisotropy in the model Z in (1.13) of Sachdev and Jalabert⁴ we obtain the XY- Z_2 gauge model of Senthil and Fisher⁸; this result holds also in two dimensions, as we will see in Section V. The model (4.12) generalized to two dimensions, but without the Berry phase, was studied recently by Sedgewick *et al.*³⁴.

We now return to the original expression for $Z_{U(1)}^{(1)}$ in (4.8) and proceed with the duality mapping: this will allow evaluation of the θ_j integrals and will also write it in a form with only positive weights. First, we perform the summation over the $m_{j\mu}$ by using the following generalized Poisson summation identity on every link of the square lattice

$$\begin{aligned} \sqrt{2\pi C} \sum_{m=-\infty}^{\infty} \exp \left[-\frac{C}{2}(x - 2\pi m)^2 + imy \right] = \\ \sum_{J=-\infty}^{\infty} \exp \left[-\frac{1}{2C} \left(J + \frac{y}{2\pi} \right)^2 + ix \left(J + \frac{y}{2\pi} \right) \right], \end{aligned} \quad (4.13)$$

where m, J are integers, and $C > 0, x, y$ are arbitrary real numbers; this replaces the sum over the $m_{j\mu}$ by a summation over a different set of integer ‘‘currents’’, $J_{j\mu}$, also residing on the links of the square lattice. The advantage of this form is that the integrals over the θ_j can be performed independently, and yield only the constraint that the $J_{j\mu}$ currents are divergenceless. In this manner, $Z_{U(1)}^{(1)}$ in (4.8) is shown to be exactly equivalent to

$$\begin{aligned} Z_{U(1)}^{(1)} = & \sum'_{\{a_{\bar{j}}, J_{j\mu}\}} \exp \left[-\frac{e^2}{2} \sum_{\bar{j}} (a_{\bar{j}} - a_{\bar{j}}^0)^2 - \right. \\ & \left. \frac{g}{2} \sum_{j,j'} K_{jj'}^{\mu\nu} \left(J_{j\mu} + \frac{\epsilon_{\mu\lambda}\Delta_{\lambda}a_{\bar{j}}}{2} \right) \left(J_{j'\nu} + \frac{\epsilon_{\nu\rho}\Delta_{\rho}a_{\bar{j}'}}{2} \right) \right], \end{aligned} \quad (4.14)$$

where the prime on the summation indicates the constraint

$$\Delta_{\mu}J_{j\mu} = 0. \quad (4.15)$$

The mapping from (4.8) to (4.14) yields only a on-site coupling between the currents with

$$K_{jj'}^{\mu\nu} = \delta_{jj'}\delta_{\mu\nu} \quad (4.16)$$

(this $K_{jj'}^{\mu\nu}$ is not to be confused with the Ising gauge coupling K in (4.10,4.12); the latter does not carry any indices). However, to reproduce the full phase diagram of the antiferromagnet $H^{(1)}$ in (4.1) it is necessary to allow for additional near-neighbor couplings in $K_{jj'}^{\mu\nu}$. As will become clear from our discussion in Section IV B 1

below, these new terms allow us to include the couplings between the z components of the \mathbf{n}_j which were dropped when we specialized the SU(2) invariant $S_{\mathbf{n}}$ in (1.9) to the easy-plane limit $S_{\mathbf{n},U(1)}$ in (4.7). With the off-site terms in $K_{jj'}^{\mu\nu}$ we will be able to restore the SU(2) symmetry along special parameter lines of $Z_{U(1)}^{(1)}$, and even obtain regimes where the spin anisotropy is easy-axis, and the spin-ordering is Ising-like.

The expression (4.14) is one of the final dual forms of $Z_{U(1)}^{(1)}$: many physical properties will be most transparent in this formulation. However, for future technical purposes, it is useful to perform a few more manipulations on it. We can solve the constraint (4.15) by writing

$$J_{j\mu} = \epsilon_{\mu\nu} \Delta_\nu p_{\bar{j}} \quad (4.17)$$

where $p_{\bar{j}}$ is an integer on the sites of the dual lattice. Then, after defining $\ell_{\bar{j}} = 2p_{\bar{j}} + a_{\bar{j}}$, it is easy to see that the summation over the $a_{\bar{j}}$ can be performed explicitly. In this manner we find that (4.14) reduces exactly to

$$Z_{U(1)}^{(1)} = \sum_{\{\ell_{\bar{j}}\}} \exp \left[K_d \sum_{\bar{j}} \varepsilon_{\bar{j}} \sigma_{\bar{j}} - \frac{g}{8} \sum_{j,j'} K_{jj'}^{\mu\nu} (\epsilon_{\mu\lambda} \Delta_\lambda \ell_{\bar{j}}) (\epsilon_{\nu\rho} \Delta_\rho \ell_{\bar{j}'}) \right], \quad (4.18)$$

where $\sigma_{\bar{j}}$ is a fluctuating Ising variable which denotes whether $\ell_{\bar{j}}$ is even or odd,

$$\sigma_{\bar{j}} \equiv 1 - 2(\ell_{\bar{j}} \bmod 2), \quad (4.19)$$

while $\varepsilon_{\bar{j}} = (-1)^{\bar{j}x}$ is a fixed oscillating field which arises from the background $a_{\bar{j}}^0$ field, and is ultimately related to the spin Berry phases. The coupling K_d is the ‘‘dual’’ of the coupling K

$$\tanh K_d \equiv e^{-2K}, \quad (4.20)$$

where K was defined as a function of e^2 in (4.11); note that K_d is a monotonically increasing function of e^2 , with $K_d = 2e^{-\pi^2/(2e^2)}$ as $e^2 \rightarrow 0$, and $K_d = e^2/4 - (\ln 2)/2$ for $e^2 \rightarrow \infty$.

1. Observables and limiting cases

We pause in our chain of duality mappings to discuss the physical interpretation of the new degrees of freedom we have introduced. The physical picture becomes clearest after an understanding of the interpretation of the currents $J_{j\mu}$ in (4.14). Analysis of the duality mapping from (4.2) to (4.14) along the lines of the dualities of quantum XY and boson models in Refs. 35,36 shows immediately that these currents are precisely those of a boson representing the spin-flip operator. In other words, if in the original spin model (4.1) we make the identification

$$\hat{S}_{j,x} + i\hat{S}_{j,y} = b_j^\dagger, \quad (4.21)$$

and perform the usual boson duality transformations (as discussed by Sørensen *et al.*³⁵) to a model of interacting integer-valued current loops, the $J_{j\mu}$ will be the spatial and temporal (*i.e.* the density) components of the current of the boson in (4.21). More precisely, we can couple an external chemical potential to the boson charge and thence deduce that

$$\hat{S}_{j,z} \sim \epsilon_{\tau\nu} \Delta_\nu \ell_{\bar{j}} = \Delta_x \ell_{\bar{j}} \quad (4.22)$$

So the spatial gradients of the $\ell_{\bar{j}}$ are related to the value of $\hat{S}_{j,z}$, and a phase with I order will have a staggered, zigzag pattern of the $\ell_{\bar{j}}$.

The above interpretation can be reinforced by examining the limiting case $e^2 \rightarrow \infty$ (or equivalently, $K_d \rightarrow \infty$). Then in (4.14), the $a_{\bar{j}}$ fluctuations are quenched to $a_{\bar{j}} = a_{\bar{j}}^0$ and so $\epsilon_{\mu\nu} \Delta_\nu a_{\bar{j}} = (-1)^{\bar{j}x} \delta_{\mu\tau}$. With this value, the partition function in (4.14) is seen to be precisely the boson current loop model examined by Otterlo *et al.*³⁶ (but in two spatial dimensions) at a mean boson density of 1/2 per site. This last density is, of course, precisely that needed to have a state with $\langle \sum_j \hat{S}_{jz} \rangle = 0$ in the spin model. With the purely on-site coupling in (4.16) this boson-loop model is expected to always be superfluid: in one spatial dimension the superfluid (or XY) correlations are only power-law, and so the spin system is in the TL phase.

With the interpretation of the spin operators in (4.21,4.22), we have just seen that at $K_d = \infty$ each site has an average density of 1/2 spin-flip bosons. This is just as expected from the usual microscopic interpretation of the original spin antiferromagnet. However, what about the case when $K_d < \infty$? In this picture, there now appear to be fluctuations in the mean boson site density, $\epsilon_{\tau\nu} \Delta_\nu a_{\bar{j}}/2$. Where do the missing bosons go? The answer is that they reside on the links of the lattice; indeed if the spins on sites j and $j + \hat{x}$ form a spin-singlet, this is expressed in terms of the bosons in (4.21) as the single boson state

$$\frac{1}{\sqrt{2}} (b_j^\dagger - b_{j+\hat{x}}^\dagger) |0\rangle \quad (4.23)$$

where $|0\rangle$ is the reference state with both spins down. So a boson on a link corresponds to a spin-singlet bond, and each site on the ends of the link will lose half a boson. So our present model for spin systems goes beyond that of Otterlo *et al.*³⁶ by allowing easily for coherent occupation of bond orbitals. This sets the stage for states with BC order, and the present interpretation is seen to be compatible with identification (2.6) of the ‘‘bond-charge’’ density with the energy associated with the $a_{\bar{j}}$ fluctuations on the dual lattice site in the center of a bond. Using the variables appearing in (4.18), it is evident that the bond modulation is now measured by

$$Q_{j,j+\hat{x}} \sim \varepsilon_{\bar{j}} \sigma_{\bar{j}}, \quad (4.24)$$

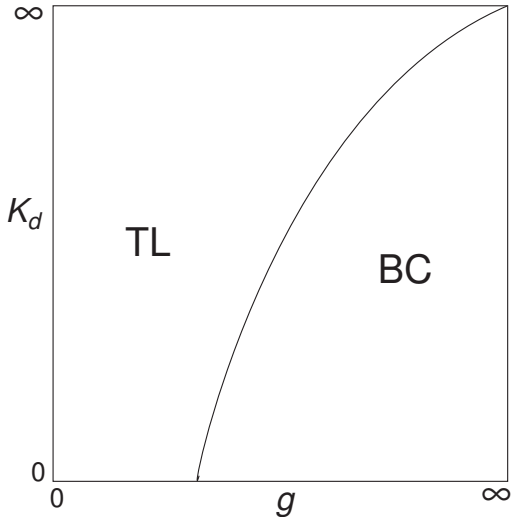


FIG. 5. Phase diagram of the one spatial-dimensional model $Z_{U(1)}^{(1)}$ for the case of the on-site coupling (4.16). The phase boundary is in the Kosterlitz-Thouless universality class, as discussed in Section IV B 2.

where \bar{j} resides on the middle of the plaquette between j and $j + \hat{x}$. With this identification, we can see that BC order is present in $Z_{U(1)}^{(1)}$ in the limit $g \rightarrow \infty$. From (4.18), we see that $\ell_{\bar{j}}$ is independent of \bar{j} , and therefore so is $\sigma_{\bar{j}}$. From (4.24), a constant $\sigma_{\bar{j}}$ leads to an oscillating Q_{ij} with BC order, with the values $\sigma_{\bar{j}} = \pm 1$ identifying the two dimerized states.

We now have enough information to construct the phase diagram of $Z_{U(1)}^{(1)}$ for the case of the purely on-site coupling (4.16). From (4.18) it is clear that there can be no phase transition at $g = 0$. Moreover, at $K_d = 0$, (4.18) reduces to a height model in 1+1 dimensions, and this must have a roughening transition at a critical value of g ; this will be discussed further in the following subsection. These results then allow us to sketch the phase diagram in Fig 5. Note there is no I phase; this will appear below when we perform generalized analysis which allows for further neighbor couplings in the $K_{jj'}^{\mu\nu}$.

2. Field theory and phase diagram

We now perform a field theoretic analysis of $Z_{U(1)}^{(1)}$ allowing for a general short-range coupling $K_{jj'}^{\mu\nu}$. The main idea, as mentioned above, is to view the partition function as a model of interfacial “heights”, $\ell_{\bar{j}}$, in 1+1 dimensions. Then the $K_{jj'}^{\mu\nu}$ control the roughness of the interface, while the first term in (4.18) indicates that the heights are preferentially even (odd) integers on every even (odd) spatial column. This height model can be analyzed by entirely standard technology, which is reviewed in Appendix E. The final result is that $Z_{U(1)}^{(1)}$ is related

to the continuum sine-Gordon model in 1+1 dimensions with action

$$S_{sG}^{(1)} = \int d^2r \left(\frac{g}{8} (\partial_\mu \phi_0)^2 - Y \cos(2\pi \phi_0) \right), \quad (4.25)$$

where r is a spacetime co-ordinate. In terms of the continuum field ϕ_0 , the I order is measured by $\sin(\pi \phi_0)$, while the BC order is measured by $\cos(\pi \phi_0)$. The coupling Y is related to the parameters of $Z_{U(1)}^{(1)}$ by (E5).

The action (4.25) is of the standard sine-Gordon type, and its properties can be read off from existing results. For small g , the coupling Y scales to 0 and its only effect is a renormalization of g to \tilde{g} . This yields the TL phase, and it is stable provided $\tilde{g} \leq 2\pi$. It is gapless and has power-law decay of correlations, controlled by the fluctuations of the free field ϕ_0 . With the identification of the BC and I order parameters below (4.25), we can now compute that they both decay with the exponent $\eta_I = 2\pi/\tilde{g}$. To compute the correlations in the x - y plane in spin space we note from (4.7) that fluctuations of the angular variable θ are controlled by the continuum action

$$S_{XY}^{(1)} = \frac{1}{2\tilde{g}} \int d^2r (\partial_\mu \theta)^2; \quad (4.26)$$

Now computing the correlator of $e^{i\theta}$ we deduce that x - y spin correlations decay as (4.2) with $\eta_{XY} = \tilde{g}/(2\pi) = 1/\eta_I$. Note that all of these exponents are identical to those obtained by abelian bosonization, as reviewed in Section IV A.

The TL phase is unstable for $\tilde{g} > 2\pi$, and the ground state acquires a gap induced by the flow of $|Y|$ to large values. For $Y > 0$, the field ϕ_0 is preferentially pinned at the values $\phi_0 = 0, 1$, and these are easily seen to correspond to the BC phase; the case with on-site couplings as in (4.16) is therefore seen to correspond to $Y > 0$, as (4.25) describes the phases in Fig 5. Similarly, for $Y < 0$, we have $\phi_0 = 1/2, 3/2$, the values corresponding to the two I states. These results imply the phase diagram shown in Fig 6. There is complete consistency between all the universal properties of Fig 6, and those obtained by abelian bosonization for the model of Fig 4. Establishing this was the primary purpose of this section.

A notable feature of Figs 4 and 6 is that $SU(2)$ spin symmetry is restored at the boundary between the TL and I phases. Moving along this line we see that the ground state initially has $SU(2)$ symmetric spin correlations decaying with an exponent $\eta_{XY} = \eta_I = 1$. However, there is eventually a continuous phase transition to the phase with BC order. So we have succeeded in understanding the phases of the $SU(2)$ model via a detour into models with only a $U(1)$ symmetry.

We conclude this section by noting that closely related results are obtained in an analysis based on the CP^1 formulation presented in Appendix A. This extension is discussed in Appendix F. This is in keeping with our contention that the \mathbf{n} field formulation of Section I and

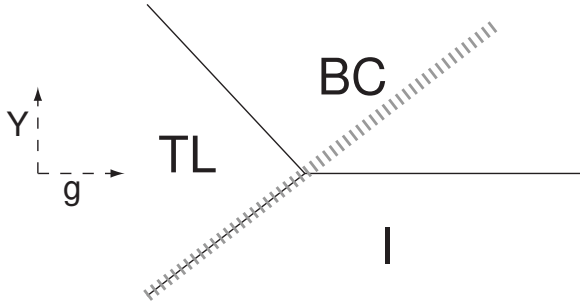


FIG. 6. Phase diagram of the one spatial-dimensional model $S_{sG}^{(1)}$ in (4.25). The same phase diagram also applies to $Z_{U(1)}^{(1)}$ in (4.14) with general off-site couplings beyond the on-site coupling in (4.16). The topology of this diagram is identical to that of Fig 4, as are all the universal long-distance properties of the TL phase, and of the phase boundaries. There is SU(2) spin symmetry along the grey hatched line. This line includes the boundary between the TL and I phases, but does not represent a phase boundary within the BC phase.

the CP^1 field formulation in Appendix A have similar phase diagrams.

V. U(1) SYMMETRY IN TWO DIMENSIONS

Bolstered by the success of our approach in one dimension, we forge ahead to the application of the same methods in two dimensions. We are interested in models of two-dimensional antiferromagnets like (1.1), but we now allow the spin exchange terms to acquire a uniaxial anisotropy like that in the first term in (4.1). We will carry out duality mappings on such spin systems with U(1) symmetry, and then search for lines in generalized parameter space where SU(2) symmetry can be restored. This should considerable light on the properties of SU(2)-symmetric quantum antiferromagnets.

Our initial analysis follows the same steps as in Section IV B; the only change is that some of the fields acquire additional vector indices, associated with the change of spacetime dimension to 3. We introduce spin anisotropy into the partition function Z in (1.13) by parameterizing the \mathbf{n} field as in (1.14) and replacing $S_{\mathbf{n}}$ in (1.9) by $S_{\mathbf{n},U(1)}$ in (4.7). Then proceeding with the duality mapping at the beginning of Section II, we obtain the following U(1) symmetric version of the partition function Z in (2.4); this generalizes (4.8) to two dimensions

$$Z_{U(1)} = \sum_{\{a_{\bar{j}\mu}, m_{j\mu}\}} \int \prod_j d\theta_j \exp\left(-S_{\mathbf{n},U(1)} - S_a - i\pi \sum_{\square} \epsilon_{\mu\nu\lambda} a_{\bar{j}\mu} \Delta_{\nu} m_{j\lambda}\right). \quad (5.1)$$

As in Section IV B, we can obtain alternative representations of (5.1) which expose its close connection to a Z_2 gauge theory. Indeed, these representations for $Z_{U(1)}$ are

identical to those for $Z_{U(1)}^{(1)}$ in (4.10) and (4.12) with the only change being that the summation over μ extends over the three spacetime directions: this alternative formulation of $Z_{U(1)}$ was presented earlier in (1.15).

Next, we proceed with the two-dimensional generalization of the duality mappings discussed below (4.12); we generalize (4.14) to

$$Z_{U(1)} = \sum'_{\{a_{\bar{j}\mu}, J_{j\mu}\}} \exp\left[-\frac{e^2}{2} \sum_{\bar{j}} (a_{\bar{j}\mu} - a_{\bar{j}\mu}^0)^2 - \frac{g}{2} \sum_{j,j'} K_{jj'}^{\mu\nu} \left(J_{j\mu} + \frac{\epsilon_{\mu\lambda\kappa} \Delta_{\lambda} a_{\bar{j}\kappa}}{2}\right) \left(J_{j'\nu} + \frac{\epsilon_{\nu\rho\gamma} \Delta_{\rho} a_{\bar{j}'\gamma}}{2}\right)\right], \quad (5.2)$$

where, as before, the prime on the summation indicates the constraint (4.15). The particular model (5.1) corresponds to the purely on-site values of the coupling $K_{jj'}^{\mu\nu}$ as in (4.16). However, as discussed in Section IV B, we find it useful to consider models with near neighbor $K_{jj'}^{\mu\nu}$ to allow for phases with easy-axis anisotropy and parameter values with enhanced SU(2) symmetry. Another useful form of (5.2) is obtained by solving the constraint (4.15) by

$$J_{j\mu} = \epsilon_{\mu\nu\lambda} \Delta_{\nu} p_{j\lambda} \quad (5.3)$$

with $p_{j\lambda}$ integer; this generalizes (4.17). With this parameterization, the two-dimensional form of (4.18) is

$$Z_{U(1)} = \sum_{\{\ell_{\bar{j}\mu}\}} \exp\left[K_d \sum_{\bar{j}} \epsilon_{\bar{j},\bar{j}+\hat{\mu}} \sigma_{\bar{j},\bar{j}+\hat{\mu}} - \frac{g}{8} \sum_{j,j'} K_{jj'}^{\mu\nu} (\epsilon_{\mu\lambda\kappa} \Delta_{\lambda} \ell_{\bar{j}\kappa}) (\epsilon_{\nu\rho\gamma} \Delta_{\rho} \ell_{\bar{j}'\gamma})\right], \quad (5.4)$$

where $\ell_{\bar{j}\mu} = 2p_{j\mu} + a_{\bar{j}\mu}$ is an integer valued vector field on the links of the dual cubic lattice, and $\sigma_{\bar{j},\bar{j}+\hat{\mu}}$ is an Ising degree of freedom which is pinned to the $\ell_{\bar{j}\mu}$ by

$$\sigma_{\bar{j},\bar{j}+\hat{\mu}} \equiv 1 - 2(\ell_{\bar{j}\mu} \bmod 2), \quad (5.5)$$

generalizing (4.19). Notice that, unlike $\ell_{\bar{j}\mu}$, $\sigma_{\bar{j},\bar{j}+\hat{\mu}}$ is *un-oriented*, and has only a single value ± 1 on each link; this is the reason for the different choice of notation for these two fields. The fixed field $\epsilon_{\bar{j},\bar{j}+\hat{\mu}}$ is likewise unoriented and takes values ± 1 . It arises, as in (4.18), from the Berry phase terms in $Z_{U(1)}$, and its values must satisfy

$$\prod_{\text{spatial } \square} \epsilon_{\bar{j},\bar{j}+\hat{\mu}} = -1 \quad (5.6)$$

about every spatial plaquette. All other plaquettes have $\prod_{\square} \epsilon_{\bar{j},\bar{j}+\hat{\mu}} = 1$. The coupling K_d is a monotonic function of e^2 given, as before, by (4.20) and (4.11).

A. Observables and limiting cases

Continuing our parallel to the discussion of one-dimensional antiferromagnets in Section IV B, we generalize the discussion of Section IV B 1 to two dimensions. The generalization of the observables is immediate. The spin-flip site boson density is now measured by the ℓ flux piercing the associated plaquette on the dual lattice:

$$\hat{S}_{j,z} \sim \epsilon_{\tau\mu\nu} \Delta_\mu \ell_{\hat{j}\nu} \quad (5.7)$$

(generalizing (4.22)). The BC order in (4.24) needs some notational modification:

$$Q_{j,j+\hat{x}} \sim \varepsilon_{\bar{j},\bar{j}+\hat{y}} \sigma_{\bar{j},\bar{j}+\hat{y}}, \quad (5.8)$$

where the direct lattice link on the left-hand-side intersects (after projecting the τ co-ordinate by half a lattice spacing) the dual lattice link on the right-hand-side. A similar relation holds with $x \leftrightarrow y$.

Next, we turning describing the physics of the limiting parameter values in the phase diagram of $Z_{U(1)}$. We will see that there is much more structure than that in the corresponding discussion in Section IV B 1.

As before, we first consider the limit $K_d \rightarrow \infty$. Now the results are essentially identical to those in one dimension: the values of $a_{\bar{j}\mu}$ are pinned to $a_{\bar{j}\mu}^0$, and so $\epsilon_{\mu\nu\lambda} \Delta_\nu a_{\bar{j}\lambda} = \eta_j \delta_{\mu\tau}$. The partition function (5.2) is exactly the boson current-loop model studied by Otterlo *et al.*³⁶. With the purely on-site coupling $K_{jj'}^{\mu\nu}$ in (4.16), they found that the boson-loop model was always a superfluid, which corresponds to a spin system with long-range XY order. With a nearest-neighbor coupling in the $K_{jj'}^{\mu\nu}$, Otterlo *et al.* found states with a boson site density wave, which corresponds here to spin states with I order.

In the limit $g \rightarrow \infty$, $Z_{U(1)}$ reduces to a non-trivial model, unlike the case in Section IV B 1. From (5.4) we deduce that the integer vector field $\ell_{\bar{j}\mu}$ must be curl-free, implying it can be expressed as the gradient of an integer-valued field on the sites of the dual lattice. The relationship (5.5) then implies that Ising field $\sigma_{\bar{j},\bar{j}+\hat{\mu}}$ is also ‘pure gauge’ *i.e.*

$$\sigma_{\bar{j},\bar{j}+\hat{\mu}} = \varsigma_{\bar{j}} \varsigma_{\bar{j}+\hat{\mu}} \quad (5.9)$$

where $\varsigma_{\bar{j}} = \pm 1$ is an Ising field on the sites of the dual lattice. So

$$Z_{U(1)}(g \rightarrow \infty) = \sum_{\{\varsigma_{\bar{j}} = \pm 1\}} \exp \left(K_d \sum_{\bar{j},\hat{\mu}} \varepsilon_{\bar{j},\bar{j}+\hat{\mu}} \varsigma_{\bar{j}} \varsigma_{\bar{j}+\hat{\mu}} \right). \quad (5.10)$$

This is the partition function of an ordinary Ising model on a cubic lattice, with a nearest neighbor exchange of modulus K_d , and the signs of the exchange chosen so that every spatial plaquette is frustrated. The expression (5.10) could also have been obtained by applying the

standard Ising duality to the Z_2 gauge theory in (1.15) in the limit $g = \infty$; the Berry phase in (1.15) appears as the frustration in (5.10). Also note that in the framework of the parameterization in (5.2), the steps leading to (5.10) correspond precisely to the discussion in Section II that the large g limit in the presence of U(1) symmetry imposed the constraint (2.10) on (2.8). The Ising model in (5.10) was studied in Ref. 16,18 with the motivation also provided by $S = 1/2$ quantum antiferromagnets. The context of U(1)-symmetric models is quite different here, and the earlier motivation is close to the SU(2) symmetric models to be considered in Section VI. From this earlier work on this frustrated Ising model, and from methods to be described in detail in Section V B, we conclude that the ‘ferromagnetic’ phase found at large K_d has BC order. Also, the Ising ‘paramagnetic’ phase at small K_d is *fractionalized* (F) with no broken lattice symmetry. This F phase had no analog in one dimension, where the large g limit yielded only the BC phase.

Turning to the limit $K_d \rightarrow 0$, $Z_{U(1)}$ in (5.4) becomes a model of interacting *half*-integer currents with short-range interactions. After a rescaling of currents and coupling constants, this model is formally equivalently to one with integer currents, which correspond in turn to boson models at integer filling studied in Refs. 35,36. These have a transition between a superfluid phase at small g and an insulating phase at large g which is in the universality class of the O(2) φ^4 field theory in 3 dimensions. For the spin model, the superfluid phase corresponds to the XY phase, while the insulating phase is F phase.

Finally, as in Section IV B 1, the $g \rightarrow 0$ limit is trivial and the ground state always has XY order.

Putting all these results together, we can sketch the phase diagram in Fig 7 for $Z_{U(1)}$. Actually, determining the structure of the phase boundaries in this figure required some additional field-theoretic analysis which appears in Section V B.

B. Field theories

We now proceed to a field-theoretic analysis of the model $Z_{U(1)}$ in (5.4) following the same method used to analyze $Z_{U(1)}^{(1)}$ in Section IV B 2. The technical details of the derivation are similar to those used in the one dimensional case in Appendix E, and their generalization to two dimensions is described in Appendix G.

The field theory obtained in this manner turns out to be very closely related to that studied recently by Lanert, Fisher and Senthil (LFS)⁹, although in a somewhat different physical context. They were studying charge fluctuations in a correlated superconductor using models of interacting boson Cooper pairs. As we noted in Section I A, and again in Section IV B 1, our antiferromagnetic spin models can also be interpreted as interacting boson Hamiltonians, but the boson is now a spin-flip operator, as in (4.21). Casting aside the different physical

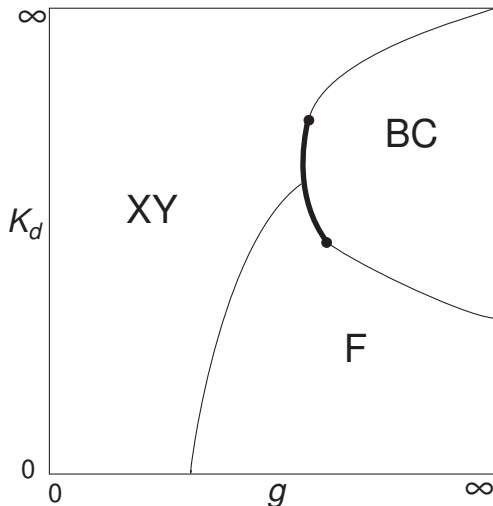


FIG. 7. Phase diagram of two spatial-dimension model $Z_{U(1)}$ in (1.15) or (5.2) or (5.4) for the case of the on-site coupling (4.16). The thin lines are second-order phase boundaries while the thick line is a first-order boundary. The field theories for the phases and the critical properties are discussed in Section V B.

interpretation of the bosons, the results of LFS can be directly applied to our models: we simply have to map their superfluid state to a XY phase of antiferromagnets, their boson site charge-density-wave to an I phase, while the interpretation of BC order remains the same in both cases. We will follow the same general approach as LFS, but will extend their results in several directions to address the questions of interest here.

In one dimension, as presented in Section IV B 2, the field theory describing the phases of the antiferromagnet was the sine-Gordon model in (4.25). In two dimensions, the analogous procedure in Appendix G shows that the central actors are point vortices in the wavefunction of the spin-flip bosons in (4.21). We will denote the complex field which creates or annihilates *single* vortices by $\phi(r)$, where r is a spacetime co-ordinate (the boson wavefunction winds by a phase of 2π around such a vortex). Also essential for a description of the phases, and emerging naturally in the derivation in Appendix G, are the *double* vortices $\Phi(r)$ (the boson wavefunction winds now by 4π). As discussed by LFS, and in Appendix G, the Berry phase terms induce frustration in the hopping Hamiltonian for the ϕ vortices: consequently, the low energy vortices have momenta near both $(0, 0)$ and $(\pi, 0)$ and it is necessary to include both sets in the field theory. We denote a convenient linear combination of fields representing vortices near these minima by $\phi_1(r)$ and $\phi_2(r)$ (see Appendix G). The motion of the double vortex, Φ , is unfrustrated, and it only has a single minimum at momentum $(0, 0)$. We list these fields, and their physical properties, in Table II; this table also contains additional fields to be introduced later in Section V C.

| Field | Description |
|------------------|---|
| ϕ_1, ϕ_2 | Complex field operators for $\pm 2\pi$ vortices in the spin-flip boson $b^\dagger = \hat{S}_+$ (see (4.21)). The Berry phase frustrates the hopping of such vortices, and their dispersion (in a convenient gauge) has minima near momenta $(0, 0)$ and $(\pi, 0)$. ϕ_1 and ϕ_2 are convenient linear combination of continuum fields representing fluctuations near these minima (see Appendix G). By the boson-vortex duality, $\pm 2\pi$ vortices in $\phi_{1,2}$ change b boson number by ± 1 , and therefore carry $S_z = \pm 1$: such vortices must be present in both ϕ_1 and ϕ_2 together to ensure a finite energy cost. |
| Φ | Complex field operator for $\pm 4\pi$ vortices in the spin-flip boson $b^\dagger = \hat{S}_+$ (see (4.21)). Its hopping is not frustrated and the dispersion has a minimum near $(0, 0)$. By the boson-vortex duality, $\pm 2\pi$ vortices in Φ change b boson number by $\pm 1/2$, and therefore carry $S_z = \pm 1/2$ <i>i.e.</i> they are spinons. The relationship to $\phi_{1,2}$ is $\Phi \sim \phi_1\phi_2$ (\sim indicates that the two sides have correlators with identical physical properties). |
| Ψ_I | Real order parameter for I order, $\Psi_I \sim \phi_1 ^2 - \phi_2 ^2$ |
| Ψ_{BC} | Complex order parameter for BC order, $\Psi_{BC} \sim \phi_1^*\phi_2$ |

TABLE II. Summary of all the continuum fields introduced in Section V and their physical properties.

| Label | Characterization |
|-------|--|
| BC | $\langle \phi_1^* \phi_2 \rangle \neq 0$ |
| I | $\langle \phi_1 ^2 - \phi_2 ^2 \rangle \neq 0$ |
| XY | $\langle \phi_1 \rangle = \langle \phi_2 \rangle = \langle \Phi \rangle = 0$ |
| F | $\langle \Phi \rangle \neq 0, \langle \phi_1 \rangle = \langle \phi_2 \rangle = 0$ |

TABLE III. Characterization of some of the state properties in Table I in terms of expectation values of the fields ϕ_1 , ϕ_2 , and Φ . States which satisfy more than one property are also possible, and obey the union of the corresponding expectation values *e.g.* the BC+F state has $\langle \phi_1^* \phi_2 \rangle \neq 0$, $\langle \Phi \rangle \neq 0$, and $\langle \phi_1 \rangle = \langle \phi_2 \rangle = 0$.

An explicit derivation of the effective action for ϕ_1 , ϕ_2 , Φ is discussed in Appendix G. Here we will begin by noting the transformations of these fields under the symmetries of the lattice Hamiltonian, and then use these to eventually write down the most general effective action consistent with these symmetries. First, as is always the case in the boson-vortex duality mapping, the fields ϕ_1 , ϕ_2 , Φ all carry charges with respect to an internal, *non-compact*, U(1) gauge field b_μ (this U(1) gauge field is entirely distinct from the *compact* U(1) gauge fields \mathcal{A}_μ (Section I) and A_μ (Section VI and Appendix A)). The fields $\phi_{1,2}$ carry b -charge 1, while Φ carries b -charge 2. Lattice symmetries lead to non-trivial mappings among these fields, as discussed by LFS:

$\pi/2$ rotation about a direct lattice site:

$$\phi_1 \rightarrow e^{i\pi/4} \phi_1, \phi_2 \rightarrow e^{-i\pi/4} \phi_2$$

x translation by a lattice spacing: $\phi_1 \rightarrow \phi_2, \phi_2 \rightarrow \phi_1$

y translation by a lattice spacing: $\phi_1 \rightarrow i\phi_2, \phi_2 \rightarrow -i\phi_1$;

$$(5.11)$$

Φ remains invariant under all of the above lattice transformations.

Before writing down the effective action, we note the connection of these fields to some of the orders characterizing the antiferromagnet as presented in Table I. The results follow from simple symmetry considerations and are summarized in Table III.

The BC order breaks only a lattice symmetry, and must clearly be neutral under the b -charge. Examination of (5.11) and the symmetries of the states in Fig 1 then easily shows that the BC order parameter is the composite field $\phi_1^* \phi_2$. The same connection can also be established directly by applying (5.8) to the analysis of Appendix G. The phase of the mean value of this order parameter distinguishes between the various states in Fig 1: $\arg(\phi_1^* \phi_2) = 0, \pi/2, \pi, 3\pi/2$ yields the four states like Fig 1a, $\arg(\phi_1^* \phi_2) = \pi/4, 3\pi/4, 5\pi/4, 7\pi/4$ yields the four states like Fig 1b, and all other values correspond to an 8-fold degenerate state with co-existing dimer and plaquette order.

For the I order, we note from (5.7) that Ising ordering is associated with a staggered pattern of boson site density;

in the boson-vortex duality this corresponds to b -charge neutral, staggered, vortex current loops. The structure of the vortex eigenmodes in Appendix G then shows that the I order is $|\phi_1|^2 - |\phi_2|^2$.

The XY order corresponds to boson superfluidity. This is only possible if none of the vortex fields have condensed, and hence the vanishing of all expectation values in Table III.

Finally, as discussed by LFS, the F states appear when Φ is preferentially condensed over $\phi_{1,2}$. In the dual boson language this means that excitations with boson charge 1/2 are liberated (these latter bosons are themselves $\pm 2\pi$ vortices in the double-vortex field Φ); from (4.21) we see that these are simply the $S = 1/2$ spinons of a F state. Also, it is evident from Table III that co-existence between the F and XY orders is not possible, while BC+F and I+F states can, in principle, exist. In the approach of Senthil and Fisher⁸ XY+F states did emerge in a larger space of models and degrees of freedom than those considered here. Here, we will show that XY+F states do not appear in the models considered so far, but are present in the models with non-collinear spin correlations to be considered in Section VI.

The derivation in Appendix G, or application of the symmetries in (5.11) shows that action describing the phases of $Z_{U(1)}$ is the spacetime integral of the Lagrangian

$$\begin{aligned} \mathcal{L} = & |(\partial_\mu - ib_\mu)\phi_1|^2 + |(\partial_\mu - ib_\mu)\phi_2|^2 + |(\partial_\mu - 2ib_\mu)\Phi|^2 \\ & + \frac{\tilde{g}}{2}(\epsilon_{\mu\nu\lambda}\partial_\nu b_\lambda)^2 + s_1(|\phi_1|^2 + |\phi_2|^2) + s_2|\Phi|^2 \\ & - w\Phi\phi_1^*\phi_2^* + \text{c.c.} + \frac{u_1}{2}(|\phi_1|^2 + |\phi_2|^2)^2 + \frac{u_2}{2}|\Phi|^4 \\ & + v_1|\phi_1|^2|\phi_2|^2 + v_2|\Phi|^2(|\phi_1|^2 + |\phi_2|^2) + v_8(\phi_1^*\phi_2)^4 + \text{c.c.} \end{aligned} \quad (5.12)$$

We have scaled all the field variables to make the coefficients of the gradient terms equal to unity; we have also set all velocities equal to unity, and, for simplicity of notation, ignored their possibly different values. The parameters s_1 and s_2 tune the system across the various phase transitions, and we will shortly discuss the phase diagram as a function of s_1 and s_2 . The cubic coupling w (not considered by LFS) is allowed by all the symmetries in (5.11), and by charge neutrality: it will play a central role in determining important features of the phase diagram. The various quartic terms couple invariant scalar densities and usually only play a peripheral role in stabilizing the action. Finally, the v_8 term serves only to choose between the different types of BC order.

The mean-field phase diagram of \mathcal{L} has a somewhat different structure depending upon the sign of v_1 . We sketch typical phase diagrams as functions of $s_{1,2}$ for these two cases in Figs 8 ($v_1 < 0$) and 9 ($v_1 > 0$). The simpler case in Fig 8 has only three phases: XY, BC, and F, and the saddle point always has $|\phi_1| = |\phi_2|$ (so there is no I order). Any two of the phases can be separated by second-order phase boundary (whose field theory and

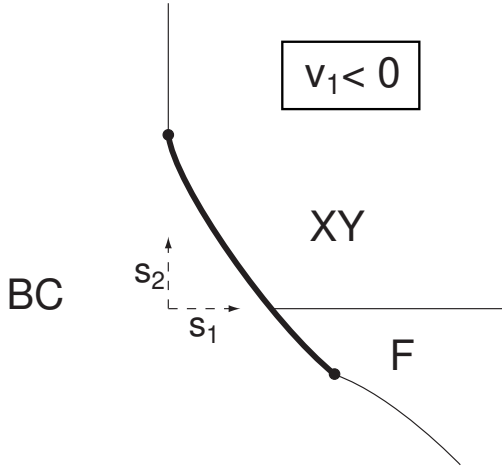


FIG. 8. Mean field phase diagram of \mathcal{L} in (5.12) as a function of s_1 and s_2 for typical parameter values and $v_1 < 0$. The non-compact U(1) gauge field b_μ is ignored in this analysis, and the action is simply minimized w.r.t. to mean values of the fields $\phi_{1,2}$, Φ . As in Fig 7, first-order boundaries are denoted by thick lines, while second-order boundaries are thin lines. The BC phase has $\langle \phi_{1,2} \rangle \neq 0$ and $|\langle \phi_1 \rangle| = |\langle \phi_2 \rangle|$, and these can be deduced from the characterizations in Table III. See also Table IV.

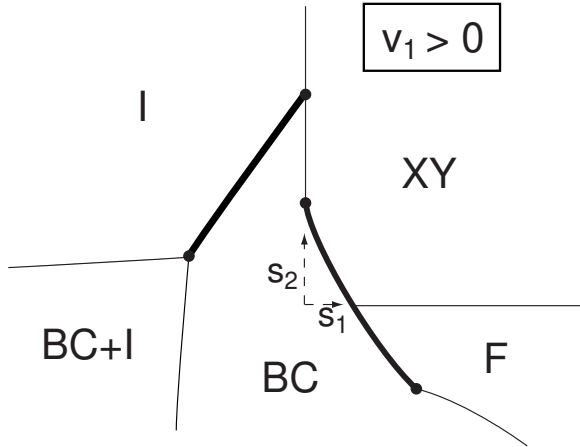


FIG. 9. As in Fig 8 but for $v_2 > 0$. The I phase has $\langle \phi_1 \rangle \neq 0$, and $\langle \phi_2 \rangle = 0$ or vice-versa, as can be deduced from Table III. The BC+I phase has $\langle \phi_{1,2} \rangle \neq 0$ and $|\langle \phi_1 \rangle| \neq |\langle \phi_2 \rangle|$, as indicated in Table IV.

order parameter can be easily determined from Table III and \mathcal{L}). However the phase boundaries necessarily become first order near the point where the three phases meet: this is a consequence of the cubic w term in \mathcal{L} , as shown recently in Appendix A of Ref. 37 in a different context but with a field theory with a very similar structure. The results of Fig 8 were used to deduce the phase diagram of $Z_{U(1)}$ in Fig 7. Note that the two diagrams have an identical topology. The absence of an I phase shows that the purely on-site coupling (4.16) in $Z_{U(1)}$ corresponds to a field theory \mathcal{L} with $v_1 < 0$.

The phase diagram in Fig 9, with $v_1 > 0$, does allow for an I phase. So it can only correspond to $Z_{U(1)}$ with non-on-site couplings $K_{jj'}^{\mu\nu}$. A crucial feature of this phase diagram is that all phases with I order are well separated from the F phase: there is no second order transition between the F phase and the I phase (although a strong first order transition can always be induced by choosing couplings judiciously). This feature will play a central role in our discussion of the restoration of SU(2) symmetry in Section V C. For now, we present a simple argument that the separation of phases with F and I order also holds beyond the mean-field analysis of \mathcal{L} . Let us begin in the fractionalized F phase. From Table III, we see that the Φ field has condensed. The b -gauge fluctuations are quenched in such a region (by the usual Higgs mechanism), and can therefore be neglected. The onset of the I phase involves a confinement transition and so one of the fields ϕ_1 , ϕ_2 must condense. Let us examine the structure of the effective action for $\phi_{1,2}$ in a region where we can safely set $b_\mu = 0$ and $\langle \Phi \rangle \neq 0$; from \mathcal{L} the quadratic form controlling $\phi_{1,2}$ fluctuations is

$$|\partial_\mu \phi_1|^2 + |\partial_\mu \phi_2|^2 + (s_1 + v_2 |\langle \Phi \rangle|^2)(|\phi_1|^2 + |\phi_2|^2) - w \langle \Phi \rangle \phi_1^* \phi_2^* - w \langle \Phi^* \rangle \phi_1 \phi_2 \quad (5.13)$$

Near a second order transition where $\phi_{1,2}$ condense, we must diagonalize the quadratic form (5.13) and condense the field combinations in the eigenmode with the lowest eigenvector. A simple analysis of (5.13) shows that, for arbitrary $\langle \Phi \rangle$, this eigenmode has $|\phi_1| = |\phi_2|$. From Table III, it follows immediately that the condensed phase cannot have I order. Therefore the F phase is surrounded entirely by with the BC phase (corresponding to condensation of $\phi_{1,2}$) or by the XY phase (corresponding to removal of the Φ condensate, as is presented in Fig 9).

C. Generalized phase diagrams and restoration of SU(2) symmetry

The ultimate objective of our analysis of antiferromagnets with U(1) symmetry is to find parameter regimes where full SU(2) symmetry is restored, thus enabling a description of the phases and phase transitions of SU(2)-invariant antiferromagnets. At the corresponding stage in our analysis of U(1) antiferromagnets in one dimension in Section IV B we had achieved this objective. We

found there that boundary between the TL and I phases was a critical line, possessing SU(2) invariant correlations at long distances with a power-law decay (as in (4.2) characterized by exponents $\eta_{XY} = \eta_I = 1$. This is, of course, the well-known property of the $S = 1/2$ antiferromagnetic Heisenberg chain. Furthermore, as indicated in Fig 6, the SU(2)-invariant line extends into the gapped BC phase, and we obtained the correct and complete theory of the quantum phase transition from the TL to BC phase for SU(2)-invariant antiferromagnets.

Let us now apply the same strategy in two dimensions. As a first step, we have to obtain a parameter regime where the ground state has HN order. Unlike the SU(2) invariant case in one dimension, the HN state is *not* critical: it has true long-range magnetic order, and an excitation spectrum of two, gapless, linearly dispersing spin waves. By analogy with one dimension, a natural candidate for HN order is the boundary between the XY and I phases in Fig 9. However, further consideration shows that this line clearly does not satisfy the necessary criteria. This is a *critical* line describing a second order transition: the critical degrees of freedom are the fields $\phi_{1,2}$ coupled to the b_μ non-compact U(1) gauge field, and the critical field theory is \mathcal{L} in (5.12) after we set the massive field $\Phi = 0$. It is expected that all correlators will have an anomalous power-law decay along this line, and these characteristics are far removed from those of the HN phase.

We have to enlarge the parameter space of our field theory to find the HN phase. To this end, note that the I (and BC) order in Table III, were associated with *composite* fields built out of $\phi_{1,2}$. It would clearly pay to elevate the I order parameter to an elementary degree of freedom, as that would then permit co-existence of *non-critical* XY and I order over a wide parameter regime, allowing for possible subspace with HN order. We therefore introduce the elementary Ising order parameter field Ψ_I , and, for completeness, the elementary BC order parameter field, Ψ_{BC} . We have now introduced all the continuum fields listed in Table II, which contains a summary of their physical interpretation.

The relationships of Ψ_I and Ψ_{BC} to the fields $\phi_{1,2}$ noted in Table II follow immediately from the state characterizations in Table III. We can now make a catalog of possible phases by considering the physical properties of all the different combinations of condensation among the fields $\phi_{1,2}$, Φ , Ψ_{BC} and Ψ_I . This leads to the exhaustive listing provided in Table IV. Note the appearance of the AF+I phase—this will be our candidate for possessing HN order along a subspace in its interior.

An understanding of the topology of the phase diagram and the nature of the quantum phase transitions requires an effective Lagrangian for all the fields. We can use the same symmetry considerations discussed near (5.11) to extend the Lagrangian \mathcal{L} in (5.12) to include Ψ_{BC} and Ψ_I . Such a procedure yields

| State | Condensed fields |
|---------|---|
| BC | $\phi_1, \phi_2, \Psi_{BC}, \Phi$ |
| I | ϕ_1 or ϕ_2, Ψ_I |
| BC+I | $\phi_1, \phi_2, \Psi_{BC}, \Psi_I, \Phi$ |
| XY | none |
| XY+BC | Ψ_{BC} |
| XY+I | Ψ_I |
| XY+BC+I | Ψ_{BC}, Ψ_I |
| F | Φ |
| F+BC | Φ, Ψ_{BC} |
| F+I | Φ, Ψ_I |
| F+BC+I | Φ, Ψ_{BC}, Ψ_I |

TABLE IV. Exhaustive specification of the states expected in the generalized parameter space of \mathcal{L}' . Notice that the left column contains state labels, and not the label of a property that may be obeyed by a state, which was the case in Table III. The right-column contains all the fields that have a non-zero expectation value in the corresponding state; if a field is not mentioned, it has vanishing expectation value in that state. The table above can be deduced directly from the characterizations in Table III, and from the field correspondences in Table II.

$$\begin{aligned}
\mathcal{L}' = \mathcal{L} &+ \frac{1}{2}(\partial_\mu \Psi_I)^2 + |\partial_\mu \Psi_{BC}|^2 + \frac{s_I}{2}\Psi_I^2 + s_{BC}|\Psi_{BC}|^2 \\
&- w_I \Psi_I (|\phi_1|^2 - |\phi_2|^2) - w_{BC} \Psi_{BC} \phi_1 \phi_2^* + \text{c.c.} \\
&+ v'_8 \Psi_{BC}^4 + \text{c.c.} + \dots
\end{aligned} \tag{5.14}$$

The ellipses represents numerous quartic terms involving couplings between the modulus squared of all the fields like $|\Psi_{BC}|^2|\Phi|^2$, $|\Psi_I|^2(|\phi_1|^2 + |\phi_2|^2)$, $|\Psi_{BC}|^4 \dots$; these serve mainly to stabilize the action and we will refrain from writing them out explicitly. We now have two additional parameters, s_{BC} and s_I , which can tune the system between its phases by controlling the condensation of Ψ_{BC} and Ψ_I respectively. The cubic couplings w_I and w_{BC} follow directly from Table II, and play a central role in determining the phase diagram.

We can now envisage a four-dimensional phase diagram as a function of the parameters s_1, s_2, s_I and s_{BC} . This is a space of immense complexity and we will explore its structure by describing a few judiciously chosen two-dimensional cross-sections.

Our primary interest is in studying the vicinity of the XY+I phase. So we describe the cross-section in the s_1 - s_I plane with $s_2 > 0$ and $s_{BC} > 0$. The mean-field phase diagram for this case is shown in Fig 10. An XY+I phase appears, as expected, and we will now study its properties in greater detail.

1. HN order in the XY+I phase

The XY+I phase only has $\langle \Psi_I \rangle$ non-zero, as was indicated in Table IV. A simple stability analysis about such

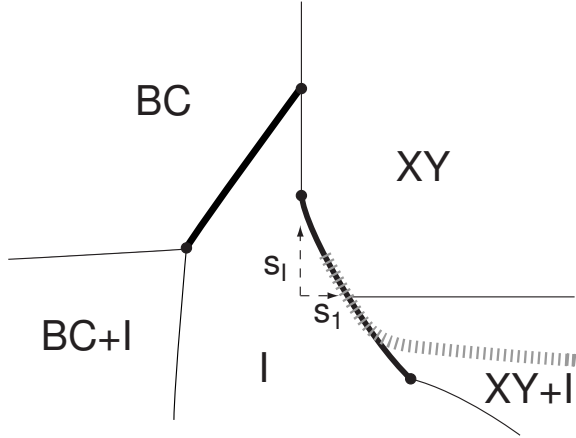


FIG. 10. Schematic mean field phase diagram of \mathcal{L}' in (5.14) as a function of s_1 and s_I with $s_2 > 0$, $s_{BC} > 0$, and $v_1 < 0$. The conventions for the phase boundaries are as in Fig 7. The grey hatched line represents a possible line along which SU(2) symmetry is restored: this line begins within the XY+I phase, and then continues along the first-order boundary between the XY and I phases; as argued in the text it cannot reach the end-point of this first-order boundary and veers off into another direction not included within this cross-section of the phase diagram.

a saddle-point shows that fluctuations of $\Psi'_I = \Psi_I - \langle \Psi_I \rangle$, Ψ_{BC} , $\phi_{1,2}$, and Φ are all gapped. However, the transverse component of the non-compact U(1) gauge field b_μ (which is not Higgsed by the neutral Ψ_I) yields a *single* gapless, linearly-dispersing mode: this corresponds to the familiar spin-wave mode of the XY order. To obtain a state with HN order, we need *two* spin-wave modes, and we can reasonably hope this may happen for special values of the parameters.

As a prelude to demonstrating this more explicitly, let us write down the form of the effective Lagrangian that will describe the HN phase. In its most symmetric form, this is simply the O(3) φ^4 field theory:

$$\mathcal{L}_H = \frac{1}{2} ((\partial_\mu \varphi_a)^2 + s_H \varphi_a^2) + \frac{u_H}{4!} (\varphi_a^2)^2, \quad (5.15)$$

where $a = x, y, z$ and $s_H < 0$. In the ordered phase, we parameterize the fluctuations of φ_a by

$$\varphi_a = (\sqrt{2}\text{Re}(\Psi_{XY}), \sqrt{2}\text{Im}(\Psi_{XY}), \langle \Psi_I \rangle + \Psi'_I), \quad (5.16)$$

where here $\langle \Psi_I \rangle = \sqrt{-6s_H/u_H}$, and Ψ_{XY} and Ψ'_I are fluctuating complex and real fields respectively. Inserting (5.16) into (5.15) we obtain the Lagrangian controlling the fluctuations about the ordered state:

$$\begin{aligned} \mathcal{L}_H = & |\partial_\mu \Psi_{XY}|^2 + \frac{1}{2} (\partial_\mu \Psi'_I)^2 + |s_H| (\Psi'_I)^2 \\ & + \sqrt{\frac{|s_H| u_H}{6}} \Psi'_I ((\Psi'_I)^2 + 2|\Psi_{XY}|^2) \\ & + \frac{u_H}{4!} ((\Psi'_I)^2 + 2|\Psi_{XY}|^2)^2 \end{aligned} \quad (5.17)$$

Two properties of this form of \mathcal{L}_H are especially noteworthy. First, there is no mass term for the complex field Ψ_{XY} , and so there are two gapless spin-wave modes at lowest order. Second, a number of cubic and quartic couplings are present, but their co-efficients have specific algebraic relations between them, tying them to the gap in the Ψ'_I mode ($\sqrt{2|s_H|}$) and the single quartic coupling u_H : these relations ensure that the gapless spin wave modes survive at all orders in perturbation theory.

We now search for an effective Lagrangian like (5.17) in \mathcal{L}' defined in (5.14). Without loss of generality, we take $\langle \Psi_I \rangle > 0$ and $w_I > 0$. Then, notice from (5.14) that the combination of the w_I cubic term and the presence of the Ψ_I condensate causes the mass of the ϕ_2 field to be significantly larger than the ϕ_1 field. So we proceed to integrate out ϕ_2 , along with the double-vortex field Φ which remains strongly gapped everywhere in Fig 10. The resulting effective Lagrangian for ϕ_1 and Ψ'_I has the ϕ_1 controlled by a model of scalar electrodynamics:

$$\begin{aligned} \mathcal{L}'' = & |(\partial_\mu - ib_\mu)\phi_1|^2 + \frac{\tilde{g}'}{2} (\epsilon_{\mu\nu\lambda} \partial_\nu b_\lambda)^2 + s'_1 |\phi_1|^2 + \frac{u'_1}{2} |\phi_1|^4 \\ & + \frac{1}{2} (\partial_\mu \Psi'_I)^2 + \frac{s'_I}{2} (\Psi'_I)^2 + \dots, \end{aligned} \quad (5.18)$$

where, at lowest order in the non-linearities,

$$s'_1 = s_1 - 2w_I \langle \Psi_I \rangle - 2w_I \Psi'_I. \quad (5.19)$$

We are now ready to make our key non-trivial observation. We use the well-established result³⁸ that the scalar electrodynamics model is dual, in the continuum, to an O(2) φ^4 field theory in three spacetime dimensions. Performing this duality on the ϕ_1, b_μ degrees of freedom in (5.18), we conclude that \mathcal{L}'' is equivalent to the following dual continuum Lagrangian

$$\begin{aligned} \mathcal{L}_D = & |\partial_\mu \Psi_{XY}|^2 + s_{XY} |\Psi_{XY}|^2 + \frac{u_{XY}}{4!} |\Psi_{XY}|^4 \\ & + \frac{1}{2} (\partial_\mu \Psi'_I)^2 + \frac{s'_I}{2} (\Psi'_I)^2 + \dots, \end{aligned} \quad (5.20)$$

where the two-component field of the O(2) φ^4 field theory has been written as the complex field Ψ_{XY} ; this field has a complicated non-local relationship to ϕ_1 and b_μ . Further, the parameters s_{XY} and u_{XY} are determined by the couplings s'_1, u'_1 , and \tilde{g}' in (5.18). The linear dependence of s'_1 on Ψ'_I in (5.19) implies that the coupling in \mathcal{L}_D also have linear dependence on Ψ'_I . With this dependence, the similarity between the (5.20) and O(3) symmetric model \mathcal{L}_H in (5.17) becomes evident: the Ψ'_I dependence of s'_1 will lead to cubic terms like those in (5.17). A suitable choice of the couplings in \mathcal{L}' can clearly ensure that its dualized version obeys the same constraints on its couplings as those required by O(3) symmetry in \mathcal{L}_H . In particular, the mass s_{XY} in \mathcal{L}_D remains pinned to 0 along this O(3)-symmetric subspace, as is needed to obtain two linearly dispersing spin-wave modes in the HN state. This establishes our claim that HN order appear in a subspace with the XY+I phase.

We have sketched a possible line with $SU(2)$ symmetry restored in Fig 10. A portion of it is in a phase with co-existing $XY+I$ order, but it also continues along the first-order boundary between the XY and I phases; all our above arguments also apply along such a boundary. However, within the phases found in Fig 10, there is no simple and natural way to extend this $SU(2)$ -symmetric line into a non-magnetic phase. If we move above along the vertical line $s_1 = 0$ in Fig 10, we eventually reach the second-order boundary between the XY and I phases: we argued earlier that this line cannot be $SU(2)$ symmetric. It is possible to choose parameters such the end-points of the two first-order lines in Fig 10 co-incide: then the $SU(2)$ symmetric line can be extended into the non-magnetic BC phase, and we have the possibility of a second-order transition between the HN and BC phases in a system with $SU(2)$ symmetry. But this case is non-generic as there does not appear to be any fundamental reason for the two end-points to merge. This conclusion is also entirely consistent with our earlier considerations in Section III.

To find a more natural scheme for a transition to a non-magnetic state with $SU(2)$ symmetry we have to search the phase diagram in a regime beyond the cross-section in Fig 10. This we will do in the following subsections.

2. $SU(2)$ symmetry with bond order

A very useful cross-section of the phase diagram is that controlled by s_I and s_{BC} . This is sketched in Fig 11 in the regime $s_1 > 0$ and $s_2 > 0$. As in Section V C, the $XY+I$ phase is a reasonable candidate for $SU(2)$ symmetry and HN order. Here we discuss the question of whether it is possible to continue the line of $SU(2)$ symmetry into the $XY+BC+I$ phase, and then further into the non-magnetic BC phase.

We begin our discussion by the spectrum of excitations in the BC phase. This is a confining phase with the fields $\phi_{1,2}$ condensed (see Table IV). As noted in Table II, the excitations with non-zero total S_z are gapped $\pm 2\pi$ vortices in $\phi_{1,2}$ (the relative phases of ϕ_1 and ϕ_2 are pinned to each other): these vortices have total $S_z = \pm 1$. In a BC phase with $SU(2)$ symmetry this doublet of excitations must be part of a $S = 1$ triplet—this is the familiar $S = 1$ gapped spin exciton expected above a dimerized insulator. We will now identify the missing $S_z = 0$ excitation which completes this degenerate triplet along a special line within the BC phase. We will also show that condensation of this triplet leads to the $BC+HN$ phase, and the latter phase naturally lies along a line within the $XY+BC+I$ phase. Thus we will be able to justify the entire trajectory of the $SU(2)$ symmetric line in Fig 11.

Within the BC or $BC+XY+I$ phases, the field Ψ_{BC} is condensed. So we can safely replace Ψ_{BC} by $\langle \Psi_{BC} \rangle$; fluctuations of Ψ_{BC} about this value are massive and do not play an important role in our considerations here. Let

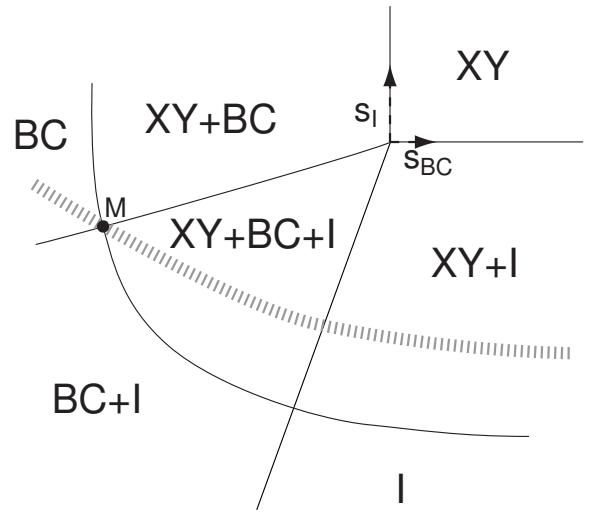


FIG. 11. Schematic mean field phase diagram of \mathcal{L}' in (5.14) as a function of s_{BC} and s_I with $s_1 > 0$ and $s_2 > 0$. The conventions for the phase boundaries are as in Fig 7. The grey hatched line represents a possible line along which $SU(2)$ symmetry is restored: this line begins within the $XY+I$ phase, continues into the $XY+BC+I$ phase, and finally into the non-magnetic BC phase; note that sequence of transitions along this line (moving right to left) is identical to that in Fig 2 (moving left to right), and also to that discussed in Section III. Upon going beyond mean-field theory, it is expected that tetracritical point M will turn into two bi-critical points separated by a short first order boundary between the $XY+BC$ and $BC+I$ phases; the line of $SU(2)$ symmetry will overlap this first-order line.

us examine the effective action for $\phi_{1,2}$ and Ψ_I fluctuations in phases with $\langle \Psi_{BC} \rangle \neq 0$. Consider the quadratic form controlling $\phi_{1,2}$; from (5.12) and (5.14), this has the form:

$$|\partial_\mu \phi_1|^2 + |\partial_\mu \phi_2|^2 + s_1(|\phi_1|^2 + |\phi_2|^2) - w_{BC} (\langle \Psi_{BC} \rangle \phi_1 \phi_2^* - \langle \Psi_{BC}^* \rangle \phi_1^* \phi_2). \quad (5.21)$$

Without loss of generality, we can assume that $w_{BC} > 0$ and $\langle \Psi_{BC} \rangle$ is real. With these values, the quadratic form (5.21) is diagonalized by the linear combinations $\phi = (\phi_1 + \phi_2)/\sqrt{2}$ and $\phi' = (\phi_1 - \phi_2)/\sqrt{2}$. The eigenvalue of ϕ' is larger than that of ϕ , and so we integrate out ϕ' and express the effective action \mathcal{L}' in terms of ϕ and Ψ_I . The result has a very simple structure. In particular, there is no cubic residual cubic coupling between Ψ_I and ϕ which arises from the w_I term in (5.14); in terms of ϕ , ϕ' , the term proportional to w_I is $\Psi_I(\phi\phi'^* + \phi'^*\phi)$, and upon integrating out ϕ' this leads only to the quartic coupling $|\phi|^2|\Psi_I|^2$ between the modulus-squared of the two fields. With these considerations, the new form of \mathcal{L}' in (5.14), in the phases with Ψ_{BC} condensed is

$$\mathcal{L}_{BC} = |(\partial_\mu - ib_\mu)\phi|^2 + \frac{\tilde{g}'}{2}(\epsilon_{\mu\nu\lambda}\partial_\nu b_\lambda)^2 + s|\phi|^2 + \frac{u}{2}|\phi|^4 + \frac{1}{2}(\partial_\mu \Psi_I')^2 + \frac{s_I}{2}(\Psi_I')^2 + \frac{u_I}{2}|\Psi_I|^4 + v_I|\phi|^2|\Psi_I|^2. \quad (5.22)$$

The $S_z = \pm 1$ excitations are the vortices in ϕ , and so we should naturally proceed to a duality transformation on the ϕ , b_μ degrees of freedom. These fields are controlled by scalar electrodynamics and so the transformation is similar to that discussed below (5.19). Scalar electrodynamics is dual to the $O(2)$ φ^4 field theory³⁸, and, as before, we express this in terms of the complex field Ψ_{XY} (which is nothing but the field operator for $\pm 2\pi$ vortices in ϕ). So \mathcal{L}_{BC} turns out to be dual to

$$\mathcal{L}_{BC}^D = |\partial_\mu \Psi_{XY}|^2 + s_{XY}|\Psi_{XY}|^2 + \frac{u_{XY}}{2}|\Psi_{XY}|^4 + \frac{1}{2}(\partial_\mu \Psi_I')^2 + \frac{s_I}{2}(\Psi_I')^2 + \frac{u_I}{2}\Psi_I'^4 + v_I'|\Psi_{XY}|^2\Psi_I'^2. \quad (5.23)$$

Now the connection between the \mathcal{L}_{BC}^D and the $O(3)$ φ^4 fields theory is plainly visible: for $s_{XY} = s_I$ and $u_{XY} = v_I' = 4u_I$ the theory in (5.23) is precisely \mathcal{L}_H in (5.15) after we identify $\varphi_a = (\sqrt{2}\text{Re}(\Psi_{XY}), \sqrt{2}\text{Im}(\Psi_{XY}), \Psi_I')$. So we have shown that $SU(2)$ symmetry is restored with these restrictions on the couplings. For $s_H = s_I = s_{XY} > 0$, the theory \mathcal{L}_H is in the BC phase and φ_a is the field operator for the required gapped $S = 1$ spin exciton; the gapped, $S_z = 0$ particle associated with Ψ_I has combined with the $S_z = \pm 1$ vortices in ϕ to yield the required triply degenerate particle. For $s_H < 0$, we have long-range HN order induced by the condensation of the $S = 1$ exciton; this corresponds to moving along the hatched line in Fig 11 from the BC phase to the XY+BC+I phase. The critical properties of the transition from the BC phase to the BC+HN phase are described by the familiar $O(3)$ φ^4 field theory in (5.15).

The above considerations clearly do not apply to the transition from the BC+XY+I phase to the XY+I phase: long-range BC order was assumed to be present above, and this becomes critical here. The line with $SU(2)$ symmetry plays no special role at this transition, and it is described simply by a field theory for Ψ_{BC} alone, which is obtained by setting all other fields in \mathcal{L}' to zero. The coupling to the gapless spin-wave modes of the XY (or HN) order is irrelevant⁶.

All the theoretical justification for the trajectory of the $SU(2)$ symmetric line in Fig 11 has now been provided. It is satisfying that the sequence of phases along this line (moving right to left) is identical to that presented in Fig 2 (moving left to right). Entirely independent theoretical arguments for the sequence in Fig 2 were presented in Section III using methods that preserved $SU(2)$ symmetry at all stages, in contrast to those discussed in the present section.

Further examination of Fig 11 also suggests an apparently exotic circumstance under which there could be a second order transition between the HN and BC states. This happens if parameters are such that the XY+BC+I phase has just been shrunk to vanishing size *i.e.* the three multicritical points in Fig 11 have just coalesced into one, and the line of $SU(2)$ symmetry passes through this coalesced point. Such a point does appear to represent a multicritical point, requiring the tuning of more than one parameter, but we cannot definitively rule out that accessing such a point in the subspace of $SU(2)$ symmetry requires only one tuning parameter. In any event, this reasoning does lead to a candidate field theory for the critical point between the HN and BC phases (multicritical or not): it is the field theory \mathcal{L}' in (5.14) with the primary fields $\phi_{1,2}$, b_μ , Ψ_{BC} and Ψ_I all critical, while Φ is massive and can be integrated out.

3. Interplay with fractionalization

The previous section paid particular attention to the role of BC order in the phase diagram of the field theory \mathcal{L}' in (5.14). This section will carry out the complementary analysis for the case of F order. We will also address the issue of whether $SU(2)$ symmetry can be found in such phases. We argued earlier, in Section II that F phases are not found in the class of $SU(2)$ symmetric systems that have been considered so far: our discussion below will further support this conclusion. However, we remind the reader that in the following Section VI we will introduce a new class of models which do have F order and $SU(2)$ symmetry.

As a prelude to our discussion, we determine a section of the mean-field phase diagram of (5.14) as a function of s_2 (which controls condensation of the field Φ essential to the appearance of F order) and s_I (which controls the I order necessary for the presence of phases with $SU(2)$ symmetry). The other two ‘masses’, s_1 and s_{BC} are

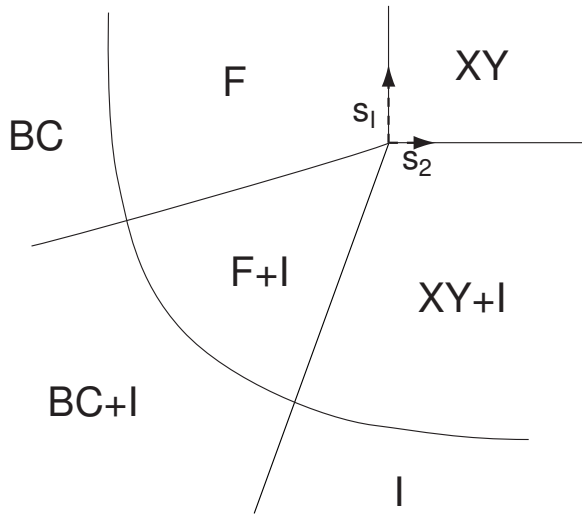


FIG. 12. Schematic mean field phase diagram of \mathcal{L}' in (5.14) as a function of s_2 and s_I with $s_I > 0$ and $s_{BC} > 0$. The conventions for the phase boundaries are as in Fig 7. As we discuss in Section VC3, there is no reasonable case for a line of SU(2) symmetry in this phase diagram, apart from within the XY+I and BC phases.

taken to be positive. The results are shown in Fig 12.

Let us focus our attention on the F phase in Fig 12 and ask if it is possible for it to possess SU(2) symmetry. A simple argument shows that this is not possible, at least in the framework of the continuum models described by \mathcal{L}' . From Table IV, only the field Φ is condensed in the F phase. As was noted in Table II, vortices with phase winding $\pm 2\pi$ in the field Φ carry boson charge 1/2, and are therefore the $S_z = \pm 1/2$ spinon excitations about the F state. (Note that such vortices were not possible in the BC states of Fig 11 and 12 because the field $\phi_{1,2}$ was condensed and this would be double-valued around a $\pm 2\pi$ vortex in the Φ field). A theory for these spinons follows by setting the massive fields $\phi_{1,2} = 0$ in \mathcal{L} in (5.12). The resulting Lagrangian for Φ is (again) simply that of scalar electrodynamics. Just as in Sections VC 1 and VC 2, we can dualize this to an $O(2)$ φ^4 field theory, which we now express in terms of the complex scalar Ψ_{sp} . This Ψ_{sp} is the field operator for the $S_z = \pm 1/2$ spinons, and is (roughly) the ‘square-root’ of the field Ψ_{XY} in (5.23); it is controlled by a ‘ $|\Psi_{sp}|^4$ ’ field theory identical in form to that for Ψ_{XY} in (5.23). Our purpose here was to search for SU(2) symmetry in the theory of Ψ_{sp} and it is evident that this is not possible in such a field theory which only has a U(1) symmetry. The single spinon states with $S_z = \pm 1/2$ are degenerate and so do form an SU(2) doublet; however, there is no reason, in the presence of the $|\Psi_{sp}|^4$ interaction, for the S-matrices of the multi-spinon states to possess SU(2) symmetry.

To further confirm this conclusion, let us look at states in the vicinity of the F state and examine whether any

of them can have SU(2) symmetry. While the XY state shares a phase boundary with F in Fig 12, note that the I phase does not: this prevents the XY+I state from being connected to the F state except across a special multicritical point. The general reasons for the separation of the I and F states were noted earlier at the end of Section VB in the discussion around (5.13)—this conclusion also holds in the presence of BC order: one can show by a very similar argument that it is not possible for the F+BC and the F+I states to share a second order phase boundary. As we discussed in Section VC 1, the XY+I state does possess a line of SU(2) symmetry along which there is HN order. We can now try to connect this to the F state in Fig 12. We clearly cannot proceed across either the F+I state or the XY state as these states have anisotropic magnetic order which explicitly break SU(2) symmetry. The only remaining possibility is to access the F state directly across the multicritical point at $s_I = s_2 = 0$. However this is also not plausible: if the multicritical point was SU(2) symmetric, we would expect it to respond symmetrically to a uniaxial anisotropy with respect to I and XY orders, and to be flanked symmetrically either by I+F and XY+F states, or by I and XY states. This is clearly not the case in Fig 12.

So in agreement with the arguments in Section II, we have found no plausible line of SU(2) symmetry in Fig 12 which can extend into the F state. Consequently, we have also not found a direct transition between the HN and F states.

VI. FRACTIONALIZATION WITH SU(2) SYMMETRY, AND NON-COLLINEAR SPIN CORRELATIONS

This section will expand upon the theory of fractionalization in two-dimensional spin systems originally presented in Refs 14–18. This formulation will exhibit the intimate connection between fractionalized phases and non-collinear spin correlations. Our treatment here will also incorporate insights gained from the recent analyses of Refs 8–10: in particular our phase diagrams here contain a new phase (the HN+F phase) not considered in the original treatment.

The treatment here will apply to frustrated $S = 1/2$ antiferromagnets on the square lattice like those in (1.1). In particular, the model with first, second, and third neighbor exchange (the so-called J_1 - J_2 - J_3 model) has magnetically ground states with spiral spin order, and fractionalized paramagnetic states could appear in its vicinity. Further, the same general theory should also apply to magnetically ordered and paramagnetic phases of other frustrated lattices in two dimensions, including the triangular lattice. The case of the triangular lattice was considered in Refs. 17,39: its three sublattice magnetically ordered state can be viewed as the limiting case of a spiral state on a distorted square lattice whose

wavevector has been pinned at a special value determined by triangular symmetry.

As in Refs 14,15, we will present the theory here using CP^1 degrees of freedom. In the body of the paper so far, we have used the $O(3)$ vector \mathbf{n}_j to represent the local orientation of the antiferromagnetic order. The close relationship of this previous formulation to the CP^1 approach is discussed in Appendix A: a reading of this appendix is a prerequisite to the discussion in the present section. The primary actor in CP^1 formulation is a complex spinor $z_{j\alpha}$ ($\alpha = \uparrow, \downarrow$) of unit modulus ($\sum_{\alpha} |z_{j\alpha}|^2 = 1$) which is related to \mathbf{n}_j by (A2), which we reproduce here for completeness:

$$n_{ja} = z_{j\alpha}^* \sigma_{\alpha\beta}^a z_{j\beta} \quad (6.1)$$

with $a = x, y, z$ a spin index, and σ^a the Pauli matrices. This representation has the disadvantage of introducing redundant degrees of freedom associated with the local compact $U(1)$ gauge symmetry $z_{j\alpha} \rightarrow e^{i\phi_j} z_{j\alpha}$. However, as was also the case in the treatment of Shraiman and Siggia⁴⁰ of doped antiferromagnets, it allows for an especially simple theory of the appearance of non-collinear, spiral spin correlations. Furthermore, the $z_{j\alpha}$ quanta carry spin $S = 1/2$, are therefore natural candidates for spinon excitations in fractionalized paramagnetic phases.

As a prelude to writing down our model, we need to understand the characterization of non-collinear spin correlations in terms of the $z_{j\alpha}$. Consider the spin correlations between two near neighbor sites $j = 1, 2$. In the context of models like (1.4) and (A3), the optimum configuration of \mathbf{n}_1 and \mathbf{n}_2 is to have them parallel to each other: such a state has $|z_{1\alpha}^* z_{2\alpha}|^2 = 1$, and simultaneously $\epsilon_{\alpha\beta} z_{1\alpha}^* z_{2\alpha} = 0$. We would like to an energetic preference for the \mathbf{n} vector to rotate by a non-zero angle in moving from site 1 to site 2: this can be ensured by demanding that $|\epsilon_{\alpha\beta} z_{1\alpha}^* z_{2\alpha}|^2 \neq 0$, while $|z_{1\alpha}^* z_{2\alpha}|^2$ remains non-zero. So, natural order parameters for non-collinear spin correlations are the two fields

$$Q_{j\varrho} \sim \epsilon_{\alpha\beta} z_{j\alpha} z_{j+\hat{\varrho},\beta}, \quad (6.2)$$

where the index ϱ will always extend over $\varrho = x, y$. These fields are not gauge invariant and preserving gauge symmetry will, of course, be essential in determining the structure of the effective action. Notice also that in the continuum limit, $Q_{\varrho} \sim \epsilon_{\alpha\beta} z_{\alpha} \partial_{\varrho} z_{\beta}$, which is the spiral order parameter used by Shraiman and Siggia⁴⁰ and in Ref. 15. The form of the order parameter chosen in (6.2) corresponds to spin spirals along the (1, 0) and (0, 1) directions of the square lattice. Clearly, it is possible to have antiferromagnets in which the spiral correlations are oriented along the (1, ± 1) or other directions: there is a corresponding modification of the order parameter in these cases, but we will not present this simple generalization explicitly here.

To fully explore the phase diagram of our model, we find it convenient to introduce explicitly the real, Néel, order parameter vector \mathbf{N}_j . This is the $O(3)$ symmetric

combination of the orders Ψ_{XY} and Ψ_I considered in Section V C. Clearly

$$N_{ja} \sim z_{j\alpha}^* \sigma_{\alpha\beta}^a z_{j\beta}, \quad (6.3)$$

where $a = x, y, z$. Also it is evident that $\mathbf{N}_j \sim \mathbf{n}_j$, but we prefer to use an independent symbol here as the physical context is different, and we do not impose a unit length constraint on \mathbf{N}_j .

We can now write down the partition function for quantum antiferromagnets with $SU(2)$ symmetry. The expression here generalizes Z_{cp} in (A3) of Appendix A by allowing for non-collinear spin correlations

$$\begin{aligned} Z_P &= \sum_{\{q_{j\mu}\}} \int_0^{2\pi} \prod_{j\mu} dA_{j\mu} \int \prod_{j\alpha} dz_{j\alpha} \delta(|z_{j\alpha}|^2 - 1) \\ &\int \prod_{j\varrho} dQ_{j\varrho} \int \prod_{j\alpha} d\mathbf{N}_j \exp \left(-S_z - S_A - \tilde{S}_B - S_Q - S_N - S_w \right) \\ S_Q &= -\frac{1}{gQ} \sum_{j\mu\varrho} Q_{j\varrho} e^{2iA_{j\mu}} Q_{j+\hat{\mu},\varrho} + \text{c.c.} + \sum_{j\varrho} V_Q (|Q_{j\varrho}|^2) \\ S_N &= -\frac{1}{gN} \sum_{j\mu} \mathbf{N}_j \cdot \mathbf{N}_{j+\hat{\mu}} + \sum_j V_N (\mathbf{N}_j^2) \\ S_w &= -w_Q \sum_{j\varrho} Q_{j\varrho}^* \epsilon_{\alpha\beta} z_{j\alpha} z_{j+\hat{\varrho},\beta} e^{iA_{j\nu}} + \text{c.c.} \\ &\quad - w_N \sum_j N_{ja} z_{j\alpha}^* \sigma_{\alpha\beta}^a z_{j\beta}. \end{aligned} \quad (6.4)$$

As stated earlier, all sums over ϱ extend only over x, y , while those over μ extends over x, y, τ . The expressions for the first three terms in the action were given earlier in (A3); these are: S_z , the hopping term for the z_{α} , S_A , the Maxwell term for the compact $U(1)$ gauge field $A_{j\mu}$, and \tilde{S}_B , the Berry phase of the underlying $S = 1/2$ spins. The symmetry of the problem clearly permits a more anisotropic nearest neighbor coupling in S_Q , but we have written down an isotropic form for notational simplicity. Suitable factors of the exponential of the compact $U(1)$ gauge field $A_{j\mu}$ have been inserted to ensure that the action is invariant under the $U(1)$ gauge transformations

$$\begin{aligned} z_{j\alpha} &\rightarrow z_{j\alpha} e^{i\phi_j} \\ Q_{j\varrho} &\rightarrow Q_{j\varrho} e^{2i\phi_j} \\ A_{j\mu} &\rightarrow A_{j\mu} - \Delta_{\mu} \phi_j \end{aligned} \quad (6.5)$$

where ϕ_j represents an arbitrary phase. The potentials in S_Q and S_N are given, as usual, by

$$V_{\sharp}(x) = \frac{1}{2} (s_{\sharp} x + u_{\sharp} x^2) \quad (6.6)$$

where $\sharp \equiv Q, N$. The allowed cubic terms between the fields have been explicitly written out in S_w . A number of quartic terms coupling the modulus squared of all the fields are also allowed but we have not written them out for simplicity.

The model Z_P in (6.4) is our global theory for the phases and phase transitions of quantum antiferromagnets. We believe it offers a complete theory of the universal properties of $S = 1/2$ antiferromagnets in two dimensions with $SU(2)$ symmetry on a variety of bi-partite and non-bi-partite lattices. Further, all its phases have the obvious generalization to cases where $SU(2)$ symmetry is broken weakly by an easy-plane or easy-axis anisotropy: HN order will transform to the corresponding XY or I order.

Various symmetries have played a crucial role in determining the structure of Z_P , and will obviously also be important in the analysis of its phase diagram. The foremost among these is the compact $U(1)$ gauge invariance associated with (6.5). Along with the gauge field $A_{j\mu}$, we have two “matter” fields: the unit charge field $z_{j\alpha}$, and the charge 2 field $Q_{j\varrho}$. The phases of such a gauge theory were discussed by Fradkin and Shenker⁴¹, and we review the essential needed results. For the pure gauge theory (without matter), the weak-coupling (small e^2) regime is continuously connected to the strong-coupling (large e^2) regime, and both of which exhibit confinement of unit charges. In the presence of charge 1 matter fields, one might expect a separate “Higgs” phase where the matter field has condensed: however, this charge 1 Higgs regime is continuously connected to the confining phase, and there are no intervening phase transitions (at least none associated with the gauge theory—other symmetries could (and do) lead to phase transitions). Upon adding the charge 2 fields, their condensation does lead to a charge 2 Higgs phase, which is separated from the remainder of the phase diagram by a phase transition: unit charges are deconfined in this Higgs phase, while they are confined elsewhere.

The second important symmetry is the global $SU(2)$ invariance: $z_{j\alpha}$ transforms like a spinor under this symmetry, while \mathbf{N}_j transforms like a vector; all other fields are $SU(2)$ singlets. This symmetry is broken in phases with HN or P order, and their properties will be discussed further in Section VIB below.

Finally, Z_P is invariant under the square lattice point group D_4 . These symmetries can also be broken, leading to new phases. As we have seen in the previous sections of this paper, the Berry phase term can induce BC order, which breaks D_4 symmetry. In a region where $Q_{j\varrho}$ is suppressed (and so we can neglect the presence of a charge 2 Higgs fields), the compact $U(1)$ gauge theory is always in a confining phase, and (as we noted above) there can be no phase transitions associated with it; nevertheless, Berry phases can induce a transition between the HN and HN+BC phases (both of which are confining) associated with D_4 symmetry breaking. In the region where $Q_{j\varrho}$ is non-negligible, another type of D_4 symmetry-breaking becomes possible. Notice from (6.2) that $Q_{j\varrho}$ transforms like a spatial vector (the E representation): it is *odd* under reflections, and its components map into each other under 90° rotations. Consequently, the Higgs phase where $Q_{j\varrho}$ is condensed can also break

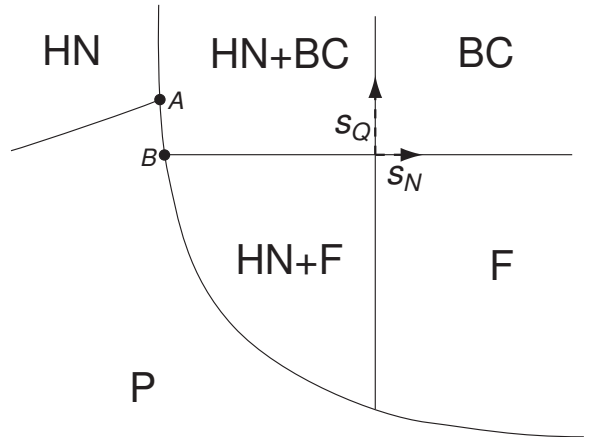


FIG. 13. Section of the proposed global phase diagram of Z_P in (6.4) as a function of s_N and s_Q for moderately large values of g , g_Q and g_N . The phases with F order are likely to have “bond-nematic” order over a substantial (and possibly) portion of their domain. Bond-nematic order corresponds to a preferential polarization of the spin correlations along the x or y axes, and spontaneously reduces the lattice symmetry from D_4 (tetragonal) to D_2 (orthorhombic). The nature of the phase boundaries near the multi-critical points A and B is uncertain, and a direct second-order transition between the HN+F and HN states also appears possible; this is discussed further in Appendix H. Most of the P phase has coplanar spin order, but portions do have non-coplanar: the latter order appears in the region contiguous to the HN+F phase; the phase boundary between coplanar and non-coplanar spin order is not shown. This phase boundary meets that between the F and HN+F phases, and so the point where the P, HN and HN+F phases meet is tetracritical.

D_4 symmetry: we will see that the paramagnetic F phase can also have “bond nematic” order^{15,42}, associated with the choice of condensation between Q_{jx} and Q_{jy} . Note also that although $Q_{jx} \rightarrow -Q_{jx}$ under a reflection along the y axis, condensation of Q_{jx} does not imply loss of this reflection symmetry: Q_{jx} also carries a compact $U(1)$ gauge charge, and this change of sign can be undone by a gauge transformation.

Careful consideration of the above symmetries, and insights from the analyses of the previous section, lead to sections of the proposed phase diagram for Z_P in Fig 13 and 14. We also present a summary of the characterizations of the various phases in terms of the fields in Z_P (and in Z'_P below) in Table V. We will describe various portions of this global phase diagram in the following subsections.

A. Connection with Z_2 gauge theory

The phases of the compact $U(1)$ gauge theory noted above provide the most complete description of the phase

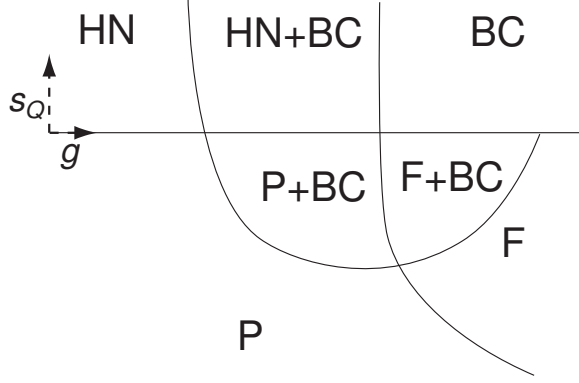


FIG. 14. As in Fig 13, but as a function of g and s_Q for s_N large and positive, and for moderately large values of g_Q and g_N .

| State | Description |
|-------|--|
| HN | \mathbf{N}_j is condensed, $Q_{j\ell}$ are massive, and unit charges of the compact $U(1)$ gauge theory Z_P are confined. As this is continuously condensed to the charge-1-Higgs phase, we can also view the z_α as condensed. This phase cannot be described by the Z_2 gauge theory Z'_P . |
| BC | \mathbf{N}_j , $Q_{j\ell}$ are massive, and unit charges of the compact $U(1)$ gauge theory Z_P (or the Z_2 gauge theory Z'_P) are confined. The Berry phases induce BC order |
| HN+BC | As in the HN state, but the Berry phases induce BC order, and this phase also appears in Z'_P . |
| F | \mathbf{N}_j and z_α are massive, while condensation of $Q_{j\ell}$ puts the compact $U(1)$ gauge theory in its charge-2-Higgs/deconfined phase; the Z_2 gauge theory is also deconfined and the z_α quanta are liberated. Bond-nematic order is likely to be present over a substantial portion of the F state. |
| F+BC | As in the F state, but BC order is also present. |
| HN+F | As in the F state, but \mathbf{N}_j is condensed. |
| P | \mathbf{N}_j , $Q_{j\ell}$ are condensed, and unit charges of the compact $U(1)$ gauge theory Z_P (or the Z_2 gauge theory Z'_P) are confined; consequently, as in the HN state, we can also view the z_α as condensed. |
| P+BC | As in the P state, but BC order is also present. |

TABLE V. Summary of all the phases in Figs 13 and 14 and their physical properties.

diagram of Z_P . However, in some portions of this phase diagram a simpler description may be provided by a Z_2 gauge theory^{14–16,18}. This reduction will also allow us to note the connection to the work of Senthil and Fisher⁸. However, it is important to note that the Z_2 theory below does *not* provide a complete description of the phases and phase transitions in Figs 13 and 14: we will argue below that it does not contain the familiar Néel (HN) state, or its phase boundaries.

The reduction to the Z_2 gauge theory is most naturally observed in the limit $r_Q \ll 0$. Here $Q_{j\ell}$ is expected to be large (at least on short scales), and by the Higgs phenomenon, this will also suppress fluctuations in the flux of $A_{j\mu}$. However, because $Q_{j\ell}$ carries charge 2, a gauge flux of π is invisible to it, while the unit charge fields $z_{j\alpha}$ do observe such a flux. To allow only such fluxes, we can safely assume that $e^{iA_{j\mu}}$ is pinned to ± 1 by the large values of $Q_{j\ell}$. So we write

$$e^{iA_{j\mu}} = s_{j,j+\hat{\mu}} \quad (6.7)$$

where $s_{j,j+\hat{\mu}} = \pm 1$ is an Ising gauge field on the links of the direct lattice; it is similar to the Z_2 gauge field in (1.15), and hence to that in Ref. 8. Clearly the field $z_{j\alpha}$ carries unit Z_2 gauge charge, while \mathbf{N}_j and $Q_{j\ell}$ are neutral.

Despite the quenching of the gauge charges associated with $Q_{j\ell}$, we cannot entirely neglect their fluctuations. This is because we still have to account for their transformations under the D_4 lattice symmetry and the associated symmetry breaking. So we introduce additional Ising variables, π_{jx} and π_{jy} by the correspondence

$$Q_{j\ell} \sim \pi_{j\ell}; \quad (6.8)$$

$\pi_{j\ell}$ also transforms under the E representation of D_4 . Ordering transitions in the $\pi_{j\ell}$ will signal D_4 symmetry breaking with the appearance of bond-nematic order. It is important to note that despite being Ising spin variables, the $\pi_{j\ell}$ are *neutral* under the Z_2 gauge field $s_{j,j+\hat{\mu}}$.

With the above parameterizations, we can reduce Z_P in (6.4) to the following Z_2 gauge theory

$$\begin{aligned}
Z'_P = & \sum_{\{s_{j,j+\hat{\mu}}=\pm 1\}} \sum_{\{\pi_{j\ell}=\pm 1\}} \int \prod_{j\alpha} dz_{j\alpha} \delta(|z_{j\alpha}|^2 - 1) \\
& \int \prod_{ja} d\mathbf{N}_j \exp(-S'_z - S_N - S'_w - S_s - S_\pi) \\
S'_z = & -\frac{1}{g} \sum_{j\mu} z_{j\alpha}^* s_{j,j+\hat{\mu}} z_{j+\hat{\mu},\alpha} + \text{c.c.} \\
S'_w = & -w_Q \sum_{j\ell} \pi_{j\ell} s_{j,j+\ell} \epsilon_{\alpha\beta} z_{j\alpha} z_{j+\hat{\ell},\beta} + \text{c.c.} \\
& - w_N \sum_j N_{ja} z_{ja}^* \sigma_{\alpha\beta}^a z_{j\beta} \\
S_s = & -K \sum_{\square} \prod_{\square} s_{j,j+\hat{\mu}} + i\frac{\pi}{2} \sum_j (1 - s_{j,j+\hat{\tau}})
\end{aligned}$$

$$S_\pi = -\frac{1}{g'_Q} \sum_{j\mu\varrho} \pi_{j\varrho} \pi_{j+\hat{\mu},\varrho} + v_\pi \sum_{j\mu} (\pi_{jx} \pi_{j+\hat{\mu},x}) (\pi_{jy} \pi_{j+\hat{\mu},y}), \quad (6.9)$$

where S_N is as defined in (6.4), the coupling g'_Q is a consequence of g_Q in Z_P , and K derives from the Maxwell term (proportional to $1/e^2$) in (A3). We have also added a term proportional to v_π , a repulsive interaction between the energies of the Ising variables π_{jx} and π_{jy} : this ensures that when these fields order, the system will choose between orderings of one or the other, and the bond-nematic or spiral order will be polarized along the (1,0) or (0,1) directions. As we noted earlier, a different choice of variables should be made for polarization of the spiral order in other directions.

The simplest application of the Z_2 gauge theory, Z'_P , is in the phases in which the $SU(2)$ symmetry is preserved. Here we may integrate out the $z_{j\alpha}$ and \mathbf{N}_j fields and the action simply becomes $S_s + S_\pi$, along with additional couplings between $s_{j,j+\hat{\mu}}$ and $\pi_{j\varrho}$ which preserve gauge invariance and D_4 symmetry. The model S_s is, of course, identical to the Z_2 gauge theory obtained in the $g \rightarrow \infty$ limit of (1.15) and was studied in Section V; it is dual to the fully frustrated Ising model in (5.10). It has a confining phase at small K with BC order, and a deconfined phase at large K in which integer Z_2 charges (like the z_α) are liberated—this is the F phase. So the present model describes the F and BC phases appearing for large r_N in Fig 13 and for large g in Fig 14. An extension of this model with more complicated couplings between the Ising gauge spins could also lead to the F+BC phase in Fig 14. The ordering of the $\pi_{j\varrho}$ variables leads to bond-nematic order: such order is already present in the BC phase and is therefore not significant there. On the other hand, in F phase the bond-nematic yields a preferential polarization of spin correlations along the x or y axes, and breaks the D_4 symmetry down to D_2 . In principle, the bond-nematic ordering and the deconfinement transitions are independent and can occur at distinct positions. However, in the large N theory of Refs. 14,15 these two transitions co-incident and the F state had bond-nematic order over its entire domain; we expect here that bond-nematic order will be present over a substantial, if not complete, portion of the phases with F order.

A similar description of these two non-magnetic phases can also be obtained starting from the compact $U(1)$ gauge theory in (6.4). Again, we integrate out the $z_{j\alpha}$ and \mathbf{N}_j and end up with the theory of a compact $U(1)$ gauge field coupled to a charge 2 scalar. The latter theory was described in Ref. 18 and possesses a transition between BC and F phases identical to that described by the Z_2 gauge theory S_s .

We now attempt to extend the above study of the Z_2 gauge theory, Z'_P , to the remaining phases in Figs 13 and 14 with broken $SU(2)$ symmetry, and will quickly run into a problem; we will have to return to the original compact $U(1)$ gauge theory, Z_P , to rectify the situation. As we will see in Section VIB, all the magnet-

ically ordered phases have $\langle \mathbf{N}_j \rangle \neq 0$. So let us assume that $\langle \mathbf{N} \rangle = N_0(0,0,1)$. Gauge-invariant fluctuations of \mathbf{N} about this direction will lead to the two required spin-wave modes. We now examine the gauge-dependent portions to check for the presence of other orderings. In the presence of $\mathbf{N} = (0,0,1)N_0$ and $w_N > 0$, we see from (6.9) that among the CP^1 fields, the $z_{j\uparrow}$ fluctuations will be preferred from the $z_{j\downarrow}$ fluctuations; this corresponds to an easy-axis anisotropy to the CP^1 model, in contrast to the easy-plane anisotropy considered in Appendix F. So we can safely neglect $z_{j\downarrow}$, and model the other component by a phase variable $z_{j\uparrow} = e^{i\theta_{j\uparrow}}$. The resulting effective action for the angle $\theta_{j\uparrow}$ and the Ising gauge field $s_{j,j+\hat{\mu}}$ in (6.9) is essentially identical to the model (1.15) which was studied in great detail in Section V (the $\pi_{j\varrho}$ Ising fields are innocuous spectators controlling the bond-nematic order). So we may directly apply the earlier results, especially the phase diagram in Fig 7 to the present situation. Because there is background Néel order with $\langle \mathbf{N} \rangle \neq 0$, the physical interpretation of the phases is now different. In particular, it is obvious that the BC phase in Fig 7 corresponds to the HN+BC phase in Figs 13 and 14, and the F phase of Fig 7 maps to the HN+F phase of Fig 13. The interpretation of the XY phase in Fig 7 is slightly more subtle: this state has a gapless Goldstone mode associated with the XY order, and in the present situation this must be combined with the two spin-wave modes of the \mathbf{N} order to yield a total of 3 gapless modes. This can only correspond to the P phase in Figs 13 and 14. As we will see below in Section VIB3 the \mathbf{N} order also gets spatially modulated in the P phase, and this is an effect that the present simple analysis misses. Similarly the XY+BC phase found in Fig 11 maps here onto the P+BC phase of Fig 14.

The most striking feature of the above analysis of phases with broken $SU(2)$ symmetry of the Z_2 gauge theory, Z'_P in (6.9), is that we achieved a description of all the phases and phase transitions in Figs 13 and 14 except those associated with the HN phase. In the above mapping of its properties to $Z_{U(1)}$ in (1.15), the HN phase requires a phase of $Z_{U(1)}$ with no broken symmetries and no fractionalization or topological order. No such phase was found in entire analysis of Section V, and so we conclude that Z'_P in (6.9) does not possess a HN phase. So we are in the slightly embarrassing position of having a sophisticated theory for the exotic states in Figs 13 and 14, but are not able to capture the simple and familiar Néel state. This situation is rectified by returning to the original compact $U(1)$ gauge theory Z_P in (6.4). As we will show in Section VIC and Appendix H, the compact $U(1)$ gauge boson (unlike the Z_2 gauge field) is able to quench the θ_{\uparrow} fluctuations without breaking any symmetries or inducing additional gapless modes, as is required in the HN state.

B. Phases with magnetic order

Now we describe more completely the phases in Figs 13 and 14 that break the spin rotation symmetry by a spontaneous magnetic polarization: such states will possess gapless spin-wave excitations. The phases in Sections VIB 1 and VIB 3 below can also co-exist with BC order, and this will (obviously) not change the structure of the gapless modes.

1. HN phase

This familiar Néel state is found in the regime with $r_Q > 0$ and $r_N < 0$. So the Q_ϱ fields are massive and can be neglected, while the \mathbf{N} field is condensed. The remaining degrees of freedom, A_μ and z_α , obey the standard action of 2+1 dimensional compact U(1) gauge field coupled to a complex scalar of charge 1, along with an additional Berry phase term. This latter theory is expected⁴¹ to always be in a confining phase: the Higgs phase where the unit charge complex scalar z_α is condensed is continuously connected to the confining phase of the pure compact U(1) gauge theory. So the present phase with Q_ϱ massive and \mathbf{N} condensed, also has z_α condensed. We will present a more complete analysis of this important phenomenon in Section VIC and Appendix H: we will find that the Berry phases can also induce a region with co-existing BC order.

This starting point of condensation of \mathbf{N} and z_α provides a straightforward description of the fluctuations in the HN phase. We perform a standard Gaussian fluctuations analysis about a mean-field saddle point at which \mathbf{N} and z_α are non-zero, and all other fields are zero. The fluctuations of the gauge field A_μ are ‘Higgsed’ by the z_α condensate, and are consequently massive. However, there are two gapless spin-wave eigenmodes which arise from eigenvectors made up the transverse components of \mathbf{N} and z_α . These are just the properties expected in the familiar collinear Néel state.

2. P phase

Let us approach the P phase from the F phase, where as we noted in Table V, the $Q_{j\varrho}$ are condensed. For simplicity, let us assume that Q_{jx} is condensed while Q_{jy} is zero. By the Higgs phenomenon, the A_μ fluctuations are then quenched and can be neglected. From Z_P we see then that long-wavelength action controlling the spectrum of the z_α spinons is then controlled by the action

$$S_z = \int d^2x d\tau \left[|\partial_\mu z_\alpha|^2 + \Delta^2 |z_\alpha|^2 - w_Q Q_x \epsilon_{\alpha\beta} z_\alpha \partial_x z_\beta + \text{c.c.} \right]; \quad (6.10)$$

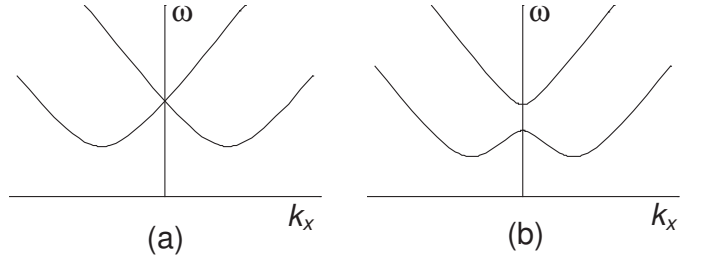


FIG. 15. Plot of the spinon dispersion in (a) the F phase (Eqn (6.11)), and (b) the HN+F phase (Eqn (6.15)). For larger N_0 , the latter has minima only at $k = 0$. There is one complex (or two real) bosonic mode at each frequency.

we have relaxed the length-constraint on the z_α and replaced it by a quadratic mass term which induces a spin gap Δ . Note that the action for spinons in (6.10) is explicitly SU(2) invariant, in contrast to the discussion of the F phase in Section VC 3. It is a simple matter to diagonalize the quadratic form in (6.10): we obtain two complex modes with dispersion

$$\omega = (k^2 + \Delta^2 \pm w_Q |k_x Q_x|)^{1/2}; \quad (6.11)$$

there are two degenerate real modes at each frequency. This dispersion relation is sketched in Fig 15a; note that it always has minima at non-zero wavevectors $k = \pm k_{\min} \equiv \pm(w_Q |Q_x|/2, 0)$ and the minimum energy is $(\Delta^2 - w_Q^2 |Q_x|^2/4)^{1/2}$. For large enough Q_x this minimum energy will vanish, and the z_α will condense at the wavevectors $\pm k_{\min}$. By a determination of the eigenvectors we see that the most general condensate has the spatial dependence (assuming, without loss of generality, that Q_x is real)

$$z_\alpha = \begin{pmatrix} d_1 & id_2 \\ id_2^* & d_1^* \end{pmatrix} \begin{pmatrix} e^{ik_{\min}x} \\ -ie^{-ik_{\min}x} \end{pmatrix}, \quad (6.12)$$

where $d_{1,2}$ are complex numbers, with only $|d_1|^2 + |d_2|^2$ determined by higher order terms in the action. We should now compute the staggered spin polarization by inserting (6.12) into (6.3). This is simplified by noting that the first factor on the right hand side is simply proportional to a general SU(2) matrix, and will only lead to an overall rotation in \mathbf{N} . So up to an arbitrary O(3) rotation, we can set $d_1 = 1$, $d_2 = 0$, and then the spin-polarization in the condensed phase is seen to have the form

$$\mathbf{N} \propto (\sin(2k_{\min}x), -\cos(2k_{\min}x), 0); \quad (6.13)$$

this is an incommensurate coplanar spiral in which \mathbf{N} precesses at the wavevector $k = 2k_{\min}$, as is expected in the P state (recall that for the underlying spins, this wavevector is measured relative to (π, π)). The critical properties of the transition at which the z_α condense (which is expected to have O(4) symmetry), and that of fluctuations

in the P states can be addressed as in Ref. 12 and will not be discussed further here. We merely note that the A_μ gauge fluctuations are quenched across the transition, and so the theory can be expressed in terms of the z_α alone; the Q_ρ are also not critical, while \mathbf{N} is pinned to the z_α via (6.3).

3. HN+F phase

The spectrum of spin excitations in the HN+F phase can be analyzed as in Section VIB2 for the F phase, but we now have to condense \mathbf{N} . Let us assume, as in Section VIA, that $\langle \mathbf{N} \rangle = N_0(0, 0, 1)$. Fluctuations of \mathbf{N} about this state will lead, as usual, to the two familiar gapless spin-wave modes. For the gapped spinon states we use the same strategy as that leading to (6.10); the presence of the \mathbf{N} condensate now modifies this to

$$S_z = \int d^2x d\tau \left[|\partial_\mu z_\alpha|^2 + \Delta^2 |z_\alpha|^2 - w_Q Q_x \epsilon_{\alpha\beta\gamma} \partial_x z_\beta + \text{c.c.} - w_N N_0 (|z_\uparrow|^2 - |z_\downarrow|^2) \right]. \quad (6.14)$$

This can now be diagonalized, and we again find two complex modes with dispersion

$$\omega = \left(k^2 + \Delta^2 \pm \sqrt{(w_Q k_x Q_x)^2 + (w_N N_0)^2} \right)^{1/2}. \quad (6.15)$$

These dispersions are sketched in Fig 15b. Unlike (6.11), the expression (6.15) can either have minima at non-zero wavevectors or only at zero wavevector; the latter applies for $w_N N_0 > w_Q^2 |Q_x|^2 / 2$. Although each frequency has doubly degenerate real modes, there is now no SU(2) symmetry in the S-matrices that describes the scattering of these modes. Condensation of the spinons at the non-zero wavevector minima of the dispersion (in the case where they exist) will lead again to the P state. Analysis corresponding to that in (6.12) and (6.13) now shows that the \mathbf{N} spin polarization is *non-coplanar* in the P phase. Further, the \mathbf{N} condensate has components at wavevectors at $k = \pm 2k_{\min}$ and at $k = 0$ (note again that for the underlying spins, these wavevectors are measured relative to (π, π)). Condensation of the spinons at the zero wavevector minimum (if it exists) leads to the HN state which has a \mathbf{N} condensate only at $k = 0$.

C. Multicritical points

The discussion in the previous subsections, combined with the analyses in Section V has given a complete description of the phases in Figs 13 and 14, and of most the boundaries between them. It remains to address the nature of some of the multicritical points.

The tetracritical points in Figs 13 and 14 all appear to be fairly conventional. As an example, consider the

point where the four phases, BC, HN+BC, HN+F, and F meet in Fig 13. The transitions in the vertical direction are described by the BC order parameter associated with the frustrated Ising model in (5.10), while that in the vertical direction is controlled by the O(3) φ^4 field theory in (5.15). The two order parameters have only a quartic energy-energy coupling involving quadratic terms which are respectively invariant under D_4 and O(3) symmetries.

It remains to sort out the physics near the multicritical points A and B in Fig 13. This appears to be a problem of great complexity. However, some progress can be made by using the observation that all four phases in the vicinity of A and B have $\langle \mathbf{N} \rangle \neq 0$. This permits a description in terms of a simplified compact U(1) gauge theory model which is amenable to a complete duality transformation, and which does not suffer from the problem of Z_2 gauge theory Z'_P of omitting the HN phase. Details of the analysis along these lines are provided in Appendix H.

VII. CONCLUSIONS

This paper has presented an extensive study of the paramagnetic states of two-dimensional, $S = 1/2$, quantum antiferromagnets with both U(1) and SU(2) spin rotation symmetries. We have focused on two central properties that characterize such states: bond-centered charge (BC) order (*e.g.* spin-Peierls order) and fractionalization (F).

Our point of departure was the ‘minimal model’ of $S = 1/2$ spin systems with local antiferromagnetic spin correlations: the O(3) non-linear sigma model with Berry phases. We were strongly influenced in this choice by the remarkable success of such an approach in producing a theory of one-dimensional antiferromagnets (reviewed and extended in Section IV), with all results in complete agreement with those obtained by bosonization methods and also with the solution of a variety of integrable models. We wrote a lattice version of the minimal model in two dimensions, the partition function Z in (1.13), and Sections II-V were devoted, directly or indirectly, to addressing its properties. We argued in Section II that the strong-coupling limit of the SU(2)-invariant Z had BC order, while that of U(1)-invariant systems was shown in Sections II and V to also allow F states. We also discussed, in Sections III and V, how the familiar magnetically ordered Néel (HN) state was connected to the BC state in systems with SU(2) symmetry: we presented a number of independent arguments which supported an intermediate co-existence (HN+BC) state.

We also presented an in-depth discussion of a number of routes to fractionalization that have appeared in the literature^{14,15,20,8,10}. These can be divided, on physical grounds, into at least three distinct classes which we review below. Near the transition to magnetically ordered states (or to superconducting states in class (B) below), these routes produce fractionalized states with

clearly distinct low energy spectra. We do not address the more subtle question of whether ground states in distinct classes can be connected to each other via some path in parameter space without an intervening phase transition—there can be considerable rearrangement between the excited states so that one can connect states with very different low energy structures without a singular change in the ground state. The routes are:

(A) In systems with a $U(1)$ spin symmetry, we approach the F state from a magnetically ordered state with XY order, which we view as ‘superfluidity’ in the $S_z = 1$ spin-flip boson $b^\dagger = \hat{S}_+$ (see (4.21)). This superfluidity can be destroyed by condensation of vortices in the phase of b^\dagger , and the F phase is produced^{8,10} by a preferential condensation of *double vortices*, Φ ; near its transition to the XY phase, the F phase has a massive $S_z = 1/2$ spinon excitation described by the complex, bosonic field operator Ψ_{sp} , as was discussed in Section V C 3. We have argued in Section V that this route to fractionalization does not survive the restoration of $SU(2)$ spin symmetry.

(B) The second route^{21,8} is technically similar to (A), but has a very different physical interpretation, and applies to systems with $SU(2)$ symmetry. The boson, b^\dagger is re-interpreted as the creation operator for Cooper pairs, and the XY phase is now a true superconductor. The condensation of double vortices (with flux hc/e) then leads to a fractionalized insulator with $S = 1/2$ fermionic spinons (which are possibly gapless). At half-filling, this route requires proximity to superconducting states, and so is only likely in systems with strong charge fluctuations which can allow the Mott charge gap to collapse.

(C) The third route¹⁴ was discussed in Section VI. Non-collinear spin correlations were shown to liberate bosonic $S = 1/2$ spinons described by the actions (6.10) and (6.14). Note that (6.10) has an explicit $SU(2)$ symmetry, and the number of spinon excitations is doubled with respect to (A).

We now use the perspective of the above ‘classification’ to present a critical review of other recent studies of $S = 1/2$ antiferromagnets in two dimensions.

The Paris group^{43–47} has performed large scale numerical studies on a variety of lattices. They have found examples of BC states, in proximity to magnetically ordered states with collinear order, in keeping with the discussion in Sections II and III. On the analog of the pyrochlore lattice in two dimensions, they have recently found⁴⁷ plaquette BC order, in accordance with the predictions of the sine-Gordon model of Appendix C 3⁴² and the quantum dimer model²⁶. They also find good candidates for fractionalized states with a well-developed gap to all excitations: these are in regimes where the classical ground state is non-collinear, and so we propose that these states are in class (C). The case of kagome lattice remains mysterious as it has a large density of very low energy singlet excitations.

We have already mentioned recent numerical evidence^{6,7} for BC order in frustrated square lattice antiferromagnets with first and second neighbor exchange interactions (the J_1 - J_2 model). Capriotti and Sorella originally claimed⁴⁸ plaquette BC order in the J_1 - J_2 model, but have recently argued⁴⁹ in favor of a state with no broken symmetries near $J_2/J_1 = 0.5$. Our studies here and the earlier work^{14,15} do not, in principle, rule out a F state in the J_1 - J_2 model, but do require a BC state to intervene (or, more exotically a HN+F state) as one moves towards the HN state at smaller J_2 . The variational approach in Ref. 49 does not work well in the region with HN order; as in our theory the BC order is intimately connected to fluctuating HN order, we suspect that the approach of Ref. 49 is also insensitive to the development of BC correlations.

Moessner, Sondhi, and collaborators²⁶ have examined generalizations of the quantum dimer model²⁵ (discussed in Appendix C 1) to a variety of lattices. They present very convincing evidence for BC phases on bipartite lattices, and for an F state on the triangular lattice; these results are in general accord with our discussion here. The dimer subspace does not include any spinon excitations, and so the classification of this F state (B or C) is not meaningful in this context.

Kashima and Imada⁵⁰ have examined a Hubbard model with first and second neighbor hopping near the metal-insulator transition. At large enough Hubbard repulsion, U , this model reduces to the J_1 - J_2 antiferromagnet, and so the corresponding region could have BC order. However the Hubbard model also induces additional ring-exchange terms at smaller U , and this should increase the tendency towards F states of class (C). Nearer the metal-insulator transition, the strong charge fluctuations could induce F states in class (B).

The striking experimental evidence⁵¹ for a F state in Cs_2CuCl_4 appears to place it very naturally in class (C), as has been discussed by Chung, Marston, and McKenzie³⁹: the neutron scattering measurements show clear evidence for incommensurate, spiral spin correlations.

It has recently become possible⁵² to perform large-scale numerical studies of a class of frustrated $S = 1/2$ antiferromagnets with a $U(1)$ spin symmetry. It would be very useful to study these in great detail, and to compare the phase diagrams with those in Section V.

Starykh *et al.*⁵³ have recently proposed a most interesting two-dimensional paramagnetic phase which does not fall into any of the classes discussed here: they have found an example of a “sliding Luttinger liquid”, in which the low energy excitations are well described by an infinite set of essentially decoupled one-dimensional antiferromagnets in the TL phase of Figs 4 and 6. However, it remains to be seen if such a phase is stable in a parameter regime with full $SU(2)$ spin symmetry.

Zaanen and collaborators⁵⁴ have introduced a Z_2 gauge theory of “sublattice parity order” in the paramagnetic states of a class of doped antiferromagnets. Their work is in a spirit similar to (C) but differs in impor-

tant aspects: the paramagnetic state has incommensurate spin correlations, but the spins remain collinear; further, there do not appear to be any neutral $S = 1/2$ excitations.

Rantner and Wen⁵⁵ and Wen⁵⁶ have recently provided a comprehensive classification of “spin-liquid” ground states in two dimensions. Many of these are fractionalized states which fall into our classes (B) and (C). However, they also propose an “algebraic spin liquid” (related to the earlier “flux phase”⁵⁷) in which there is a gapless U(1) gauge boson strongly interacting with gapless fermionic spinons. We are skeptical about the stability of such a state. The original analysis⁵⁵ dealt with a field theory of a non-compact U(1) gauge field, whereas a microscopic derivation always yields a compact U(1) field. The latter possesses instantons which have been the center of attention in our analysis here, and which have been the driving force behind the appearance of BC order. Rantner and Wen⁵⁵ neglected the instantons, whereas Wen⁵⁶ argued for the irrelevance of the operator creating a *single* instanton under suitable conditions. However, this irrelevance is not a sufficient criterion for neglecting the effects of a *finite density* of instantons. The latter effects can be addressed by the Kosterlitz recursion relations⁵⁸, which examine the renormalization of the instanton action by integrating out a tightly bound instanton/anti-instanton dipole. In spacetime dimensions $D > 2$ such renormalizations are disruptive, and cannot be simply absorbed into an innocuous renormalization of a “stiffness” (as is the case in $D = 2$ in the superfluid phase of the Kosterlitz-Thouless transition). A number of models of the statistical mechanics of “charges” in $D = 3$ have been examined in the literature (with interactions between opposite charges separated by spacetime distance R behaving like $\sim -1/|R|$ (Ref. 58), $\sim \ln(|R|)$ (Ref. 59), and $\sim |R|$ (Ref. 60)), and all results are the same: there is a strong renormalization induced by the dipoles, and this always liberates the charges at large scales; this liberation includes the regime where a naive analysis of the single vortex fugacity suggests that unbound charges are suppressed. The instanton gas is then in the Debye-Hückel plasma screening phase, and there is no phase of confined charges for $D > 2$. It is this screened plasma of instantons which is responsible for the BC order and confined spinons we have studied here, and we believe it will also disrupt the algebraic spin liquid.

ACKNOWLEDGMENTS

We thank E. Demler, M. P. A. Fisher, S. Girvin, B. I. Halperin, O. Starykh, and O. Sushkov for helpful discussions. We are especially grateful to T. Senthil for numerous insightful remarks. This research was supported by US NSF Grant DMR 0098226.

APPENDIX A: CP^1 FORMULATION

We discuss here an alternative lattice model for the ground states of quantum antiferromagnets in two dimensions. It is closely related to the model Z in (1.13), which was in turn derived from the coherent state path integral of quantum spin systems. The approach here is closer to the model of Ref. 4: it has the advantage of allowing a simple generalization which accounts for incommensurate spin correlations and fractionalized phases in systems with SU(2) spin symmetry (discussed in Section VI), and of having a simpler large g limit. Its main disadvantage is that it enlarges the number of degrees of freedom on the lattice scale, and the connection to the underlying quantum spin Hamiltonian is not as direct.

The central actors in this formulation are complex spinors $z_{j\alpha}$ ($\alpha = \uparrow, \downarrow$) on the sites of the direct spacetime lattice. These obey the constraint

$$\sum_{\alpha} |z_{j\alpha}|^2 = 1 \quad (\text{A1})$$

on every site, and are related to the \mathbf{n}_j by

$$n_{ja} = z_{j\alpha}^* \sigma_{\alpha\beta}^a z_{j\beta} \quad (\text{A2})$$

where $a = x, y, z$ is a spin index, and the σ^a are the Pauli matrices. Trading in the \mathbf{n}_j for the $z_{j\alpha}$ introduces a compact U(1) gauge redundancy under which $z_{j\alpha} \rightarrow z_{j\alpha} e^{i\phi_j}$, with ϕ_j arbitrary. This is closely related to (1.8), but will now be an explicitly realized in every term in the Hamiltonian.

A companion player in the present formulation is a compact U(1) gauge field $A_{j\mu}$. This transforms under the above gauge transformation in the obvious manner $A_{j\mu} \rightarrow A_{j\mu} - \Delta_{\mu}\phi_j$, and the action is invariant under $A_{j\mu} \rightarrow A_{j\mu} + 2\pi$. As we will see below, $A_{j\mu}$ is closely related to $\mathcal{A}_{j\mu}$.

We can now write down the new formulation of the partition function:

$$\begin{aligned} Z_{cp} &= \sum_{\{q_{j\mu}\}} \int_0^{2\pi} \prod_{j,\mu} dA_{j\mu} \int \prod_{j\alpha} dz_{j\alpha} \delta(|z_{j\alpha}|^2 - 1) \\ &\quad \times \exp\left(-S_z - S_A - \tilde{S}_B\right) \\ S_z &= -\frac{1}{g} \sum_{j,\mu} z_{j\alpha}^* e^{iA_{j\mu}} z_{j+\hat{\mu},\alpha} + \text{c.c.} \\ S_A &= \frac{1}{2e^2} \sum_{\square} (\epsilon_{\mu\nu\lambda} \Delta_{\nu} A_{j\lambda} - 2\pi q_{j\mu})^2 \\ \tilde{S}_B &= \sum_j \eta_j A_{j\tau} \end{aligned} \quad (\text{A3})$$

The parallel between Z_{cp} and Z should be clear: S_z replaces $S_{\mathbf{n}}$, S_A replaces S_A , and \tilde{S}_B replaces S_B . The phase diagram of Z_{cp} as a function of g and e^2 should be similar to that of Z , as we argue below and in Appendix F.

It is tempting to analyze Z_{cp} by taking the continuum limit of S_A valid for small e^2 : in this case S_A reduces to the standard continuum action for a $U(1)$ gauge field, and Z_{cp} reduces to the theory of a complex spinor, z_α , coupled to a non-compact $U(1)$ gauge field. However, this approach is not correct for any non-zero e^2 : it ignores the compactness of the $U(1)$ gauge field, and the associated instantons, which confines charged fields in 2+1 dimensions.

A proper understanding of Z_{cp} is achieved by an analysis appropriate for large e^2 . A crucial identity in this limit is the exact expression

$$\sum_{\alpha} z_{j\alpha}^* z_{j+\hat{\mu},\alpha} = \left(\frac{1 + \mathbf{n}_j \cdot \mathbf{n}_{j+\hat{\mu}}}{2} \right)^{1/2} e^{i\mathcal{A}_{j\mu}}, \quad (\text{A4})$$

a suitable gauge choice has to be made on the left-hand-side, corresponding to the choice of \mathbf{n}_0 in the definition of $\mathcal{A}_{j\mu}$. Using this, we can explicitly perform the integral of $A_{j\mu}$ in Z_{cp} and map it into a model which has a structure similar to Z . This is most easily done at $e^2 = \infty$, when the integral over $A_{j\mu}$ can be done independently on every site, without any preliminary decoupling procedure (we have already argued that the $e^2 \rightarrow \infty$ limit should be smooth, and the physics at $e^2 = \infty$ should not differ from that at finite e^2). A simple evaluation of the integral shows that

$$\begin{aligned} Z_{cp}(e^2 = \infty) &= \int \prod_j d\mathbf{n}_j \delta(\mathbf{n}_j^2 - 1) \exp(-S_B - \tilde{S}_{\mathbf{n}}) \\ e^{-\tilde{S}_{\mathbf{n}}} &= \prod_j I_1 \left(\frac{\sqrt{2(1 + \mathbf{n}_j \cdot \mathbf{n}_{j+\hat{\tau}})}}{g} \right) \\ &\times \prod_{\mu=x,y} I_0 \left(\frac{\sqrt{2(1 + \mathbf{n}_j \cdot \mathbf{n}_{j+\hat{\mu}})}}{g} \right), \quad (\text{A5}) \end{aligned}$$

where $I_{0,1}$ are modified Bessel functions which are monotonically increasing functions of their arguments, and increase exponentially fast at large arguments. In the evaluation of the integral it is useful to shift $A_{j\mu}$ by $\mathcal{A}_{j\mu}$ and this leads to the Berry phase S_B expressed in terms of the $A_{j\tau}$ rather than the \tilde{S}_B expressed in terms of the $A_{j\tau}$ in (A3). For small g it is also interesting to note that the integral over $A_{j\mu}$ is dominated by values for which

$$A_{j\mu} \approx \mathcal{A}_{j\mu}, \quad (\text{A6})$$

although this approximation was not used in the evaluation of $\tilde{S}_{\mathbf{n}}$ — thus the A flux is pinned to values close to the flux associated with \mathbf{n} fluctuations. The explicit form of $\tilde{S}_{\mathbf{n}}$ differs from that of $S_{\mathbf{n}}$, but the two actions should have essentially identical physical properties for any finite g . Both actions are minimized when the \mathbf{n}_j are all parallel (a state with HN order), and both increase monotonically as the angle between any two neighboring \mathbf{n}_j is increased. The action $\tilde{S}_{\mathbf{n}}$ does not have precisely the same form along the spatial and temporal links, but

this should lead only to an innocuous and uninteresting renormalization of a spin-wave velocity. This establishes the close connection between the properties of Z and Z_{cp} .

Another connection can be seen in the $g \rightarrow \infty$ limit of Z_{cp} . In this limit, a direct application of the duality methods developed in Section II establishes the exact result

$$Z_{cp}(g = \infty) = Z_h, \quad (\text{A7})$$

where Z_h is the height model partition function defined in (2.12). So all of the results for Z_h discussed in Appendix C apply directly to Z_{cp} .

APPENDIX B: LARGE g LIMIT WITH $SU(2)$ SYMMETRY

This Appendix will describe the evaluation of $W(a_\mu)$ in (2.7) for the $SU(2)$ symmetric action $S_{\mathbf{n}}$ in (1.9) for large g .

One way to proceed is to accept the equivalence between Z and Z_{cp} just discussed, and perform the average not over $S_{\mathbf{n}}$, but over S_z with $\mathcal{A}_{j\mu}$ replaced by $A_{j\mu}$: this will lead to essentially the same results as those appearing below.

Alternatively, we can follow a procedure that is roughly the inverse of that discussed towards the end of Appendix A. We first, formally, write down an effective action for $\mathcal{A}_{j\mu}$ fluctuations by

$$e^{-S'_A(\mathcal{A}_{j\mu})} \equiv \int \prod_j d\mathbf{n}_j \delta(\mathbf{n}_j^2 - 1) \delta(A_{j\mu} - \mathcal{A}_{j\mu}) e^{-S_{\mathbf{n}}}. \quad (\text{B1})$$

The resulting action will be invariant under gauge transformation of the $A_{j\mu}$ and also periodic under shifts of $A_{j\mu}$ by 2π . However, because of the complicated form of (1.7), this action is difficult to write down explicitly, even at $g = \infty$. Nevertheless, it is evident from a ‘‘high temperature’’ expansion of $S_{\mathbf{n}}$ that correlations of the flux decay exponentially fast *i.e.*

$$\langle \exp(iE_\mu(r_{\bar{j}}) - iE_\mu(0)) \rangle_{S'_A} \sim e^{|r_{\bar{j}}|/\xi}, \quad (\text{B2})$$

where $E_\mu(r_{\bar{j}}) = (\epsilon_{\mu\nu\lambda} \Delta_\nu A_\lambda)_{\bar{j}}$, and the correlation length $\xi = 1/(2 \ln g)$. So it is reasonable to model S'_A by the simplest lattice action which is consistent with all the symmetries and which reproduces (B2) at long scales:

$$S'_A = \frac{1}{2g^2} \sum_{\square} (\epsilon_{\mu\nu\lambda} \Delta_\nu A_{j\lambda} - 2\pi q_{j\mu})^2. \quad (\text{B3})$$

Now we can easily evaluate $W(a_\mu)$ by the same duality transformations developed in Section II and obtain

$$\begin{aligned}
W(a_\mu) &= \left\langle \exp \left(-i \sum_{\square} \epsilon_{\mu\nu\lambda} a_{\bar{j}\mu} \Delta_\nu A_{j\lambda} \right) \right\rangle_{S'_A} \\
&= \sum_{\{h_{\bar{j}}\}} \exp \left(-\frac{g^2}{2} \sum_{\bar{j}} (a_{\bar{j}\mu} - \Delta_\mu h_{\bar{j}})^2 \right) \quad (\text{B4})
\end{aligned}$$

This last expression is our main result for $W(a_\mu)$, and it clearly shows the a -Meissner nature of the large g regime; notice its similarity to the London-limit action for the electromagnetic field in a superconductor—after allowing the discrete variables a and h to be continuous, we see that a plays the role of the electromagnetic vector potential, and h that of the phase of the superconducting order. So (B4) indicates that a -flux will be expelled, and the phase is well characterized by (2.9). More precisely, we can easily evaluate the expression for Z in (2.8) and obtain

$$Z = \sum_{\{h_{\bar{j}}\}} \exp(-f(\Delta_\mu h_{\bar{j}} - a_{\bar{j}\mu}^0)) \quad (\text{B5})$$

where the function $f(n)$ is given by

$$e^{-f(n)} \equiv \sum_{m=-\infty}^{\infty} \exp\left(-\frac{e^2}{2}m^2 - \frac{g^2}{2}(m-n)^2\right). \quad (\text{B6})$$

The expression (B5) for Z is very closely related to that for the height model partition function, Z_h , in (2.12); the latter corresponds to the choice $f(n) = e^2 n^2/2$. More generally, $f(n)$ is an even, monotonically function of n , and we expect that the properties of the height model should be quite insensitive to the detailed form of $f(n)$. The expression (B6) can be viewed as a renormalization of the coupling e^2 due to \mathbf{n} fluctuations.

APPENDIX C: PROPERTIES AND MAPPINGS OF THE HEIGHT MODEL

This appendix will review the properties of the height model, Z_h , in (2.12), and also present its equivalence to a number of other models of paramagnetic states of quantum antiferromagnets.

It is useful to first rewrite Z_h in a form closer to that used in earlier work. We decompose the fixed field $a_{\bar{j}\mu}^0$ into curl and divergence free parts by writing it in terms of new fixed fields, $\mathcal{X}_{\bar{j}}$ and $\mathcal{Y}_{j\mu}$ as follows:

$$a_{\bar{j}\mu}^0 = \Delta_\mu \mathcal{X}_{\bar{j}} + \epsilon_{\mu\nu\lambda} \Delta_\nu \mathcal{Y}_{j\lambda}. \quad (\text{C1})$$

The values of these new fields are shown in Fig 16. Inserting (C1) into (2.12), we can now write the height model in its simplest form

$$Z_h = \sum_{\{H_{\bar{j}}\}} \exp\left(-\frac{e^2}{2} \sum_{\bar{j}} (\Delta_\mu H_{\bar{j}})^2\right), \quad (\text{C2})$$

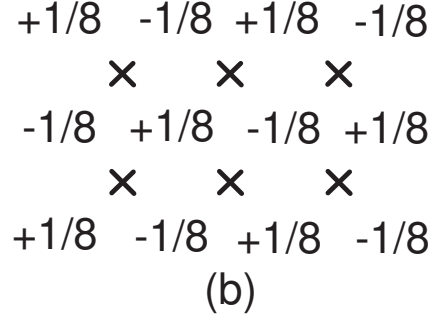
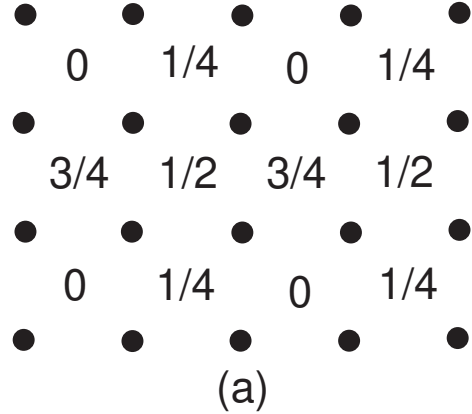


FIG. 16. Specification of the non-zero values of the fixed fields (a) $\mathcal{X}_{\bar{j}}$ and (b) $\mathcal{Y}_{j\mu}$ introduced in (C1). The notational conventions are as in Fig 3. Only the $\mu = \tau$ components of $\mathcal{Y}_{j\mu}$ are non-zero, and these are shown in (b).

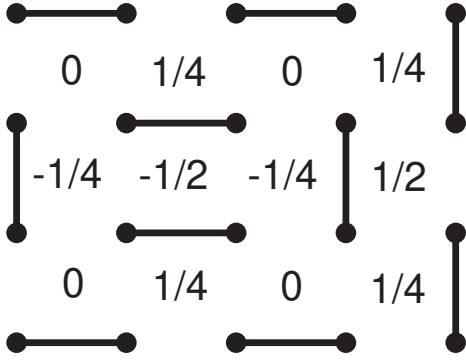


FIG. 17. Mapping between the quantum dimer model and Z_h . Each dimer on the direct lattice is associated with a step in height of $3/4$ on the link of the dual lattice that crosses it. All other height steps are $1/4$.

where

$$H_{\bar{j}} = h_{\bar{j}} - \mathcal{X}_{\bar{j}} \quad (\text{C3})$$

is the new height variable we shall work with. Notice that the $\mathcal{Y}_{j\mu}$ have dropped out, while the $\mathcal{X}_{\bar{j}}$ act only as fractional offsets to the integer heights. From (C3) we see that the height is restricted to be an integer on of the four sublattices, an integer plus $1/4$ on the second, an integer plus $1/2$ on the third, and an integer plus $3/4$ on the fourth; the fractional parts of these heights are as shown in Fig 16a. The steps between neighboring heights are always an integer plus $1/4$, or an integer plus $3/4$.

1. Quantum dimer model

The connection²² with the quantum dimer model^{25,26} emerges upon examining the large e^2 limit of Z_h . In this limit, the action is minimized by choosing the smallest possible modulus of steps between neighboring heights: these are either $1/4$ or $3/4$. It is not possible to reduce the number of $3/4$ steps to zero, and height configurations with the minimal number of $3/4$ steps have an exact one-to-one correspondence with the set of dimer coverings of the direct lattice (heights which differ merely by a uniform shift of all heights by the same integer are treated as equivalent). This correspondence is illustrated in Fig 17. Temporal fluctuations of the heights between two such minimal action configurations correspond to quantum tunnelling between different dimer states, and hence the connection with the quantum dimer model.

2. Coulomb plasma of instantons

Elevate the height variable to a continuous real field by the Poisson summation formula; this allows us to rewrite (C2) as

$$Z_h = \sum_{\{m_{\bar{j}}\}} \int_{-\infty}^{\infty} \prod_{\bar{j}} dH_{\bar{j}} \exp \left(-\frac{e^2}{2} \sum_{\bar{j}} (\Delta_{\mu} H_{\bar{j}})^2 - 2\pi i \sum_{\bar{j}} m_{\bar{j}} (H_{\bar{j}} + \mathcal{X}_{\bar{j}}) \right) \quad (\text{C4})$$

Now perform the Gaussian integral over the $H_{\bar{j}}$ and obtain the height model partition function written as a sum over the plasma of “charges” $m_{\bar{j}}$.

$$Z_h = \sum_{\{m_{\bar{j}}\}} \exp \left(-\frac{2\pi^2}{e^2} \sum_{\bar{j}\bar{j}'} m_{\bar{j}} G(\bar{j} - \bar{j}') m_{\bar{j}'} - 2\pi i \sum_{\bar{j}} m_{\bar{j}} \mathcal{X}_{\bar{j}} \right), \quad (\text{C5})$$

where G is the lattice Green’s function in (3.1). For large $|r|$, $G(r) \sim 1/|r|$, and hence this is a Coulomb plasma of charges in $2+1$ dimensions. Working backwards through the series of duality transformations, we can deduce that these charges are the ‘hedgehogs’ in the \mathbf{n} field. Each charge also carries a Berry phase of $1, i, -1, -i$, on the four dual sublattices, represented by the last term in (C5)—these phases are identical to the hedgehog Berry phases computed by Haldane²⁷ by entirely different methods. The plasma is always in its “Debye-screened” phase for all values of e^2 , and so isolated hedgehog are “free”. As we review in the following subsection, this free plasma of charges always has BC order, induced by the Berry phases.

3. Sine-Gordon model

The most practical formulation of the height model is in terms of a frustrated sine-Gordon model. To obtain this, we insert a phenomenological “core” action $e^{-E_c m_{\bar{j}}^2}$ in (C4), and in the limit of large E_c , sum over just $m_{\bar{j}} = 0, \pm 1$ on every site. This expresses Z_h as the functional integral over what is now the sine-Gordon field, $H_{\bar{j}\mu}$, with the action

$$S_{sG} = \frac{e^2}{2} \sum_{\bar{j}} [(\Delta_{\mu} H_{\bar{j}})^2 - y \cos(2\pi(H_{\bar{j}} + \mathcal{X}_{\bar{j}}))] \quad (\text{C6})$$

The properties of the model S_{sG} have been discussed at length in Ref. 5, and so we need not reproduce the analysis here. The main result is that the height $H_{\bar{j}}$ is always in its “smooth” phase (and the plasma above is therefore in its Debye screening phase), characterized by a definite value of the average height $\overline{H} \langle H_{\bar{j}} \rangle$ (where the average is over quantum fluctuations and over all sites), and such a phase necessarily has BC order. The fractional value of \overline{H} specifies the nature of the BC order. As in Section V C, we introduce the BC order parameter

$$\Psi_{BC} = \sum_{\bar{j}} e^{2\pi i H_{\bar{j}}}. \quad (\text{C7})$$

Then, from the results of Ref. 5,24 we see that the values $\arg\langle\Psi_{BC}\rangle = \pi/4, 3\pi/4, 5\pi/4, 7\pi/4$ correspond to the four BC states in Fig 1a, the values $\arg\langle\Psi_{BC}\rangle = 0, \pi/2, \pi, 3\pi/2$ correspond to the four BC states in Fig 1b, while any other value of $\arg\langle\Psi_{BC}\rangle$ yields an eight-fold degenerate state involving superposition of the orders in Fig 1a and b (lattice symmetries show that the states with $\Psi_{BC} \rightarrow \Psi_{BC}^*$, and $\Psi_{BC} \rightarrow e^{in\pi/2}\Psi_{BC}$ (n integer) are all equivalent).

APPENDIX D: CORRELATIONS OF DEFECTS IN THE φ^4 FIELD THEORY

This appendix shows how defect correlations may be computed in a continuum φ^4 field theory. The methods used here are a generalization of an approach due to Halperin²⁸. We will outline the technical steps in the calculation, as no details were given in Ref. 28.

We are interested in a field theory with action

$$S_\varphi = \frac{1}{2} \int \frac{d^D k}{(2\pi)^D} \frac{|\varphi_a(k)|^2}{Q(k)} + \frac{u}{4!} \int d^D r (\varphi_a^2(r))^2 \quad (D1)$$

where $D = 3$ is the dimension of spacetime, and $a = 1 \dots N$ for a theory with $O(N)$ symmetry. The propagator $Q^{-1}(k) = m_0^2 + k^2$ at small k , while at k larger than some cutoff, Λ , $Q(k)$ decreases sufficiently fast with increasing k to make the interacting theory ultraviolet finite. The ‘mass’, m_0^2 is tuned by varying the coupling g in the underlying model Z .

We consider first the case $N = D = 3$. Then we have point hedgehog defects. In the present continuum formulation, Halperin showed that the topological charge density can be written as

$$\rho_h(r) = \delta^D [\varphi_a(r)] \det [\partial_\mu \varphi_a(r)] \quad (D2)$$

We are interested in evaluating correlators of $\rho_h(r)$ under the action S_φ in a perturbation theory in u . The main technical difficulty in such a calculation arises from the delta function in (D2). However this may be easily treated by a standard Lagrange multiplier technique.

We illustrate the method by computing the two-point correlator of $\rho_h(r)$ at $u = 0$. In the standard field theoretic method, correlators of φ , and its derivatives, may be easily obtained by first evaluating the generating function

$$\left\langle \exp \left(- \int d^D r J(r) \varphi(r) \right) \right\rangle_{S_\varphi}. \quad (D3)$$

For simplicity of notation, we will work in this paragraph with a single component field φ ; the generalization to multiple values of α is immediate. At $g = 0$, (D3) evaluates to

$$\exp \left(\frac{1}{2} \int d^D r_1 d^D r_2 J(r_1) J(r_2) Q(r_1 - r_2) \right), \quad (D4)$$

where $Q(r)$ is the Fourier transform of $Q(k)$. Now generalize (D3) by including two delta functions of φ

$$\left\langle \delta(\varphi(r_3)) \delta(\varphi(r_4)) \exp \left(- \int d^D r J(r) \varphi(r) \right) \right\rangle_{S_\varphi} \quad (D5)$$

with $r_3 \neq r_4$. We write the first delta function as

$$\delta(\varphi(r_3)) = \int_{-\infty}^{\infty} \frac{d\lambda}{2\pi} e^{-i\lambda\varphi(r_3)}, \quad (D6)$$

and similarly for the second delta function. We can now evaluate the φ averages in (D5), and then explicitly perform the integrals over the two λ 's. In this manner we obtain our key result for the value of (D5) at $g = 0$:

$$(D5) = \frac{1}{2\pi\sqrt{\Delta(r_3 - r_4)}} \times \exp \left(\frac{1}{2} \int d^D r_1 d^D r_2 J(r_1) J(r_2) \tilde{Q}(r_1, r_2) \right) \quad (D7)$$

where $\Delta(r) \equiv Q^2(r = 0) - Q^2(r)$ and

$$\begin{aligned} \tilde{Q}(r_1, r_2) = & Q(r_1 - r_2) - \frac{1}{\Delta(r_3 - r_4)} \left[\right. \\ & Q(r_1 - r_3)Q(r_2 - r_3)Q(0) \\ & + Q(r_1 - r_4)Q(r_2 - r_4)Q(0) \\ & - Q(r_1 - r_3)Q(r_2 - r_4)Q(r_3 - r_4) \\ & \left. - Q(r_1 - r_4)Q(r_2 - r_3)Q(r_3 - r_4) \right] \quad (D8) \end{aligned}$$

Observe that (D8) is a Gaussian in J , and so φ correlations remain Gaussian even in the presence of the delta function. In comparing (D8) with (D4), we notice only two differences. First, the overall amplitude of the correlators has been modified by the prefactor $1/(2\pi\sqrt{\Delta})$. Second, Q has been replaced by \tilde{Q} ; notice that the additional terms in (D8) become subdominant as r_1 and r_2 move far apart provided $Q(r)$ is a smoothly decreasing function of r (which is the case even at the critical point). This latter fact indicates that at large distances we may as well neglect the delta functions entirely: they merely renormalize the correlators with an overall prefactor, which is not of interest in the universal properties anyway. It is now a straightforward matter to compute the two-point correlator of ρ_h by repeated applications of (D7) and (D8). First by sending $r_3 \rightarrow r_1$ and $r_4 \rightarrow r_2$ we can obtain the correlator of the gradients of φ :

$$\begin{aligned} \langle \delta(\varphi(r)) \partial_\mu \varphi(r) \delta(\varphi(0)) \partial_\nu \varphi(0) \rangle_{S_\varphi} = \\ \frac{1}{2\pi\sqrt{\Delta(r)}} \left[-\partial_\mu \partial_\nu Q(r) - \frac{r_\mu r_\nu}{r^2} \frac{Q(r)(Q'(r))^2}{\Delta(r)} \right], \quad (D9) \end{aligned}$$

where $r \neq 0$, we have assumed that $Q(r)$ is a function only of $|r|$, and the prime indicates a derivative with respect to the argument of $Q(|r|)$. Now we can compute $C_h(r)$, defined in (3.2), by a straightforward application of Wick's theorem, and we obtain Halperin's result²⁸:

$$C_h(r \neq 0) = 6P_1(r)P_2^2(r) \quad (\text{D10})$$

where

$$P_1(r) = \frac{-Q''(r)\Delta(r) - (Q'(r))^2Q(r)}{2\pi\Delta^{3/2}(r)}$$

$$P_2(r) = \frac{-Q'(r)}{2\pi r\Delta^{1/2}(r)}. \quad (\text{D11})$$

There is additional singular contribution to $C_h(r)$ at $r = 0$, proportional to $\delta(r)$, which has been computed by Halperin: this contribution is precisely that needed for $C_h(r)$ to satisfy the neutrality condition (3.3).

Our approach above can be easily generalized to develop a perturbation theory for $C_h(r \neq 0)$ in u . We expect that the neutrality condition (3.3) will be satisfied at each order in u , as it is a topological constraint imposed by the existence of the smooth field $\varphi(r)$.

We now have the machinery to determine the long-distance decay of $C_h(r)$ at the critical point of S_φ . The key observation, noted above, is that the delta functions may be neglected in determining the leading functional form of this decay (note however, that the delta-function related contributions were essential in satisfying the neutrality condition (3.3), as it depended also on the short distance behavior of $C_h(r)$). The subdominance of the delta-function related contributions at long distances holds also at each order in u , and so we conclude that the scaling dimension of ρ_h is given simply by

$$\dim[\rho_h(r)] = \dim[\det[\partial_\mu\varphi_a]]$$

$$\equiv (9 + \eta_h)/2, \quad (\text{D12})$$

where the second expression defines the anomalous dimension η_h . The expression on the right-hand-side of the first equation is a local composite operator, and its scaling dimension can be determined in an expansion in $\epsilon = 4 - D$ by standard field theoretic methods. It is not difficult to show that this composite operator has no renormalizations to two loops (although they do appear at higher loop order); hence we immediately obtain (3.6,3.5). We also discussed in Section III that we do not expect the conservation law (3.3), which is special to $D = 3$, to disrupt the validity of the ϵ expansion at $\epsilon = 1$. The scaling dimension in (D12) also specifies the singularity in the density of hedgehogs at the critical point of S_φ ; for the original model Z this critical point is at $g = g_{2c}$ (see Fig 2) and

$$\bar{\rho}_h = \langle |\rho_h| \rangle = C_1(g)\Lambda^{-3} + C_\pm |g - g_{2c}|^{(9+\eta_h)/2} \quad (\text{D13})$$

where $C_1(g)$ is a smooth function of g , finite at $g = g_{2c}$. The non-universal constants C_\pm apply on the two sides of the transition. Notice that the singularity is very weak and essentially unobservable.

We conclude this Appendix by stating the generalization of these results to the O(2) case, with $N = 2$, $D = 3$; this applies to the spin systems with U(1) symmetry. In

this case, the generalization of the expression (D2) for the defect density is the following expression²⁸ for the vortex current $\mathcal{J}_\mu(r)$:

$$\mathcal{J}_\mu(r) = \delta^2[\varphi_a(r)] \epsilon_{\mu\nu\lambda} \partial_\nu \varphi_1(r) \partial_\lambda \varphi_2(r). \quad (\text{D14})$$

The above methods show that at $u = 0$, the correlator of $\mathcal{J}_\mu(r)$ is given by

$$C_{v,\mu\nu}(r) = \langle \mathcal{J}_\mu(r) \mathcal{J}_\nu(r) \rangle$$

$$= 2P_2^2(r) \frac{r_\mu r_\nu}{r^2} + 2P_1(r)P_2(r) \left(\delta_{\mu\nu} - \frac{r_\mu r_\nu}{r^2} \right), \quad (\text{D15})$$

where $P_{1,2}$ were defined in (D11). This result corrects an error in Halperin's result, quoted in (6.33) of Ref. 28. It can be checked that the result in (D15) satisfies

$$\int d^3r C_{v,\mu\nu}(r) = 0 \quad ; \quad \partial_\mu C_{v,\mu\nu}(r) = 0. \quad (\text{D16})$$

The first result states that the net vorticity vanishes, while the second expresses the conservation of the vortex current. Both these properties will hold at each order in u , and this allowed us to obtain (3.16). The long-distance behavior of \mathcal{J}_μ correlations at the critical point is controlled by the scaling dimension

$$\dim[\mathcal{J}_\mu(r)] \equiv (6 + \eta_v)/2$$

$$= \dim[\epsilon_{\mu\nu\lambda} \partial_\nu \varphi_1 \partial_\lambda \varphi_2]$$

$$= 4 - \epsilon + \eta + \mathcal{O}(\epsilon^3). \quad (\text{D17})$$

In the present situation, as was discussed in Section III, we do expect the conservation law (D16) to play a crucial role in $D = 3$, and to impose the exact result $\eta_v = -2$ for $\epsilon = 1$.

APPENDIX E: FIELD THEORY IN ONE DIMENSION

This appendix outlines the steps which relate the lattice model $Z_{U(1)}^{(1)}$ in (4.18) to the field theory in (4.25).

We first elevate the height ℓ_j to a continuous real field by the Poisson summation identity. The presence of the parity variables, σ_j , requires a slight generalization of this identity to

$$\sum_{\ell=-\infty}^{\infty} f(\ell, \sigma) = \frac{1}{2} \lim_{E_c \rightarrow 0} \int_{-\infty}^{\infty} d\phi \sum_{m=-\infty}^{\infty} e^{i\pi m \phi}$$

$$\times \left[f(\phi, 1) + (-1)^m f(\phi, -1) \right] e^{-E_c m^2} \quad (\text{E1})$$

where $\sigma \equiv 1 - 2(\ell \pmod{2})$, and f is an arbitrary function. As is conventional, it is safe to analyze these interface models in the limit of large "core" energy E_c , which accounts for short-distance renormalizations. Then, application of (4.25) to (4.18) shows that

$$Z_{U(1)}^{(1)} = \int \prod_{\bar{j}} d\phi_{\bar{j}} \exp \left[- \sum_{\bar{j}} \left(\frac{g}{8} (\epsilon_{\mu\nu} \Delta_{\nu} \phi_{\bar{j}})^2 - 2e^{-4E_c} \cos(2\pi\phi_{\bar{j}}) - 2e^{-E_c} \tanh(K_d) \epsilon_{\bar{j}} \cos(\pi\phi_{\bar{j}}) \right) \right]. \quad (\text{E2})$$

In terms of these variables, the BC order parameter is $Q_{j,j+\hat{x}} \sim \epsilon_{\bar{j}} \cos(\pi\phi_{\bar{j}})$ and I order is determined by $\hat{S}_{jz} \sim \Delta_x \phi_{\bar{j}}$.

It is useful to now integrate out some short-distance, high-energy fluctuations in (E2). We write

$$\phi_{\bar{j}} = \phi_0(r_{\bar{j}}) + \epsilon_{\bar{j}} \phi_1(r_{\bar{j}}) \quad (\text{E3})$$

and minimize the action with respect to the massive field ϕ_1 . This yields

$$\phi_1(r_{\bar{j}}) = -\frac{2\pi}{g} \tanh(K_d) e^{-E_c} \sin(\pi\phi_0(r_{\bar{j}})) \quad (\text{E4})$$

Inserting this back into (E2), and performing the gradient expansion for the field ϕ_0 we get the action of the sine-Gordon theory in (4.25) with

$$Y = 2e^{-4E_c} - \frac{\tanh^2(K_d) \pi^2 e^{-2E_c}}{g}. \quad (\text{E5})$$

The expression (E4) now shows that the I order parameter (measured by a staggered $\hat{S}_{j,z}$) is $\sim \sin(\pi\phi_0)$, while the BC order (measured by a staggered $Q_{j,j+\hat{x}}$) is $\sim \cos(\pi\phi_0)$.

APPENDIX F: CP^1 MODELS WITH EASY-PLANE ANISOTROPY

In the body of the paper, we applied the easy-plane anisotropy implied by (1.14) to the central partition function Z in (1.13), and so obtained $Z_{U(1)}$. This latter model was studied in great detail in Section V. We also claimed that the physics of the phases of the $SU(2)$ invariant Z was essentially identical to the CP^1 model Z_{cp} in Appendix A. As a consistency check, we will apply the easy-plane anisotropy to Z_{cp} here: it is then reassuring to find below properties that are very similar to those in Section V.

Comparing (1.14) and (A2), we see that the easy-plane limit corresponds to $|z_{j\uparrow}| = |z_{j\downarrow}|$. So we parameterize $z_{j\alpha} = e^{i\theta_{\alpha}}$, and then the gauge-invariant angle $\theta = \theta_{\uparrow} - \theta_{\downarrow}$. Inserting this in (A3), and writing the periodic couplings in Villain form, we obtain the form of Z_{cp} with $U(1)$ symmetry and easy-plane anisotropy:

$$Z_{cp,U(1)} = \sum_{\{q_{\bar{j}\mu}, m_{j\uparrow\mu}, m_{j\downarrow\mu}\}} \int_0^{2\pi} \prod_{j\mu} dA_{j\mu} \int \prod_j d\theta_{j\uparrow} d\theta_{j\downarrow} \times \exp \left(-S_A - \tilde{S}_B - S_{\uparrow} - S_{\downarrow} \right)$$

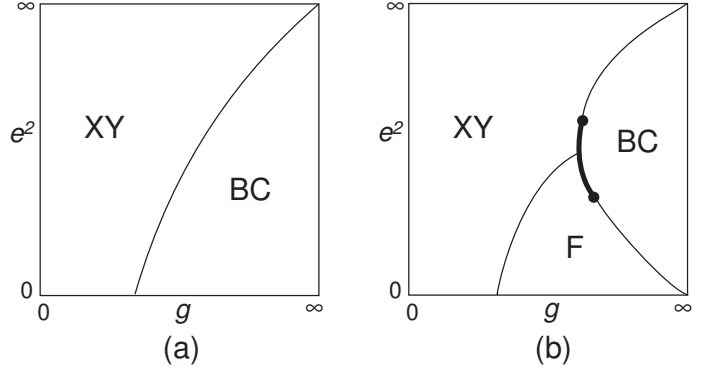


FIG. 18. As in Fig 7, but for the model $Z_{cp,U(1)}$ in (F2). Two possible phase diagrams are shown. In (a), the BC order vanishes as $e^2 \rightarrow 0$, and the $e^2 = 0$ line of the BC state is fractionalized.

$$S_{\uparrow} = \frac{1}{2g} (\Delta_{\mu} \theta_{j\uparrow} - 2\pi m_{j\uparrow\mu} - A_{j\mu})^2$$

$$S_{\downarrow} = \frac{1}{2g} (\Delta_{\mu} \theta_{j\downarrow} - 2\pi m_{j\downarrow\mu} - A_{j\mu})^2, \quad (\text{F1})$$

where S_A and \tilde{S}_B are defined in (A3). We can easily apply the duality methods of Sections II and V to (F1) and obtain a partition function for integer valued vectors fields $a_{\bar{j}\mu}, p_{\bar{j}\mu}$ residing on the links of the dual lattice:

$$Z_{cp,U(1)} = \sum_{\{a_{\bar{j}\mu}, p_{\bar{j}\mu}\}} \exp \left(-\frac{e^2}{2} (a_{\bar{j}\mu} - a_{\bar{j}\mu}^0)^2 - \frac{g}{2} \sum_{\square} (\epsilon_{\mu\nu\lambda} \Delta_{\nu} p_{\bar{j}\lambda})^2 - \frac{g}{2} \sum_{\square} (\epsilon_{\mu\nu\lambda} \Delta_{\nu} p_{\bar{j}\lambda} - \epsilon_{\mu\nu\lambda} \Delta_{\nu} a_{\bar{j}\lambda})^2 \right). \quad (\text{F2})$$

This model is closely related to (5.2) for the case of the on-site coupling (4.16). The connection becomes evident when we rewrite the last two terms in (F2) as

$$g \sum_{\square} \left(\epsilon_{\mu\nu\lambda} \Delta_{\nu} p_{\bar{j}\lambda} - \frac{1}{2} \epsilon_{\mu\nu\lambda} \Delta_{\nu} a_{\bar{j}\lambda} \right)^2 + \frac{g'}{4} \sum_{\square} (\epsilon_{\mu\nu\lambda} \Delta_{\nu} a_{\bar{j}\lambda})^2 \quad (\text{F3})$$

with $g' = g$. For $g' = 0$, the model (F2) is identical to the model (5.2). Adding such a ‘Maxwell’ term with $g' = g$ does appear to be an innocuous change, and it is clear that the basic physics of the class of models described by (F2) and (5.2) should be the same.

For the specific value $g' = g$, the phase diagram of (F2) does have some differences from that of (5.2) in Fig 7 (however, the topological relationship of the phases remains the same), and two possible phase diagrams are shown in Fig 18. Some insight is gained by looking at limiting values of the parameters in (F2). For $e^2 = \infty$, (F2) is identical to the corresponding limit of (5.2): both models reduce to the boson-current loop model of Otterlo

*et al.*³⁶ which has XY order for all values of g ; this XY order corresponds to ‘superfluidity’ in the gauge-invariant angle θ . Similarly, the $g = 0$ limit is also identical in the two models with XY order always present. A difference appears in the limit $g = \infty$: now (F2) becomes equivalent the height model in (2.12) whose ground state always has BC order, while (5.2) reduced to the frustrated Ising model in (5.10) which had both F and BC ground states. Finally, the limit $e^2 = 0$ becomes clearest in the form (F1): now the gauge field A_μ is entirely quenched and we have two independent XY models associated with the angles $\theta_{\uparrow,\downarrow}$. These have an XY ordering transition, and $z_{\uparrow,\downarrow}$ quanta become free massive spinons in the disordered phase: this is evidently an F phase.

An important unanswered question is the fate of the F phase found above at $e^2 = 0$ for non-zero values of e^2 . In the case of (5.2) we also found the F phase along the line $g = \infty$ and so it was clear that F order survived over a finite domain for $e^2 > 0$. This is not so clear here for (F1,F2). The compact U(1) gauge theory is confining, and the liberation of a finite density of instantons for $e^2 > 0$ could immediately confine the spinons and lead to BC order. This possibility is reflected in Fig 18a. However, in the absence of numerical studies of (F2) we leave open the possibility in Fig 18b that the F phase survives for a range of value of e^2 .

Similar considerations apply to the easy-plane CP^1 model in one dimension, and its properties are essentially identical to those discussed in Section IV for $Z_{U(1)}^{(1)}$.

APPENDIX G: FIELD THEORY IN TWO DIMENSIONS

This appendix will provide the missing steps between the model (5.4) and the field theory (5.12). The method is a combination of that applied in one dimension in Appendix E, and the analysis of LFS⁹.

First, we follow the two-dimensional analog of the steps leading to (E2). The main change is that the real scalar field $\phi_{\bar{j}}$ is replaced by a real vector field which we denote $b_{\bar{j}\mu}/\pi$. By these methods (5.4) maps to

$$Z_{U(1)} = \int \prod_{\bar{j}} db_{\bar{j}\mu} \exp \left[-\frac{g}{8\pi^2} \sum_{\square} (\epsilon_{\mu\nu\lambda} \Delta_\nu b_{\bar{j}\lambda})^2 + \sum_{\bar{j}\mu} \left(2e^{-4E_c} \cos(2b_{\bar{j}\mu}) + 2e^{-E_c} \tanh(K_d) \epsilon_{\bar{j},\bar{j}+\hat{\mu}} \cos(b_{\bar{j}\mu}) \right) \right], \quad (G1)$$

where $\epsilon_{\bar{j},\bar{j}+\hat{\mu}}$ is defined in (5.6). We can now make all the terms in (G1) invariant under a non-compact U(1) symmetry by introducing an angular variable ϑ_j and mapping

$$b_{\bar{j}\mu} \rightarrow -\Delta_\mu \vartheta_j + b_{\bar{j}\mu} \quad (G2)$$

in (G1). The representation (G1) then corresponds to a particular gauge choice in the non-compact U(1) gauge

theory. The remaining analysis is then identical to that in LFS. First, we introduce two complex scalars, the field operators for single vortices, $\phi_{\bar{j}} \sim e^{i\vartheta_j}$, and the field operator for double vortices $\Phi_{\bar{j}} \sim e^{2i\vartheta_j}$. Then, the second term in (G1) is proportional to a simple hopping term for $\Phi_{\bar{j}}$

$$- \sum_{\bar{j},\mu} \Phi_{\bar{j}}^* e^{2ib_{\bar{j}\mu}} \Phi_{\bar{j}+\hat{\mu}}. \quad (G3)$$

This $\Phi_{\bar{j}}$ quanta clearly have a minimum near $k = 0$, and so a naive continuum limit may be taken on (G3). In contrast, the dispersion of $\phi_{\bar{j}}$ is provided by the last term in (G1), and is

$$- \sum_{\bar{j},\mu} \epsilon_{\bar{j},\bar{j}+\hat{\mu}} \phi_{\bar{j}}^* e^{ib_{\bar{j}\mu}} \phi_{\bar{j}+\hat{\mu}}. \quad (G4)$$

The $\epsilon_{\bar{j},\bar{j}+\hat{\mu}}$ frustrates the hopping of the $\phi_{\bar{j}}$ and it is necessary to properly diagonalize (G4) in momentum space for $b_{\bar{j}\mu} = 0$. This was performed by LFS who showed that for a suitable gauge choice in (5.6), the $\phi_{\bar{j}}$ had equivalent minima near spatial momenta $(0,0)$ and $(\pi,0)$. We choose the same linear combinations of fields near these minima as defined by LFS. Now we are prepared to take the continuum limit of all the terms in (G1), and the result leads to (5.12).

APPENDIX H: GAUGE THEORY WITH $\langle N \rangle \neq 0$

This appendix will study the vicinity of the points A and B in Fig 13. We will use the same strategy as that followed in Section VIA but will apply it to the compact U(1) gauge theory Z_P in (6.4) rather than to the Z_2 gauge theory Z'_P in (6.9).

The initial strategy is the same as that followed in Section VIA for the Z_2 gauge theory. We quench the field N_j at its condensate $N_0(0,0,1)$ and neglect its spin-wave fluctuations (as in the discussion in Section III A, the latter will lead to weak additional power-law tails to the interactions considered below and do not alter the basic physical properties). This allows us to preferentially focus on $z_{j\uparrow}$ and neglect $z_{j\downarrow}$; we write the former in terms of an angular variable as $z_{j\uparrow} = e^{i\theta_{j\uparrow}}$. Note that this is an easy-axis anisotropy to the CP^1 fields, in contrast to the easy-plane limit considered in Appendix F. For the $Q_{j\ell}$ degrees of freedom in (6.4), we assume, for simplicity, that the spiral correlations have preferentially polarized in the x direction: so we write $Q_{jx} = e^{i\theta_{jQ}}$ and neglect Q_{jy} . With this transformations and (innocuous) approximations we can obtain from Z_P the following effective action for the angular variables $\theta_{j\uparrow}$, θ_{jQ} and the compact U(1) gauge field $A_{j\mu}$ (all terms have been written in a Villain form to facilitate duality transforms):

$$Z_N = \sum_{\{q_{\bar{j}\mu}, m_{j\uparrow\mu}, m_{jQ\mu}\}} \int_0^{2\pi} \prod_{\bar{j}\mu} dA_{\bar{j}\mu} \int \prod_j d\theta_{j\uparrow} d\theta_{jQ}$$

$$\begin{aligned} & \times \exp\left(-S_A - \tilde{S}_B - S_\dagger - \tilde{S}_Q\right) \\ \tilde{S}_Q &= \frac{1}{2g_Q} (\Delta_\mu \theta_{jQ} - 2\pi m_{jQ\mu} - 2A_{j\mu})^2, \end{aligned} \quad (\text{H1})$$

where S_A and \tilde{S}_B are defined in (A3), and S_\dagger is defined in (F1). Note that this action differs in structure from (F1) only in the prefactor of 2 for the gauge field in \tilde{S}_Q ; this double charge is, of course, crucial to the structure explored here. The duality methods developed in Section II and V are easily applicable to (H1): we obtain the following action for integer valued vectors fields $a_{\bar{j}\mu}, p_{\bar{j}\mu}$ residing on the links of the dual lattice

$$\begin{aligned} Z_N &= \sum_{\{a_{\bar{j}\mu}, p_{\bar{j}\mu}\}} \exp\left(-\frac{e^2}{2}(a_{\bar{j}\mu} - a_{\bar{j}\mu}^0)^2 - \frac{g_Q}{2} \sum_{\square} (\epsilon_{\mu\nu\lambda} \Delta_\nu p_{\bar{j}\lambda})^2\right. \\ & \quad \left. - \frac{g}{2} \sum_{\square} (2\epsilon_{\mu\nu\lambda} \Delta_\nu p_{\bar{j}\lambda} - \epsilon_{\mu\nu\lambda} \Delta_\nu a_{\bar{j}\lambda})^2\right). \end{aligned} \quad (\text{H2})$$

Some physical properties of Z_N will be more transparent in this dual formulation. Note also that (H2) has only positive weights and so should be amenable to Monte Carlo simulations.

We are interested here in the phase diagram of Z_P as a function of the three couplings g , g_Q , and e^2 . Much insight can be gained by looking at various limiting cases: the results of such an analysis of the phase diagram are displayed in Fig 19. Our primary interest is in the phases at center of the cube shown in Fig 19 where the states found at the boundaries will meet and compete. A complete understanding of this strongly coupled region will probably require Monte Carlo simulations of (H2), which we have not undertaken.

The identification of the phases in Fig 19 accounts for the presence of the background \mathbf{N}_0 condensate, and so the phase labels are appropriate to the theory Z_P in (6.4). However, taken by itself, Z_N is a model of a compact U(1) gauge theory coupled to two angular variables, and its phases can also be described in the language of the models of Section V. Z_N possesses a gauge-invariant angular variable, $\theta_\dagger - \theta_Q/2$, which can acquire “superfluid” or XY order; as in Section VIA this XY order maps to the P phase after accounting for the \mathbf{N}_0 condensate. Also as in Section VIA, the gauge degrees of freedom can induce BC or F phases, which become HN+BC and HN+F phases in the context of (6.4) and Fig 19.

The relationship between Z_N and the models of Section V can be made explicit by examining the limit $g_Q \rightarrow 0$, where the charge 2 scalar $e^{i\theta_Q}$ condenses. Then it is evident from (H2) that Z_N at $g_Q = 0$ is exactly equivalent to (5.2) which is in turn related by duality to the Z_2 gauge theory (1.15). The results of Section V then lead to the phase diagram at the bottom of Fig 19. We had argued in Section VIA that Z'_P mapped onto $Z_{U(1)}$ in the region with $\langle \mathbf{N} \rangle \neq 0$; as Z'_P was also obtained from Z_P in the limit of a strong charge 2 condensate, the con-

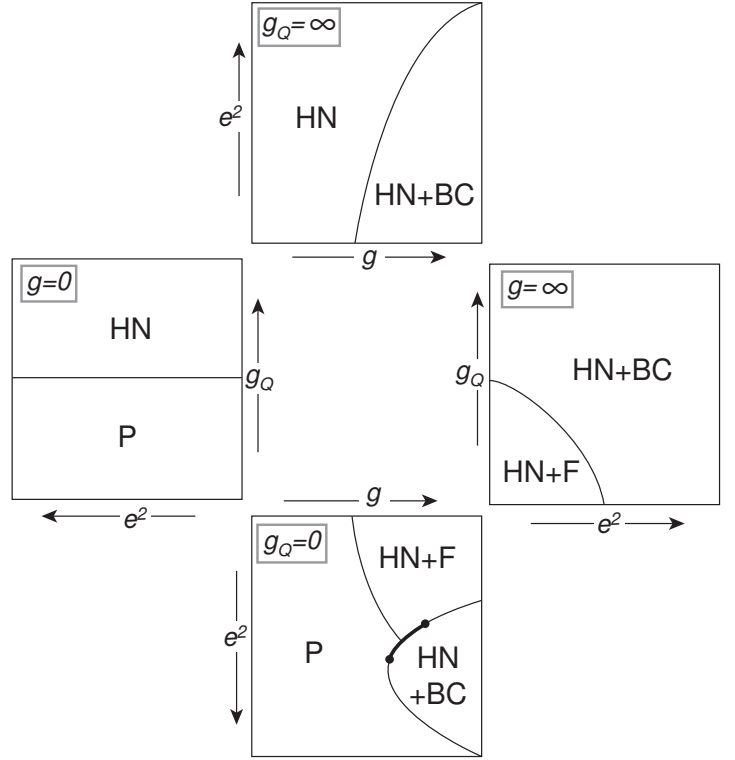


FIG. 19. Phase diagram of Z_N in (H1) and (H2) as a function of the three couplings g , g_Q , and e^2 . The labels of the states account for the background \mathbf{N} condensate needed in the derivation of Z_P , and are appropriate to the phases of Z_P in (6.4). The figure is to be visualized by imagining that these couplings run along the axes of a three-dimensional cube; the sides of the cube have been opened out flat into the plane of the paper. The arrows indicate that the associated coupling runs from 0 to ∞ along its direction.

nection between Z_N and the Z_2 gauge theory (1.15) for small g_Q is just as expected.

We also discussed in Section VI A that Z'_P , and hence the small g_Q limit of Z_N , misses a crucial piece of physics: it is not able to describe the HN phase. The present model Z_N is able to repair this key deficiency in the opposite limit of large g_Q . The most important property of Z_N in this limit is that it possesses a phase without any broken symmetries or fractionalization, and this leads to the HN phase in Fig 19. In this respect the compact U(1) gauge theory Z_N is far removed from the Z_2 gauge theory $Z_{U(1)}$ in (1.15) which did not have any such featureless phase; this phase appears in the region corresponding to that with XY order in the Z_2 gauge theory—unlike the discrete Z_2 gauge fields, the $U(1)$ are able to quench the superfluid order by “Higgsing” it into a massive phase. The appearance of HN order is, of course, satisfactory, and was the reason we stated our preference for Z_P over Z'_P . To demonstrate the existence of this featureless phase, consider the limit of large g_Q in (H2): there we can set $\epsilon_{\mu\nu\lambda}\Delta_\nu p_{\bar{j}\lambda} = 0$, and Z_N reduces to precisely the model studied in Ref. 4 by Monte Carlo simulations—this is a model of a compact U(1) gauge field A_μ coupled to a single charge-1 scalar. In its simplest form, such a model has only a single featureless phase continuously connecting the confining and Higgs regions; however, with the Berry phases present here a BC ordering transition can occur. The resulting phase diagram is shown at the top of Fig 19.

Moving on, we can also look at the limit of large g exhibited in Fig 19. Here, the charge-1 scalar can be ignored, and we have the theory of a charge-2 scalar coupled to a compact U(1) gauge field with Berry phases. This was examined in Ref. 18 and the resulting phase diagram appears on the right of Fig 19. Its phase transition involving competition between BC and F order is described by the fully frustrated Ising model in (5.10), and this last mapping becomes exact for small g_Q .

Finally, we consider the limit of small g appearing on the left of Fig 19. Now the charge-1 scalar completely quenches the gauge field, and the theory becomes that of an ordinary three-dimensional XY model; the XY ordering transition is that between the P and HN phases.

Saarloos, Phys. Rev. B **62**, 14844 (2000).

- ⁸ T. Senthil and M. P. A. Fisher, Phys. Rev. B **62**, 7850 (2000).
- ⁹ C. Lannert, M. P. A. Fisher, and T. Senthil, Phys. Rev. B **63**, 134510 (2001).
- ¹⁰ E. Demler, C. Nayak, H.-Y. Kee, Y. B. Kim, and T. Senthil, cond-mat/0105446.
- ¹¹ S. Chakravarty, B. I. Halperin, and D. R. Nelson, Phys. Rev. B **39**, 2344 (1989).
- ¹² For a review and original references, see S. Sachdev, *Quantum Phase Transitions*, Chapter 13, Cambridge University Press, Cambridge (1999).
- ¹³ B. Berg and M. Luscher, Nucl. Phys. B **190**, 412 (1981).
- ¹⁴ N. Read and S. Sachdev, Phys. Rev. Lett. **66**, 1773 (1991).
- ¹⁵ S. Sachdev and N. Read, Int. J. Mod. Phys. B **5**, 219 (1991).
- ¹⁶ R. Jalabert and S. Sachdev, Phys. Rev. B **44**, 686 (1991).
- ¹⁷ S. Sachdev, Phys. Rev. B **45**, 12377 (1992).
- ¹⁸ S. Sachdev and M. Vojta, J. Phys. Soc. Jpn. **69**, Suppl. B, 1 (2000).
- ¹⁹ A related theory is in Ref. 20 and will be discussed briefly in Section VII. We also note that there were earlier proposals for fractionalized states involving the concept of the chiral spin liquid (V. Kalmeyer and R. B. Laughlin, Phys. Rev. Lett. **59**, 2095 (1987) and X.-G. Wen, F. Wilczek, and A. Zee, Phys. Rev. B **39**, 11413 (1989)), but it was subsequently realized^{14,20,21,8} that the time-reversal symmetry-breaking in these states was unnecessary and unrelated to the underlying physics of fractionalization.
- ²⁰ X.-G. Wen, Phys. Rev. B **44**, 2664 (1991).
- ²¹ L. Balents, M. P. A. Fisher, and C. Nayak, Phys. Rev. B **60**, 1654 (1999); Phys. Rev. B **61**, 6307 (2000).
- ²² W. Zheng and S. Sachdev, Phys. Rev. B **40**, 2704 (1989).
- ²³ E. Fradkin and S. A. Kivelson, Mod. Phys. Lett. B **4**, 225 (1990).
- ²⁴ S. Sachdev and N. Read, Phys. Rev. Lett. **77**, 4800 (1996).
- ²⁵ D. Rokhsar and S. A. Kivelson, Phys. Rev. Lett. **61**, 2376 (1988).
- ²⁶ R. Moessner and S. L. Sondhi, Phys. Rev. Lett. **86**, 1881 (2001); R. Moessner, S. L. Sondhi, and E. Fradkin, cond-mat/0103396; R. Moessner, O. Tchernyshyov, S. L. Sondhi, cond-mat/0106286; R. Moessner, S. L. Sondhi, and P. Chandra cond-mat/0106288.
- ²⁷ F. D. M. Haldane, Phys. Rev. Lett. **61**, 1029 (1988).
- ²⁸ B. I. Halperin in *Physics of Defects*, Les Houches XXXV NATO ASI, R. Balian, M. Kleman, J.-P. Poirier Eds, pg 816, North Holland, New York (1981).
- ²⁹ N. D. Autunes, L. M. A. Bettencourt, and A. Yates, hep-ph/9901391.
- ³⁰ G. Murthy and S. Sachdev, Nucl. Phys. B **344**, 557 (1990); A. V. Chubukov, S. Sachdev, and J. Ye, Phys. Rev. B **49**, 11919 (1994).
- ³¹ F. D. M. Haldane, Phys. Rev. B **25**, 4925 (1982).
- ³² S. Sachdev, *Quantum Phase Transitions*, Chapter 14, Cambridge University Press, Cambridge (1999).
- ³³ C. K. Majumdar and D. K. Ghosh, J. Phys. C **3**, 911 (1970).
- ³⁴ R. D. Sedgewick, D. J. Scalapino, and R. L. Sugar, cond-mat/0012028.
- ³⁵ E. S. Sørensen, M. Wallin, S. M. Girvin, and A. P. Young, Phys. Rev. Lett. **69**, 828 (1992); M. Wallin, E. S. Sørensen,

¹ P. W. Anderson, Science, **235**, 1196 (1987).

² S. Sachdev, Science, **288**, 475 (2000).

³ N. Read and S. Sachdev, Phys. Rev. Lett. **62**, 1694 (1989).

⁴ S. Sachdev and R. Jalabert, Mod. Phys. Lett. B **4**, 1043 (1990).

⁵ N. Read and S. Sachdev, Phys. Rev. B **42**, 4568 (1990).

⁶ O. P. Sushkov, J. Oitmaa, and Zheng Weihong, Phys. Rev. B **63**, 104420 (2001).

⁷ M. S. L. du Croo de Jongh, J. M. J. van Leeuwen, W. van

- S. M. Girvin, and A. P. Young, Phys. Rev. B **49**, 12115 (1994).
- ³⁶ A. van Otterlo, K.-H. Wagenblast, R. Baltin, C. Bruder, R. Fazio, and G. Schön, Phys. Rev. B **52**, 16176 (1995).
- ³⁷ K. Park and S. Sachdev, cond-mat/0104519.
- ³⁸ C. Dasgupta and B. I. Halperin, Phys. Rev. Lett. **47**, 1556 (1981).
- ³⁹ C. H. Chung, J. B. Marston, and R. H. McKenzie, J. Phys.: Condens. Matter **13**, 5159 (2001).
- ⁴⁰ B. I. Shraiman and E. D. Siggia Phys. Rev. Lett. **62**, 1564 (1989); Phys. Rev. B **42**, 2485 (1990).
- ⁴¹ E. Fradkin and S. H. Shenker, Phys. Rev. D **19**, 3682 (1979).
- ⁴² C. H. Chung, J. B. Marston, and S. Sachdev, cond-mat/0102222.
- ⁴³ G. Misguich, C. Lhuillier, B. Bernu, C. Waldtmann, Phys. Rev. B **60**, 1064 (1999).
- ⁴⁴ W. LiMing, G. Misguich, P. Sindzingre, C. Lhuillier, Phys. Rev. B **62**, 6372 (2000).
- ⁴⁵ J. B. Fouet, P. Sindzingre, and C. Lhuillier, Eur. Phys. J. B **20**, 241 (2001).
- ⁴⁶ B. Bernu, L. Candido, D. M. Ceperley, Phys. Rev. Lett. **86**, 870 (2001).
- ⁴⁷ J.-B. Fouet, M. Mambrini, P. Sindzingre, and C. Lhuillier, cond-mat/0108070.
- ⁴⁸ L. Capriotti and S. Sorella, Phys. Rev. Lett. **84**, 3173 (2000).
- ⁴⁹ L. Capriotti, F. Becca, A. Parola, and S. Sorella, cond-mat/0107204.
- ⁵⁰ T. Kashima and M. Imada, cond-mat/0104348.
- ⁵¹ R. Coldea, D. A. Tennant, A. M. Tsvetlik, and Z. Tylczynski, Phys. Rev. Lett. **86**, 1335 (2001).
- ⁵² F. Hebert, G. G. Batrouni, R. T. Scalettar, G. Schmid, M. Troyer, and A. Dorneich, cond-mat/0105450.
- ⁵³ O. A. Starykh, R. R. P. Singh, and G. C. Levine, cond-mat/0106260.
- ⁵⁴ J. Zaanen, O. Y. Osman, H. V. Kruis, Z. Nussinov, and J. Tworzydło, cond-mat/0102103.
- ⁵⁵ W. Rantner and X.-G. Wen, Phys. Rev. Lett. **86**, 3871 (2001).
- ⁵⁶ X.-G. Wen, cond-mat/0107071.
- ⁵⁷ I. Affleck and J. B. Marston, Phys. Rev. B **37**, 3774 (1988).
- ⁵⁸ J. M. Kosterlitz, J. Phys. C **10**, 3753 (1977).
- ⁵⁹ G. Murthy, Phys. Rev. Lett. **67**, 911 (1991).
- ⁶⁰ D. R. Nelson, Phys. Rev. B **26**, 269 (1982).